POLITECNICO DI MILANO
DEPARTMENT OF ELECTRONICS, INFORMATION AND BIOENGINEERING
DOCTORAL PROGRAMME IN BIOENGINEERING

ASSESSMENT OF ATRIAL FIBRILLATION TRIGGERS AND THEIR ROLE IN ITS PROGRESSION

Doctoral Dissertation of:

Francisco Javier Saiz Vivó

Supervisors:

Prof. Luca Mainardi

Prof. Valentina Corino

Dr. Mirko de Melis

Tutor:

Prof. Paolo Giuseppe Ravazzani

Committee Members:

Prof. Pablo Laguna

Prof. Axel Bauer

Prof. Andrea Aliverti

December, 2022

XXXIII Cycle

Francisco Javier Saiz Vivó, 2022
Assessment of atrial fibrillation triggers and their role in its progression.

Date of current version: December 20th, 2022

This Ph.D. thesis has been developed within the Dipartimento di Elettronica, Informazione e Bioingegneria (DEIB) from Politecnico di Milano (Milan, Italy), and the Bakken Research Center from Medtronic (Maastricht, Netherlands)

This thesis was supported by a fellowship from the European Union's Horizon 2020 research and innovation programme under the Marie Skłodowska-Curie grant agreement No.766082: "MultidisciplinarY training network for ATrial fibRillation monItoring, treAtment and progression" (MY-ATRIA). Some parts of this thesis have been developed within secondments in the Department of Biomedical Engineering from Lund University (Lund, Sweden), and the Skåne University Hospital (Lund, Sweden).

ASSESSMENT OF ATRIAL FIBRILLATION TRIGGERS AND THEIR ROLE IN ITS PROGRESSION

Summary and Conclusions

Atrial fibrillation (AF) is a progressive disease often initially manifested by intermittent episodes terminating spontaneously and eventually leading to sustained forms of AF for a subset of patients. This rhythm disorder is the most common arrhythmia encountered in clinical practices with predictions of affecting 6-12 million people in the USA by 2050 and 17.9 million in Europe by 2060. However, the underlying mechanisms are still under investigation.

The main objective of this thesis is to propose methodological advancements for the characterization of the AF triggers and episodes detected by implantable cardiac monitors (ICM) in cohorts of continuously monitored patients, to attain a better understanding of AF and its mechanisms that may lead to improvement in clinical decisions, as those related to catheter ablation strategies which could lead to a more effective patient triage that could reduce the economic and personal burden of the ablation procedure by increasing the success rate of long-term AF termination.

To accomplish this, the patient population used throughout the thesis was composed by combining two different cohorts: the Reveal LINQ Usability study (N=151, 33.1% female, 66.9% male, 56.6 ± 12.1 years old) obtained by Medtronic, and a database acquired from the National Institute of Cardiovascular Diseases in Bratislava (N=40, 20% female, 80% male, 55.9 ± 9.9 years old). Due to algorithm requirements, each chapter of the thesis uses a different subset of patients extracted from these cohorts.

In the first part of this thesis, the characterization of AF triggers, and an automatic unsupervised AF trigger classification method based on a combination of heart rate variability (HRV) features extracted from ICMs in a cohort of continuously monitored patients is presented. These HRV features were evaluated, and principal component analysis (PCA) was used to determine the most representative features and compute their linear combination, i.e., the principal components. The unsupervised classification method used in this study was k-means algorithm in which the triggers were placed into different clusters based on their principal components. The optimum number of clusters was determined by the silhouette coefficient and any cluster which contained fewer than 5% of the observations was discarded as an outlier cluster. The results obtained when analysing the HRV features from the different clusters extracted from the Flashbacks, the 500 beats preceding the AF onset, showed that distinct triggers could be found. Although the inference of clinical information from unsupervised classification of patterns has relative reliability, the

triggers that could potentially be identified in the clusters ware premature atrial complexes (PACs), atrial tachycardia (AT), atrial flutter and spontaneous AF, i.e., no trigger. Based on literature, we believe that patients with different triggers might respond differently to certain catheter ablation strategies. Therefore, the characterization of AF triggers could aid clinicians in selecting the optimum ablation strategy for their patients.

Then, the AF episode characterization involved the modelling of the atrial fibrillatory rate (AFR) based on changes in autonomic tone quantified by RR series characteristics and the temporal aggregation of AF episodes. For the assessment of the modelling of the AFR, the f-wave signals, from which AFR is estimated, were extracted using a QRST cancellation process, from a single lead ECG of the first 2 minutes of the AF episodes. The AFR was then estimated as the fundamental frequency of a harmonic model fitted to the extracted f-waves. We used a fixed-effect (FE) model and compared the results to a mixed-effect (ME) approach to study both the population and patient specific effects of RR series in AFR and another ME modelling approach which allowed correction for confounding factors such as effect of episode duration, previous ablation, and circadian variations, to model the variations of AFR based on changes in autonomic tone quantified by RR series characteristics. The mixed-effect models were shown to have a better fit to the data than the fixed-effect models. This approach also showed that AFR was faster in episodes with longer duration, less organized RR intervals and after several ablation procedures. For the AF episode patterns characterization, the alternating bivariate Hawkes model was used. Two parameters of the alternating bivariate Hawkes model were used to characterize the pattern: AF dominance during the monitoring period ($\log(\mu)$) and temporal clustering of episodes (β_1). This characterization was then used to investigate, for the first time, whether post-ablation recurrence of AF could be predicted by evaluating episode patterns. In addition, we compared the risk assessment of AF recurrence capabilities between the Hawkes parameters and stablished measurements of AF dominance and temporal aggregation such as AF burden and AF density. While the combination of AF burden and AF density is related to a non-significant hazard ratio, the Hawkes parameters showed increased risk of AF recurrence within 1 year after the procedure for patients with high AF dominance and high episode clustering and may be used for pre-ablation risk assessment.

Finally, this thesis evaluated the feasibility of using clinical data and heart rate variability (HRV) features extracted from an ICM to predict recurrences in patients prior to undergoing catheter ablation for AF. HRV derived features were extracted from the Flashback and from the first 2 minutes of the last AF episode recorded by an ICM before undergoing first catheter ablation. Several single classification methods including Support Vector Machines (SVM), with linear, polynomial (SVMp)

and Gaussian (SVMg) kernels, Classification and Regression Trees (CART) and K-Nearest Neighbour (KNN) algorithms are evaluated to predict AF recurrence. In addition, the capabilities of ensemble learning methods in which a weighted combination of the single classifiers is used as the predictor of AF recurrence was explored. The sequential forward floating search (SFFS) algorithm was used to select the optimum feature set for each classification method. The results showed that clinical and HRV features can be used to predict rhythm outcome using an ensemble classifier for superior accuracy. The proposed ensemble algorithm's performance metrics for predicting AF recurrence after catheter ablation where: accuracy 0.82; sensitivity 0.76, specificity 0.87, F1-score 0.82 and Area under the ROC curve 0.85. This would enable a more effective pre-ablation patient triage that could reduce economic and personal burden of the procedure by increasing the success rate of first catheter ablation.

This thesis is based on retrospective analyses that carry certain limitations including the relatively low number of patients enrolled from different cohorts, the unavailability of clinical and medication information, the heterogeneity of the characteristics of the patients, or the lack of validation of an independent cohort. Nonetheless, the database offered a unique characterization of patients diagnosed with AF and is crucial for deciding the optimum course of treatment such as catheter ablation, which has relatively low success rates. ICMs with high AF detection accuracy offer the unique advantage of long-term monitoring periods and continuous monitoring of the patient. With the rapidly increasing use of these devices for AF patients, the need for methods to characterize AF triggers and AF episodes which could be used in in tools that can help in clinical decisions, is increasingly important.

In particular and if confirmed in future studies, the use of these characterization methods to, for instance, aid clinicians in deciding the best catheter ablation strategy is potentially of significant clinical relevance for several reasons: first, catheter ablation of AF substrate is a procedure with high economic and personal burden; secondly, due to the epidemic character of AF prevalence, these interventions cannot be offered (even in countries with developed health-care systems) to all patients and third, the selection of patients with higher probability of long-term elimination of AF has high priority. With this in mind, once a potential catheter ablation candidate is identified, the patient could be implanted and followed up while in the waiting list. Using the algorithms proposed and the data collected, the clinician could evaluate the status of the patient every couple of weeks and decide their position on the waiting list as well as start planning for the ablation strategy: that which will increase their chance of long-term AF termination.

Keywords: Ablation; Advanced Signal Processing; Atrial fibrillation; Atrial fibrillation burden; Atrial fibrillatory rate; Classification; Episode clustering; Heart rate variability; Implantable cardiac monitors; Electrocardiogram; Machine Learning; Mixed-effect models; Prediction; Recurrences; Risk stratification; Temporal aggregation

Acknowledgements

The completion of this thesis would not have been possible without the help and support of many people, to whom I would like to express my gratitude.

First of all, I would like to thank my supervisors, Valentina D.A. Corino, Luca T. Mainardi and Mirko de Melis, for all their constant support, availability, patience and enthusiasm that I have received along all these years. Valentina and Luca, thank you for your encouragement not only during this PhD but also during the Master thesis. If I have been able to do this, it is in big measure as a result of all I had learnt (and continued learning) with and from you during those early years in Milan when I was introduced to research and atrial fibrillation. Being able to return to Milan during these years has been a pleasure and thank you for welcoming me back to the B3-Lab whenever I was there. Mirko, thank you for making me feel at home in Maastricht (despite the weather!) and for giving me the trust and space to grow as a researcher and as a person. One of the best things I take from these years is the experience gained in a research driven company such as Medtronic. Thank you for helping me navigate the waters of industry and giving me the tools to communicate effectively with fellow researchers but also with customers and stakeholders.

I would like to extend my thankfulness to Leif Sörnmo and Frida Sandberg, for their continuous help and fruitful discussions that have contributed to the realization of this thesis and hopefully will lead to many future projects together. I will always be thankful for welcoming me to Lund and to the department of Biomedical Engineering where I was lucky to be able to spend a couple of months. Even if the pandemic cut my stay short, you gave me the chance to return to Lund and share fikas and veggie burgers with you. The first person to greet me when I arrived in Lund was Alba and I want to thank you for your kindness and support during my stay there and during our collaboration. I would also like to thank Pyotr Platonov and Fredrik Holmqvist for opening the doors of their Cathlab at Skåne University Hospital and giving me the opportunity of learning first-hand the needs of physicians during ablation procedures. Your insight and experience have help shape this thesis and I hope we'll continue to work together on our annotation tool.

I have been more than lucky having the possibility of doing this PhD within the Horizon 2020 Marie Skłodowska-Curie Actions programme, during which I have had the pleasure of sharing this journey with my fellow ESRs, Jordan, Rebecca, Giorgio, Muhamed, Ricardo, Hesam, Mostafa, Guadalupe, Luca, Chiara and Jennifer. I would like to thank them, and everyone involved in MY-ATRIA for their support and making every summer (and winter) school unforgettable. The time (and beers) we shared in Milan, Lund, Jaca, Karlsruhe, and whenever we happened to meet as part of our secondments or at conferences were a pleasure and part of the highlights of these years. You are still all invited to Valencia!

Y todos estos años, tanto o más importante para mí ha sido el apoyo recibido fuera del laboratorio y la oficina. A mis amigos, los de siempre y a los que se han ido sumando en mis años de universidad, gracias porque pese a la distancia y a lo desperdigados que estamos, compartir con vosotros los buenos y malos ratos, ha hecho siempre que las alegrías fueran dobles y las penas, la mitad. Mención especial para mi Squad, gracias por siempre sacar tiempo (a veces demasiado) para reunirnos en Chinas o en Condominio. Ha sido una gran manera de teneros cerca pese a estar lejos.

Y sin duda, a mi familia. Habéis vivido esta tesis en primera persona, con todo lo que ello conlleva. Me habéis esperado siempre con un abrazo y os aseguro que os he llevado siempre conmigo. Estoy seguro de que si alguien está orgulloso de mi trabajo, esos son mis abuelos Benita y Paco y mi abuelo Antonio. Para mí, encontrarme con vuestras sonrisas (y algún que otro plato de lentejas) al llegar a casa, ha sido siempre la mejor de las medicinas. Quiero agradecer también a las dos personas que han hecho su especialidad sacarme de quicio y a las que quiero mucho: mis hermanas, Raquel y Marta. Estoy muy orgulloso de vosotras, de lo que habéis conseguido, y de lo que estoy seguro, conseguiréis. Mucho ánimo con la residencia y el doctorado, y recordad disfrutar del camino. Echando la vista atrás, se hace corto. Vero, no hay palabras para agradecer tu confianza y apoyo incondicional estos años que he estado fuera. Para mi has sido un pilar fundamental y sé que no ha sido fácil verme hacer las maletas tantas veces. El tiempo que vivimos el Baldovi fue un regalo y espero que pronto podamos volver a vivirlo. ¡Te quiero muchísimo! Por último, pero para nada menos importante, especial mención a mis padres, para los que solo puedo decir: gracias por todo. Soy quien soy y he llegado hasta donde he llegado gracias a vosotros. Gracias por inspirarme a perseguir mis objetivos y a no rendirme nunca. Sin vosotros no lo habría conseguido y por ello, os estaré siempre agradecido.

Gracias a todos. Thank you everyone.

Javi

Contents

List of Figures

List of Tables

Chapter 1 Introduction

1.1. Motivation

Atrial fibrillation (AF) is a progressive disease often initially manifested by intermittent episodes terminating spontaneously and eventually leading to sustained forms of AF for a subset of patients [1]. As the general population ages, the incidence of AF rises from 0.7% in subjects from 55-59 years to almost 18% in 85-year-old patients [2]. Nowadays, this particular rhythm disorder has become the most common arrhythmia encountered in clinical practice with predictions of affecting 6-12 million people in the USA by 2050 and 17.9 million in Europe by 2060 [3]. However, the underlying mechanisms are still under investigation.

Over the decades, catheter ablation, and more specifically, pulmonary vein isolation (PVI), has become a common treatment of AF patients [4], especially for those whose antiarrhythmic drug therapy was inefficient (or not tolerated) for rhythm stabilization [5,6] or those who were highly symptomatic [7]. However, long-term efficacy of catheter ablation reported in AF single-procedures does not exceed 70% [8]. These relatively low success rates are translated not only into an increase of the personal burden of the patient which have higher rates of emergency department visits (43.4% vs. 32.2%: $p<0.001$) and subsequent hospitalizations (35.6% vs. 21.5%; $p<0.001$) but also, in an increase of medical costs ($52,281 vs. $13,412; $p<0.001$) [9].

Several well-established scoring systems aiming at predicting rhythm outcome after catheter ablation, including thromboembolic risk predictors like $\mathrm{CHADS_2}$ or $\mathrm{CHA_2DS_2}$-VASc, have shown modest prediction capabilities [10]. Other specific rhythm outcome predictors such as APPLE [11], SUCCESS [12], and MB-LATER [13] have achieved better results. However, most studies have the drawback of relying on 24-hour Holter monitoring to detect AF recurrences, which was shown to have a rather poor detection rate for subclinical AF of 5.5% [14].

Implantable cardiac monitors (ICMs) offer the advantage of long-term monitoring and use highly sensitive AF detection algorithms, with detection rates up to 96% [15]. Some studies have shown how ICMs can be used as a tool to inform medical management of post-ablation patients [16] as well as to guide subsequent ablations after AF recurrence [17].

In this thesis, methodological advances are proposed to improve the risk stratification of AF patients based on AF trigger and AF episode characterization as well as to improve AF recurrence prediction in patients which are continuously monitored by an ICM. This could lead to a more effective pre-ablation patient triage

that could reduce economic and personal burden of the procedure by increasing the success rate of first catheter ablation to achieve long-term AF termination.

1.2. The Heart

The heart is a muscular organ with the main function of pumping blood into the circulatory system. This fist-sized organ is constituted of four chambers: two atria and two ventricles which are connected by the atrioventricular (AV) valves also known as the tricuspid and the mitral valve. Each pair of chambers, conformed by one atrium and one ventricle, work together to supply blood to the systemic (or peripheral) and the pulmonary circulatory systems. Biologically speaking, in the cardiac cycle, two different stages can be identified: the ventricular diastole and systole. In the late diastole (or ventricular filling), deoxygenated blood from the veins and oxygenated blood from the lungs flows from the right and left atria into the right and left ventricles respectively through the AV valves. The last phase of the diastole is the atrial systole, during which the atria contract so that the remaining blood inside them flows into the ventricles. This phase is responsible for filling almost one third of the ventricles. The ventricular systole consists of an isometric ventricular contraction which increases the pressure inside the ventricles until the aortic and pulmonary valves burst open and the ventricular ejection takes place. The ejection phase takes 3 times longer than the contraction phase. Finally, the isovolumetric relaxation takes place where the ventricular fibres relax causing the pressure to drop. When the pressure decreases enough, the AV valves reopen and the atria are filled again, restarting the cycle. Figure 1.1 (A) illustrates the different chambers of the heart and the course of blood through them.

In a healthy heart, the cardiac cycle is coordinated by a mass of self-excitable cells located in the right atrium called the sinoatrial (SA) node. The SA node is responsible of generating autonomously the electrical impulses used to contract the muscles of the myocardium, thanks to a property called autorhythmicity. The SA node, the so-called natural pacemaker of the heart generates the electrical impulses at a rate modulated by the autonomic nervous system (ANS). A second system of specialized fibers is in charge of distributing these electric impulses throughout the myocardium. Three pathways: anterior, middle, and posterior internodal tracts connect the SA node to the atrioventricular (AV) node. The passage of the impulse is delayed in the AV node, to allow the atrial contraction to further increase the blood volume in the ventricles before the systole takes place, before it continues to the bundle of His,

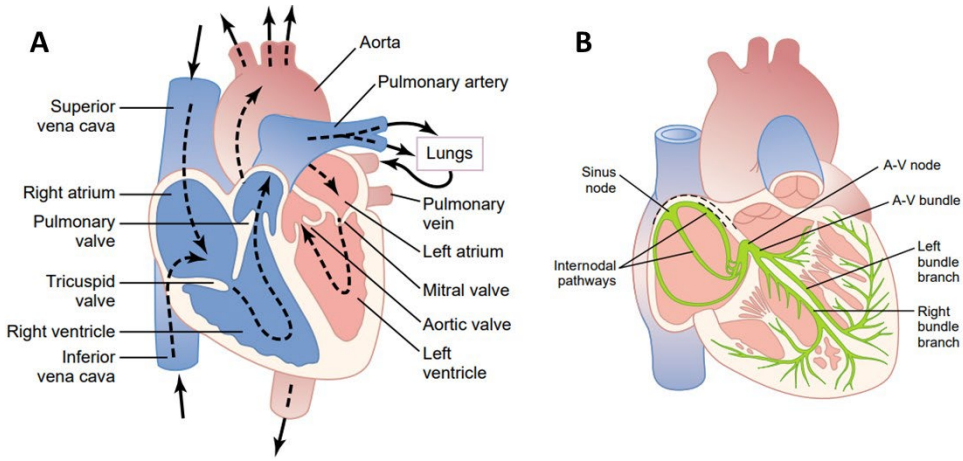

Figure 1.1. Anatomic overview of the heart: chambers and blood flow (A) and conduction network (B). From [18].

which in turn devices into the right and left bundle branch, and finally reaches the Purkinje network (Figure 1.1 (B)). The Purkinje network rapidly propagates the impulse to the different layers of cardiac muscle in order to achieve a coordinated contraction within the ventricles. During the normal functioning of the heart, the heart rate (HR) is directly controlled by the rate of impulses from the SA node, referred to normal sinus rhythm (SR) and has a rate of about $100 - 120\ beats/min$ in absence of the ANS influence [19]. However, if any of these paths were to be blocked or the electrical impulses were to be diffused randomly, different pathological heart conditions would arise [20].

1.3. Atrial Fibrillation

One of these pathological heart conditions, and the focus of study of this thesis, is atrial fibrillation (AF). Atrial fibrillation is a supraventricular tachyarrhythmia characterized by chaotic and uncoordinated atrial activation and contraction that produces an irregular ventricular response. While the exact mechanisms of AF remain unknown, this asynchrony may be due to the appearance of secondary (ectopic) pacemaker activity and/or areas of decreased conduction that enable and facilitate re-entrant activity. The chaotic activation and contraction of the atrial muscles makes the AV node discharge at irregular intervals as after the node is activated, its tissue gets depolarized, and it needs to be repolarized before being activated again. During the repolarization, and for a certain period after it called the

refractory period, the tissue cannot be depolarized again. This limits the number of impulses that get through, as several impulses arriving close to each other may not all be conducted. Hence, causing a highly irregular rate of ventricular contractions, and consequently, a highly irregular heart rhythm often faster than SR ($120 - 160\ beats/min$).

AF represents a major health problem as it is the most prevalent sustained arrhythmia encountered in clinical practice [21], affecting globally over 43.6 million individuals [6]. Increasing age is a prominent AF risk factor [22], increasing from 2-4% in subjects from 55-59 years to almost 18% in octogenarians [2], but other comorbidities including hypertension, diabetes mellitus, heart failure (HF), coronary artery disease (CAD), obesity and obstructive sleep apnoea are also important. In [23] it is stated that "The typical patient with AF is often referred to as an elder one with diabetes, left ventricular hypertrophy (LVH), and/or other electrocardiographic pathological findings, coronary heart disease (CHD) or valvular heart disease, coronary heart failure (CHF), or a history of previous stroke".

While many patients suffering from AF present a variety of recognizable symptoms, most commonly palpitations, chest pain, tiredness and shortness of breath [6], approximately one-third of the cases are diagnosed with no or nonspecific symptoms, i.e., are asymptomatic [24], suggesting an underestimation of the prevalence. AF is not only related to its variety of symptoms and reduced quality of life in >60% of patients [25] which is often translated to anxiety disorders [26] and a higher burden of depressive symptoms [27], but also constitutes a major risk factor for blood clots, stroke, HF and other heart-related complications [6]. Most importantly, AF is associated with a 3.5-fold mortality increase [28] generally related to HF and stroke, which has a 5-fold risk increase associated with AF [29].

The diagnosis of AF is based on rhythm documentation with an electrocardiogram (ECG) tracing. On the ECG, AF is observable since P waves, produced by a coordinated atrial depolarization during the atrial systole, are replaced with rapid oscillations of fibrillatory waves, i.e., f waves, that vary in amplitude, shape, and rate as consequence of the chaotic depolarization of atrial tissue. The frequency of these fibrillatory waves, i.e., the atrial fibrillatory rate (AFR) is generally accepted as a surrogate marker for local refractoriness and is a key characteristic of AF which is extensively studied in clinical contexts [30]. Atrial activity characterization through AFR has been used to evaluate the effects of Class I and III antiarrhythmic drugs [31–33] and has been linked to the spontaneous termination of AF [34,35], AF type (paroxysmal/non-paroxysmal) [36], and the progression of atrial structural remodelling and fibrosis [37]. The f-waves represent the atrial activity and are

extracted by removing the ventricular activity from the ECG signal as illustrated in Figure 1.2.

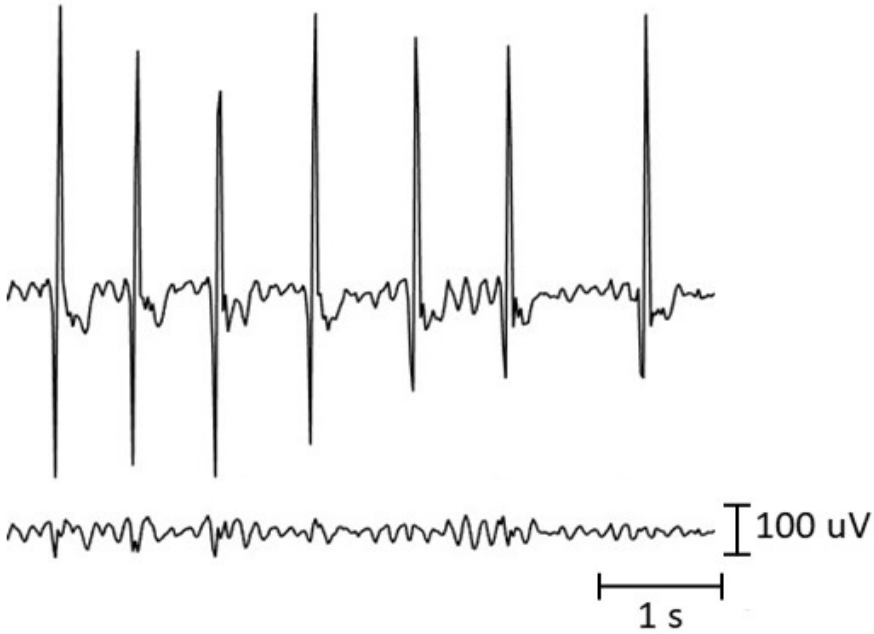

Figure 1.2 Example of f-waves extracted from single-lead ECG. The ECG (top) and the corresponding extracted f-wave signal (bottom) are displayed.

AF is also associated with the heart rate or RR intervals observable in the ECG being irregular and frequently faster than in SR. This happens as a result of the AV node filter role resulting in a high level of disorganization of ventricular impulses. By convention, an ECG tracing of at least 30s showing heart rhythm with no discernible P waves and irregular RR intervals is required to establish the diagnosis of AF [38].

Figure 1.3 shows the ECG tracings typically observed during SR and AF where the rhythm becomes irregular, and the P-waves are replaced with f-waves.

To describe the temporal dynamic pattern of AF, in terms of presence and duration of AF episodes, the term AF burden (defined as the amount of time spent in AF) has been introduced and subjected to study [39]. By considering AF burden, AF is regarded as a quantitative entity and physicians move beyond merely treating AF as a binary condition (presence or absence of AF). While the relationship with AF burden with specific outcomes is not well characterized [41], it may be associated with higher risk of incident HF [42] and all-cause mortality [43].

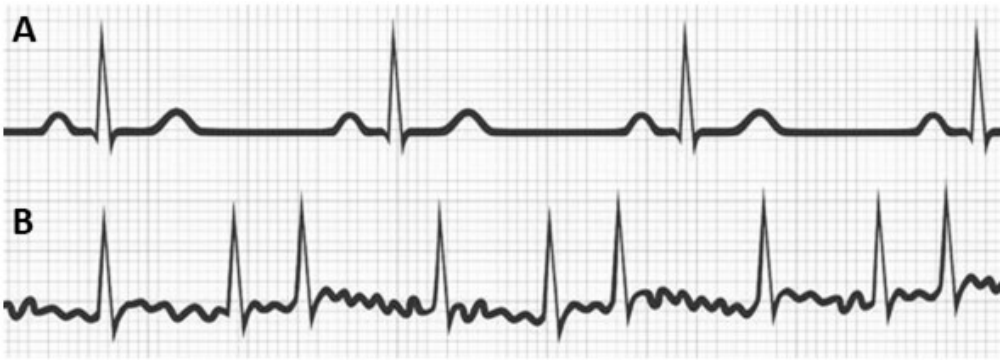

Figure 1.3 ECG tracing representation of (A) normal sinus rhythm and (B) atrial fibrillation. Modified from [40].

1.3.1. AF mechanisms

Atrial fibrillation's pathology is complex, with different mechanisms influencing the onset, duration, and termination of AF episodes.

Remodelling of atrial structure: Structural heart disease, hypertension, diabetes, and AF itself act as stressors which induce structural remodelling in the atria [44]. Structural remodelling, usually accompanied by fibrosis, results in an electrical dissociation between different regions of the atria [45], which favours re-entry and maintenance of AF [46]. The most important pathophysiological alterations in atrial tissue associated with AF include changes of the extracellular matrix, fibroblast functions and fat cells [47], ion channel alterations [48], myocyte alterations [49], endothelial and vascular alterations [50], and changes to the autonomic nervous system [51].

Electrophysiological mechanisms: Atrial fibrillation causes changes in atrial electrophysiology by progressively shortening the atrial refractory period and AF cycle length. In contrast, structural heart changes tend to prolong the atrial refractory period hence illustrating the heterogeneity of AF in different patients [48]. Regarding the generation and maintenance of AF, three main hypotheses are identified: (1) a focal initiation and maintenance hypothesis, where a focal source in the pulmonary veins can trigger AF and serve as localized re-entry point, and an ablation of this source can suppress recurrent AF [52]. (2) A multiple wavelet hypothesis, which states that AF can be perpetuated by several independent wavelets propagating though the atria in a chaotic manner [53]. This hypothesis

postulates that as long as the number of wavefronts remains over a certain critical level, they will be capable of sustaining the arrhythmia. (3) The presence of a mother rotor defined as a stable, high-frequency rotating pattern that drives AF [54].

Genetic predisposition: A strong heritable component, independent of concomitant cardiovascular conditions, has been found in AF, especially early-onset AF [55]. Changes in atrial action potential characteristics, atrial remodelling, and modified penetration of rare gene defects have been suggested as potential mechanisms resulting in increased AF risk [56].

1.3.2. AF types

Atrial fibrillation is a progressive disease often initially manifested by short and isolated episodes terminating spontaneously and eventually leading to more frequent and sustained forms of AF for a subset of patients [1]. Traditionally, based on onset, duration, and spontaneous termination of episodes, five different AF patterns are distinguished [6]:

First diagnosed AF: AF which occurs when the arrhythmia has not been diagnosed before and its irrespective of its duration or the presence and severity of AF-related symptoms.

Paroxysmal AF (PAF): This type of AF generally terminates spontaneously, usually within the first 48 hours, but can be terminated with intervention within 7 days of onset.

Persistent AF: AF which is continuously maintained beyond 7 days, including episodes terminated by cardioversion, either with drugs or by electrical cardioversion.

Long-standing persistent AF: Continuous sustenance of AF for more than one year in which cardioversion has failed or not been attempted, and rhythm control strategy has been adopted.

Permanent AF: AF that is accepted by the patient and physician. It represents the therapeutic attitude of not further attempting to restore and maintain sinus rhythm rather than a pathophysiological AF attribute. If and when a rhythm control strategy is decided to be adopted, the arrythmia could be re-classified as ‘long-standing persistent AF’.

The AF type is not considered to be static as, for example, a paroxysmal AF patient may very well transition into persistent AF. This classification of AF is still very widely used in the clinical setting. However, with the increasing use of implantable cardiac monitors capable of long-term monitoring, clinically determined AF patters have been found not to correspond well to the AF burden [39,57].

1.4. Patient management: ABC pathway

Reflecting the complex and somehow uncertain underlying mechanisms of AF, patient management has remained suboptimal. Recently, a simple Atrial fibrillation Better Care (ABC) pathway ('A' Anticoagulation/Avoid stroke, 'B' Better symptom management; 'C' Cardiovascular and Comorbidity optimization [58]) was proposed to streamline the management of AF patients.

1.4.1. A – Anticoagulation/Avoid stroke

AF increases the risk of stroke five-fold as the incomplete contractions of the atria may cause blood to coagulate and form blood clots. However, stroke risk in AF is not homogeneous and depends on various risk factors. For this reason, the first step in avoiding stroke is to identify low risk patients who do not require any antithrombotic therapy via validated stroke risk stratification scores, usually, the $\mathrm{CHA_2DS_2\text{-}VASc}$ score (Congestive heart failure, Hypertension, Age ≥75, Diabetes mellitus, Stroke, Vascular disease, Age 65-75 years, Sex (female)). Step 2 is to offer stroke prevention to those patients with one or more risk factors of stroke, involving oral anticoagulation (OAC) after the proper assessment of bleeding risk. The last step is to decide on the preferred OAC which include dose-adjusted vitamin K antagonists (VKAs) such as warfarin with a well-managed time in therapeutic range (TTR) or the now preferred option in many guidelines: non-VKA oral anticoagulants (NOACs) such as rivaroxaban [59].

1.4.2. B – Better symptom control

After considering the admission of OACs to avoid stroke, the next consideration includes management of symptoms (for those symptomatic patients) and deciding between one of two options: rhythm control or rate control[60].

Rhythm control

The rhythm control strategy focuses on restoration and maintenance of SR, primarily indicated for patients with AF-related symptoms in an attempt of improve QoL, and can be achieved through a combination of treatment approaches, including electrical or pharmacological cardioversion, antiarrhythmic medication, and catheter ablation.

Cardioversion

Sinus rhythm can be restored in AF patients through pharmacological or electrical cardioversion. Pharmacological cardioversion to SR is indicated in haemodynamically stable patients and while it is less effective than electrical cardioversion [61], restoring SR in approximately 60-80% of patients with recent-onset AF versus the 80%-90% restoration rate of electrical cardioversion [62], it does not require sedation. Flecainide [63], propafenone [64], vernakalant [65] and amiodarone [66] are some examples of effective antiarrhythmic drugs for pharmacological cardioversion. For a selected subset of patients with rare paroxysmal AF episodes, a "pill-in-pocket" approach, where the patient self-administers an oral dose of flecainide or propafenone, might be preferred [67].

For severely haemodynamically compromised patients, a synchronized direct current electrical cardioversion is the method of choice to quickly and effectively convert AF to SR [6]. The standard device for electrical cardioversion is the biphasic defibrillator [68] with anterior-posterior electrode positions for a more effective rhythm restoration [69].

Long-term antiarrhythmic drug therapy

The aim of antiarrhythmic drug (AAD) therapy is to reduce AF related symptoms [6]. Clinically successful AAD therapy may reduce rather than eliminate AF and although compared to no therapy, AAD approximately doubles SR maintenance [70] , it is less effective than AF catheter ablation [71,72]. To reduce the risk of side effects, such as adverse events, proarrhythmic events and even death, a shorter duration of AAD therapy is preferred [70,73,74]. As an example, treatment with flecainide for 4 weeks (short-term) was well-tolerated and prevented up to 80% of AF recurrences when

compared to long-term treatment [75]. The main AADs available to prevent AF include amiodarone, dronedarone, flecainide, sotalol and dofetilide [70].

Catheter ablation

Over the decades, catheter ablation has become a common treatment of AF patients [7], especially for those whose antiarrhythmic drug therapy was inefficient (or not tolerated) for rhythm stabilization [5,6] or those who were highly symptomatic [7]. Since the common triggers for paroxysmal AF initiation are ectopic beats originating from the pulmonary veins (PV) [52], catheter ablation is primarily achieved by complete pulmonary vein isolation (PVI) [4]. Pulmonary vein isolation is achievable by creating lesions encircling the pulmonary veins by point-by-point radiofrequency (RF) ablation or cryoballoon ablation. Figure 1.4 illustrates the PVI procedures using cryoballon ablation and RF ablation.

In the cryoballoon ablation process, ablative lesions are created using intra-catheter temperatures at around -50 °C delivered to each pulmonary vein in a “single-shot” application. Operators use using fluoroscopic guidance to place the device at each pulmonary vein antrum, advancing it toward the pulmonary vein to achieve occlusion, and then cooling the tissue by filling the balloon with the liquid refrigerant.

In the RF process, the PVI is attempted by creating a contiguous circular lesion around each pulmonary vein antrum with point-by-point applications of radiofrequency energy while navigating the catheter under the guidance of a 3-D electroanatomical mapping system [76].

While cryoballoon procedures have showed reduced hospitalizations and lower complication rates [77], both types of energy have shown similar AF termination and maintenance outcomes [78–80].

In more advanced AF types such as persistent and long-standing persistent AF, a more extensive ablation may have additional benefits [81]. This may include liner lesions in the atria, isolation of the superior vena cava or the left atrial appendage, ablation of complex fractionated atrial electrograms (CFAE), rotors, or non-pulmonary foci. However, the additional benefit of PVI plus extra lesions (PVI+) against PVI alone, justifying its use during the first procedure, is yet to be confirmed. Figure 1.5 illustrates examples of PVI and PVI+ ablation strategies.

Although AF ablation is more effective than AAD therapy in restoring and maintaining SR [71,72] in patients with symptomatic paroxysmal, persistent, and long-standing persistent AF, long-term efficacy of catheter ablation reported in AF single-procedures does not exceed 70% [8].

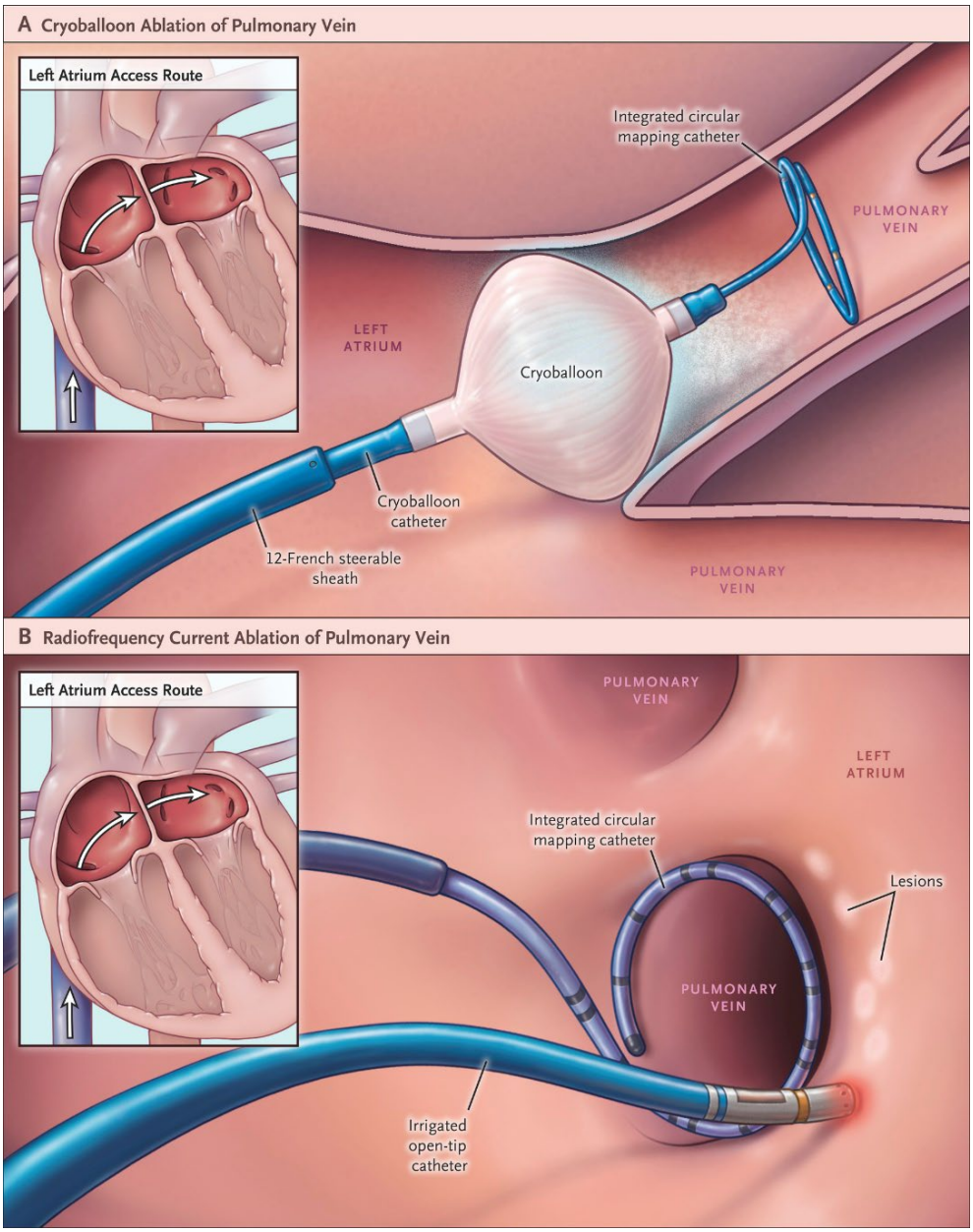

Figure 1.4. Pulmonary vein ablation procedure using (A) Cryoballoon ablation, and (B) Radiofrequency current ablation. Image from [80]. *Used with permission.*

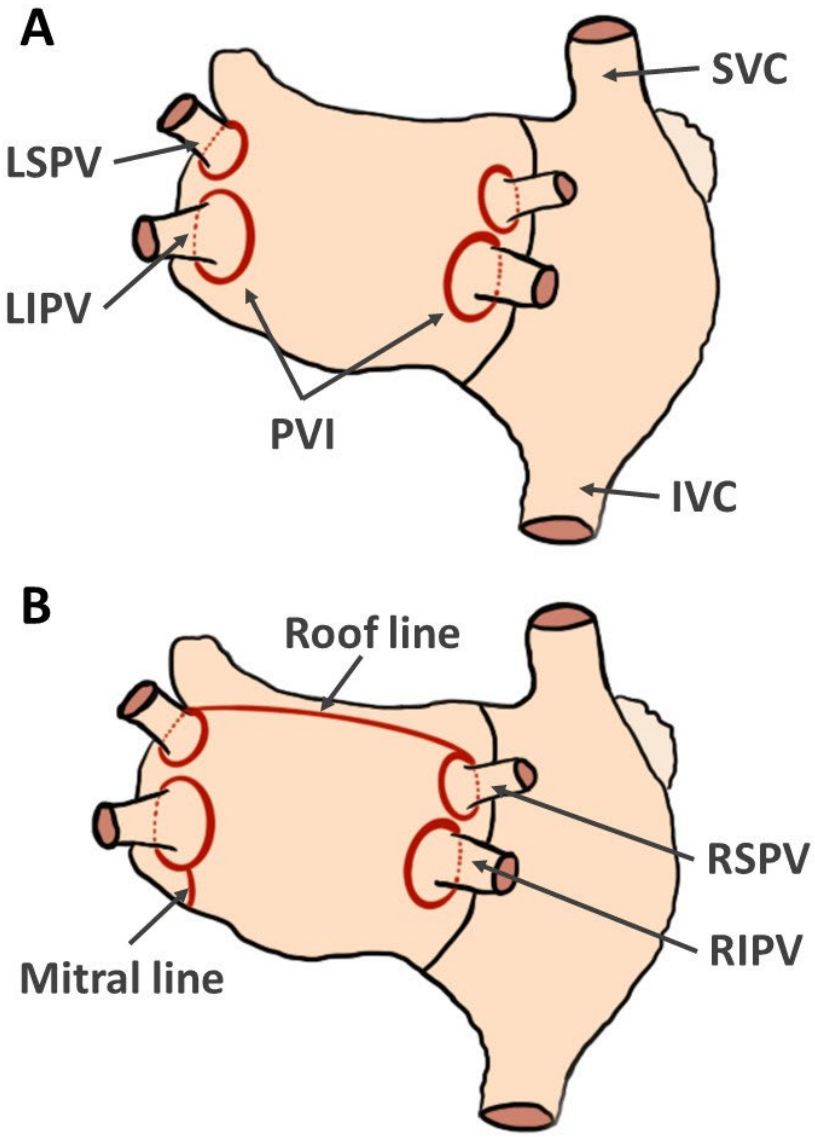

Figure 1.5 Examples of ablation strategies. (A) Pulmonary vein isolation (PVI), and (B) PVI plus extra lesions, in this case, Roof and Mitral lines.

IVC: Inferior Vena Cava; LIPV: Left inferior pulmonary vein; LSPV: Left superior pulmonary vein; RIPV: Right inferior pulmonary vein; RSPV: Right superior pulmonary vein; SVC: Superior Vena Cava

These relatively low success rates are translated not only into an increase of the personal burden of the patient which have higher rates of emergency department visits and subsequent hospitalizations but also, in an increase of medical costs [9].

Several risk factors for AF recurrence after ablation have been identified and scoring systems aimed at predicting rhythm outcome have been developed. Thromboembolic risk predictors such as $\mathrm{CHADS_2}$ or $\mathrm{CHA_2DS_2}$-VASc have shown modest prediction capabilities [10]. Other specific rhythm outcome predictors including APPLE (one point for Age > 65, Persistent AF, imPaired estimated glomerular filtration rate (eGMR $< 60\ ml/min/1.73m^2$), LA diameter $\geq 43\ mm$, Ejection fraction $< 50\%$) [82], SUCCESS, based on the APPLE score and adding one extra point for each previously performed ablation [12], and MB-LATER (one point for Male, Bundle branch block, LA diameter $\geq 47\ mm$, Type of AF [0 points for paroxysmal, 1 point for persistent, 2 points for long-standing persistent], and ER-AF, i.e., early recurrence AF during 3-months blanking period [83])[13] have achieved better results. While the model variables can be measured before ablation (except early recurrence in MB-LATER) and could therefore be used pre-procedurally to predict the likelihood of recurrence, no single score has been presently identified as consistently superior to others.

Rate control

Rate control is an integral part of AF management and is often sufficient to improve AF-related symptoms. It can be achieved with AV node ablation and pacing or with drugs that increase the degree of block that the AV node offers [84], thus decreasing the number of impulses that conduct into the ventricles, to sustain a heart-rate target of <110 bpm, unless symptoms call for stricter rate control [85].

Acute and long-term rate control can be pharmacologically achieved with beta-blockers, often the first-line rate-controlling agent [6], non-dihydropyridine calcium channel blockers (NDCC), such as verapamil or diltiazem which can improve AF-related symptoms compared to beta-blockers [84], and with cardiac glycosides, such as digoxin and digitoxin which, although their prescriptions have been declining in the past years [86], they are still commonly prescribed to sicker patients [87]. As a last resort, AADs such as amiodarone, dronedarone or sotalol, which also have rate-limiting properties, can also be used for rate control. However, they should be used only for rhythm control. The choice of rate control drugs, or a combination thereof, depends on the symptoms, comorbidities, and potential side-effects.

When medication fails, ablation of the AV node and pacemaker implantation can also be attempted to control ventricular rate. The procedure has low complication rate

and low long-term mortality risk [88,89] but will render patients pacemaker dependent for the rest of their lives. For this reason, AV nodal ablation should be limited to patients whose symptoms cannot be managed by pharmacological rate-control or by reasonable rhythm control strategies [6].

1.4.3. C – Cardiovascular and comorbidity risk reduction

The last component in the ABC pathway includes the identification and management of concomitant diseases, cardiometabolic risk factors, and unhealthy lifestyle choices.

Hypertension is the most common cardiovascular risk factor associated with AF where hypertense patients have a 1.7-fold higher risk of developing AF compared to normotensives [90]. In addition, interactions between AF and heart failure [91] and coronary artery disease [92] have been shown. Diabetes mellitus is also an independent risk factor for AF, especially in younger patients [93] with a prevalence of AF twice as high in patients with diabetes compared with patients without diabetes [94]. Obstructive sleep apnoea (OSA), the most common form of sleep-disordered breathing, is highly associated in increased risk of cardiovascular events and mortality [95]. A prospective analysis has also shown that approximately 50% of AF patients had OSA compared with 32% of control group [96].

AF can also be tackled by targeting lifestyle choices. Obesity [97,98], excessive alcohol consumption [99,100], and vigorous physical activity mainly related to long-term or endurance sport participation [101], have shown to increase the risk of incident AF. For this reason, patients are advised to manage their obesity if needed [102], reduce their alcohol intake, where alcohol abstinence if preferred [103], and while are encouraged to remain physically active to prevent AF incidence or recurrence, avoid excessive endurance exercise (such as marathons).

1.5. Recording techniques

The diagnosis of AF or detection of AF recurrence post therapy is usually based on rhythm documentation using an ECG showing the typical pattern of AF. Undiagnosed AF is common [104] as AF often occurs in a subclinical form, i.e., patients have only mild and unspecific symptoms, if any [105], or are mostly paroxysmal in nature,

making it difficult to be detected by intermittent monitoring such as conventional 24-, 48- or 72-hour Holter devices [106]. For this reason, AF screening programs, especially in older populations (>65 years), are encouraged and several mobile health technologies have emerged for AF screening and detection [107], including wearables such as smart watches, or patient initiated photoplethysmogram-based smartphone apps. Many of them are not clinically validated so caution in their clinical use is needed. In order to establish a definitive diagnosis of AF when detected by a screening tool, a single-lead ECG tracing of $\geq 30\,s$ or 12-lead ECG showing AF analysed by an expert physician is needed.

1.5.1. Holter monitors

A Holter monitor, also referred to as an ambulatory electrocardiographic system, is a small, battery-powered medical device that measures the patient's cardiac activity typically for 24, 48 or 72 hours. This type of devices is mainly used for rhythm detection and analysis including to establish the link between palpitations and abnormal heart rhythms [108], evaluate transient episodes of cardiac arrhythmias [109], monitor the efficacy and safety of pharmacological and non-pharmacological therapies [110], or to analyse and evaluate the function of pacemakers or other implantable devices [111].

The current state Holter technology records and stores data from 2 to 3 ECG leads attached to the patient's chest. Although Holter monitoring has the ability to continuously record ECG data without the need for patient participation, the relatively short monitoring duration of the monitoring can be inadequate if symptoms are infrequent. A study comparing 24-hour Holter monitoring with a single-lead adhesive patch-type device (APD) showed that 72-hour monitoring with the APD increased the detection rate of paroxysmal AF by 2.2-fold [112].

1.5.2. Implantable Cardiac Monitors

Implantable cardiac monitors (ICM) are subcutaneously implanted arrhythmia monitoring devices. These leadless devices continuously monitor the cardiac rhythm of the patient and record single-lead ECG signals automatically when an episode is detected or by patient activation when the patient has a symptomatic episode. ICMs

have proven to be significantly superior at AF detection compared to the commonly used intermittent follow-up strategy based on quarterly 24-hour Holter monitoring. In this study, the ICM was able to identify more AF episodes than intermittent 24-hour Holter performed every 3 months. The Holter monitoring was shown to have a sensitivity of 0.6 with a negative predictive value of 0.64 in identifying AF recurrence patients [113]. The use of ICMs for the diagnosis of AF after surgical AF ablation [113], catheter AF ablation [16,17,114], atrial flutter ablation [115], and cryptogenic stroke [116] has been increasing in the clinical practice.

This thesis will focus and use the data extracted from the Reveal LINQ (Medtronic, Inc).

Reveal LINQ

The Medtronic Reveal LINQ is a novel ICM which is $1.18\ cm^3$ in size and utilizes wireless telemetry for remote monitoring of patients with suspected arrhythmias. It continuously monitors the patient's ECG and other physiological parameters such as activity and it's designed to record the occurrence of an arrhythmia in a patient automatically. The following arrhythmias can be detected: tachyarrthymia, bradyarrhythmia, pause, atrial tachyarrhythmia, or atrial fibrillation. In addition, while experiencing or immediately after a symptomatic event, the patient can activate the device to record his/her cardiac rhythm.

The device is implanted within the fourth intercostal space (V2-V3 orientation) as shown in Figure 1.6, and senses and detects the rhythm, storing part of it with a sampling frequency of 256 Hz.

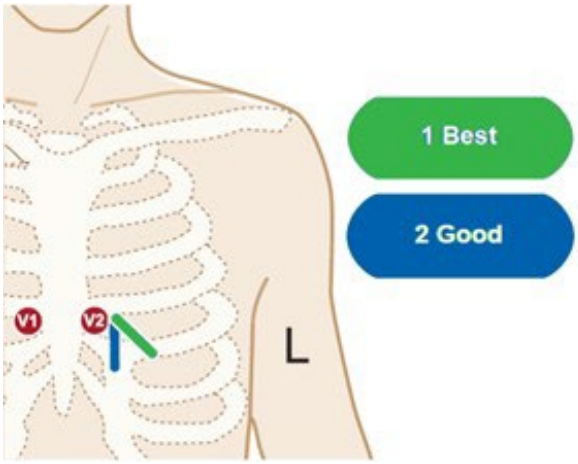

Figure 1.6 Recommended subcutaneous implant locations. Image from Reveal LINQ LNQ11 manual. Used with permission.

Once an AF episode is detected, the device stores the episode onset date and time, the first 2 minutes of the AF episode detected as well as the ventricular sense, i.e., the position of the R-peaks, for further clinical validation and, once the episode is over, the duration of the episode. The device can store up to 30 episodes of data, with the new episode overwriting the oldest one when the buffer is full. In addition, the device stores the daily AF burden in minutes for the entire monitoring period as well as other physiological parameters such as patient activity, daily heart rate variability calculated as the sum of the squares of the median heart rate computed every 5 minutes, and daily average heart rate during the day and at night.

AF detection algorithm

The AF detection algorithm included in the Reveal LINQ is based on RR interval incoherence patterns to compute an AF evidence score every 2 min [15,117] and a P-wave evidence score [118,119]. The P-wave evidence score was developed to reduce inappropriate AF detection in the original RR interval pattern-based algorithm. A schematic representation of the AF detection algorithm is illustrated in Figure 1.7.

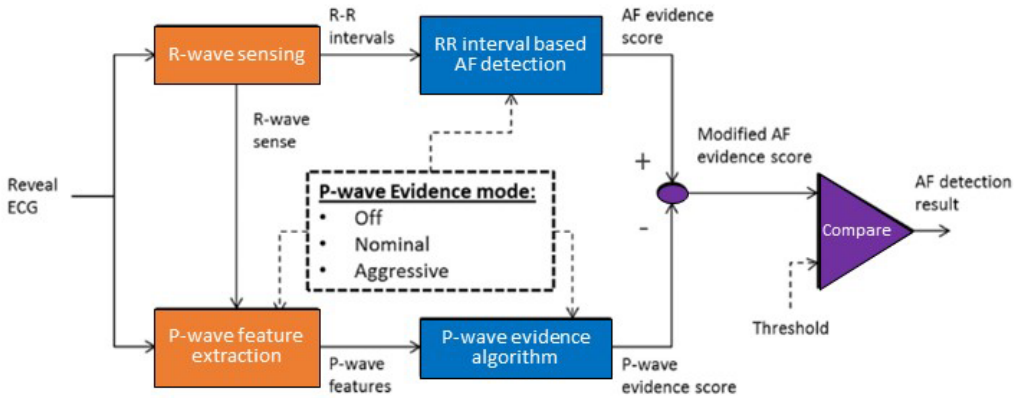

Figure 1.7 Schematic for the combination of the P-wave evidence algorithm with the RR interval-based AF detection algorithm. Modified from [118].

The RR interval-based AF detection algorithm is the original AF detection algorithm used in the predecessor of the Reveal LINQ, the Reveal XT ICM. This algorithm looks for patterns of incoherence in a Lorenz plot of difference in RR intervals (δRR) defined as:

$$\delta RR(i) = RR(i) - RR(i-1). \tag{1.1}$$

The Lorenz plot is a scatter plot of $\delta RR(i-1)\ vs\ \delta RR(i)$ which encodes the uncorrelated nature of RR intervals in the direction of change of three consecutive RR intervals. The different areas of the Lorenz plot are masked and the AF evidence score is computed as explained in [117].

During sinus rhythm, the centre part of the Lorenz plot is mostly populated as shown in Figure 1.8(A), whereas during AF, all segments are populated (Figure 1.8(C)). Figure 1.8(B) shows the distribution during a series of premature atrial contractions (PACs) leading to irregular RR intervals exhibiting a distribution different from SR and AF signature. The points populating the different areas are counted to calculate the AF evidence score.

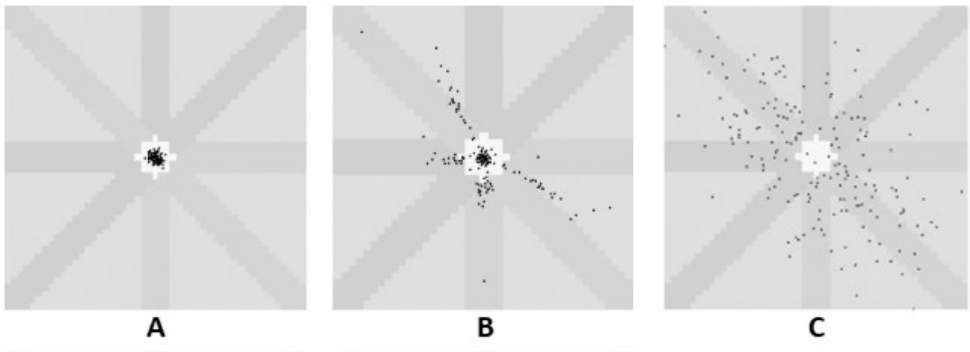

Figure 1.8 Lorenz plot of δRR intervals for 2 minutes of data during (A) normal sinus rhythm, (B) series of premature atrial contractions, and (C) atrial fibrillation. The plots exhibit several forms of irregularity. The Lorenz plots are extended from -600ms to +600ms along both axes. The differently shaded areas mark the masked areas considered when computing the AF evidence score. Modified from [117].

In order to reduce the number of inappropriate AF detections due to runs of atrial ectopy, oversensing due to noise or T-waves/P-waves, undersensing due to small R-waves, or bigeminal and trigeminal rhythms for example, the AF evidence score is corrected with the P-wave evidence score. The P-wave evidence score is based on the presence of a single P-wave and absence of fibrillatory waves (f-waves) or noise between two consecutive R-waves [118]. The ECG windows of 600-ms baseline before the R-waves of 4 consecutive beats are averaged. Subsequently, the presence of P-waves, f-waves, and baseline noise are identified from the morphological features. The P-wave evidence is then accumulated over the 2-minute detection interval to compute the evidence score as shown in Figure 1.9.

This algorithm can work in two different modes depending on the intention of usage: the “nominal” mode for AF monitoring which enhances AF burden accuracy, and the

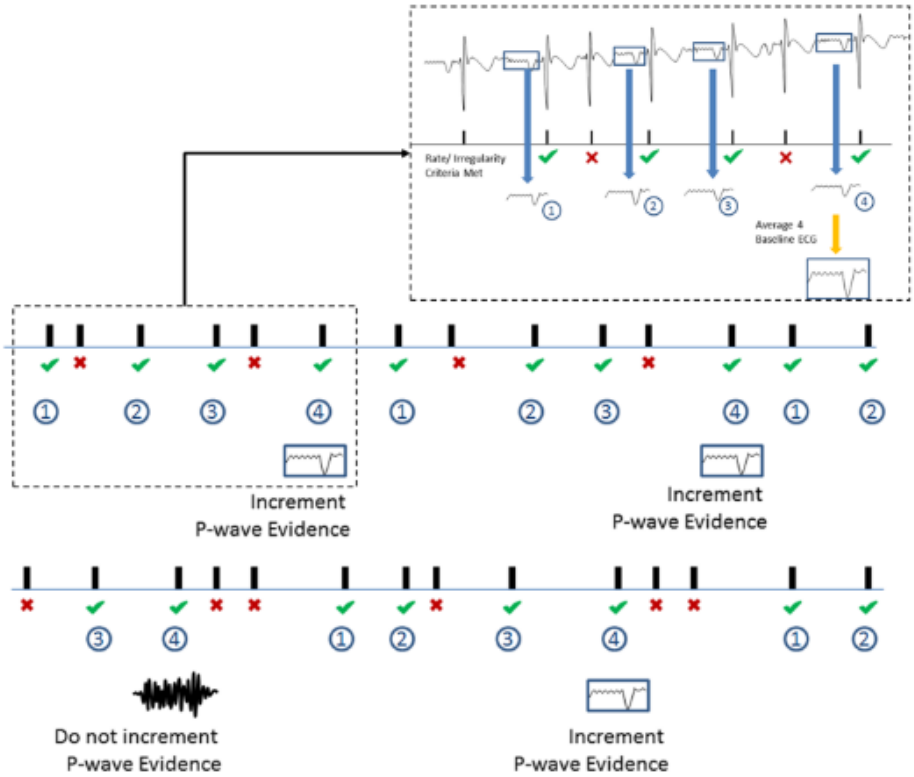

Figure 1.9 Segment of a 2-minute detection period illustrating the P-wave evidence accumulation procedure. The inset illustrates the 4-beat averaging procedure for P-wave detection. For every 4 beats that fulfill the rate/irregularity criteria, the baselines of the 600 ms preceding the beats are extracted and averaged as can be seen under every 4th criteria-fulfilling beat. If there is presence of a single P-wave and absence of atrial flutter waves (multiple P-waves) or noise in the averaged baseline, the P-wave evidence criterion is met, and the P-wave evidence score is incremented. This score is then accumulated over 2-minute detection interval and used as evidence against AF. From [118].

"aggressive" mode designed for AF diagnosis and non-AF patients which increases the specificity and improves the diagnostic yield of the algorithm. In case of runs of ectopic beats, both the P-wave evidence and the RR interval-based AF evidence score will be high. However, in the case of AF, only the AF evidence score will be high.

The P-wave evidence score is then subtracted from the AF evidence score before comparing it to the detection threshold. Once the modified AF evidence score is higher than the detection threshold, an AF episode is detected. The AF detection threshold is programmed during implant.

1.6. Objectives and outline of the thesis

The main objective of this thesis is to propose methodological advancements for the characterization of the AF triggers, i.e., heart rhythms that could induce AF and episodes detected by ICMs in a group of continuously monitored patients as described in Chapter 2. A better understanding of AF and its mechanisms that may lead to an improvement in clinical decisions, as those related to catheter ablation strategies which could lead to a more effective patient triage that could reduce the economic and personal burden of the ablation procedure by increasing the success rate of long-term AF termination. In particular, methodological advances in AF trigger characterization based on heart rate variability (HRV) features (Chapter 3), AF episode characterization focusing on assessing the circadian variations of fibrillatory waves and the temporal aggregation of AF episodes (Chapter 4 and Chapter 5, respectively), and a new algorithm designed for catheter ablation outcome based on clinical and HRV features extracted from both the last AF trigger and the AF episode before the procedure (Chapter 6), are presented. Finally, Chapter 7 and Chapter 8 present the main conclusions of the thesis, discuss the future extension of the work, and list the publications generated throughout the thesis.

The content of Chapters 3-6 of the thesis are organized as follows:

Chapter 3: AF Trigger Characterization

Studies have shown an improvement of catheter ablation for AF termination success rate, reaching 89%, in a second ablation procedure in patients with a specific AF trigger onset [17]. Motivated by the importance of AF triggers, this chapter explores AF trigger characterization and presents an automatic unsupervised AF trigger classification method. From a cohort of 132 patients ($56 \pm 10\ years$), 528 Flashbacks, i.e., the trend of around 500 ventricular beats preceding the AF onset stored in an ICM, were extracted and heart rate variability (HRV) computed. The Flashbacks are classified into 5 different clusters after the Principal Component Analysis (PCA) was computed on the HRV features. Two principal components explained more than 95% of the variance and were a combination of the mean RR interval, square root of the mean squared differences of successive RR intervals (RMSSD), standard deviation of the RR intervals (SDNN) and Poincare descriptors, SD1 and SD2. Five different clusters were identified using the silhouette coefficient and k-means clustering. When evaluating the differences in the HRV features for the different clusters, RMSSD and SD1 were significantly different among all clusters

($p < 0.05$, with Holm's correction) showing that distinct patterns can be found using this method.

Chapter 4: Atrial Fibrillatory Rate

This chapter investigates the use of heart rate variability (HRV) features as a measure of the changes in the autonomic tone to model variations in the atrial fibrillatory rate (AFR) in a cohort of atrial fibrillation (AF) patients continuously monitored with an implantable cardiac monitor (ICM). This study offers a chance of a more detailed characterization for patients diagnosed with AF and a better understanding of the patients' condition. The f-wave signals, from which AFR is estimated, were extracted using a QRST cancellation process, from a single lead ECG of the first 2 minutes of the AF episodes. The AFR then estimated as the fundamental frequency of a harmonic model fitted to the extracted f-waves. This chapter assesses the use of both fixed-effect and mixed-effect (ME) approaches. The latter allowing correction for confounding factors such as effect of episode duration, previous ablation, and circadian variations, to model the variations of AFR. The analysis included the AFR from 2453 f-waves extracted from a cohort of 99 patients ($57 \pm 12\ years$) which were continuously monitored with and ICM monitored for 9.2 (0.2-24.3) months as median (min-max). AFR was significantly affected by previous catheter ablations ($\mathrm{p} < 0.05$), episode duration ($\mathrm{p} < 0.05$), and irregularity of the RR interval series as quantified by sample entropy ($\mathrm{p} < 0.05$). This chapter concludes that AFR was faster in episodes with longer duration, less organized RR intervals and after several ablation procedures.

Chapter 5: Temporal aggregation

AF episode patterns characterization methods have been introduced without establishing clinical significance. This chapter includes a description of the alternating bivariate Hawkes model which is used to characterize the AF dominance and the temporal clustering degree of AF episodes within a certain monitoring period. Two parameters of the alternating bivariate Hawkes model were used to characterize the pattern: AF dominance during the monitoring period ($\log(\mu)$) and temporal clustering of episodes (β_1). This characterization is then used to investigate, for the first time, whether post-ablation recurrence of AF can be predicted by evaluating episode patterns. In addition, this chapter compares the risk assessment of AF recurrence capabilities between the Hawkes parameters and stablished measurements of AF dominance and temporal aggregation such as AF burden and AF density. The four parameters were computed from an average of 29 AF episodes per patient on a cohort of 54 patients ($56 \pm 11\ years$), with an

implantable cardiac monitor, before undergoing the first AF catheter ablation. The risk of AF recurrence after catheter ablation using the Hawkes parameters $\log(\mu)$ and β_1, AF burden and AF density was evaluated. While the combination of AF burden and AF density is related to a non-significant hazard ratio, the combination of $\log(\mu)$ and β_1 is related to a hazard ratio of 1.95 (1.03–3.70; p<0.05). The Hawkes parameters showed increased risk of AF recurrence within 1 year after the procedure for patients with high AF dominance and high episode clustering and may be used for pre-ablation risk assessment.

Chapter 6: AF recurrence prediction

Single-procedure catheter ablation success rate is as low as 52% in atrial fibrillation (AF) patients. This chapter evaluates the feasibility of using clinical data and heart rate variability (HRV) features extracted from an ICM to predict recurrences in patients prior to undergoing catheter ablation for AF. HRV derived features were extracted from the 500 beats preceding the AF onset and from the first 2 minutes of the last AF episode recorded by an ICM of 74 patients ($57 \pm 12\ years$; 26% non-paroxysmal AF; $57\%\ AF$ recurrence) before undergoing first AF catheter ablation. Several single classification methods including Support Vector Machines (SVM), with linear, polynomial (SVMp) and Gaussian (SVMg) kernels, Classification and Regression Trees (CART) and K-Nearest Neighbour (KNN) algorithms are evaluated to predict AF recurrence. In addition, the capabilities of ensemble learning methods in which a weighted combination of the single classifiers is used as the predictor of AF recurrence is explored. The sequential forward floating search (SFFS) algorithm was used to select the optimum feature set for each classification method. The Optimum Weighted Voting (OWV) method, which used an optimum combination of the single classifiers, was the best overall classifier (Accuracy = 0.82, Sensitivity = 0.76 and Specificity = 0.87). This chapter concluded that clinical and HRV features can be used to predict rhythm outcome using an ensemble classifier which would enable a more effective pre-ablation patient triage that could reduce economic and personal burden of the procedure by increasing the success rate of first catheter ablation.

Chapter 2 Cohort Description

2.1. Motivation

The algorithms developed throughout this thesis are focused on data extracted from the Reveal LINQ implanted in AF patients scheduled for catheter ablation. The patients included had to have a particular set of requirements. Generally, the patient had to have been implanted with an ICM (the Reveal LINQ), have been followed up for a period, referred to as the monitoring period, and during which would have undergone a catheter ablation procedure.

The patient population used was collected by Medtronic combining two different cohorts: the Reveal LINQ Usability study, a database obtained by Medtronic, and a database acquired from the National Institute of Cardiovascular Diseases in Bratislava, Slovakia [120], hereinafter, Slovakia study.

The patients included in both studies provided written informed consent to the study protocols which were reviewed and approved by the human research ethics committee of each participating institution in accordance with the Declaration of Helsinki.

This chapter acts as a summary of the patient population common to the different chapters to avoid repetition.

2.2. Usability Study

The Reveal LINQ usability study is a prospective multicenter single-arm clinical study (ClinicalTrials.gov Identifier: NCT01965899) which was designed to have two phases, the first enrolling 30 patients with any indication for an ICM and the second enrolling 121 patients with a documented history of AF and ablation candidates [119].

The baseline characteristics of the enrolled patients are listed in Table 2.1.

For phase I, the primary indication for ICM insertion included syncope (n=19), suspected AF (n=2), AF ablation monitoring (n=2), AF management (n=2), palpitations (n=3), cryptogenic stroke (n=1), or other reason specified as bradycardia by conversion of AF (n=1). In Phase II, the primary indication for ICM insertion included suspected AF (n=2), AF ablation monitoring (n=103) and AF management (n=16).

Table 2.1. Baseline demographics of patients enrolled in Reveal LINQ usability study

Patient Characteristics	Enrolled subjects (N=151)
Gender	
Male	101 (66.9%)
Female	50 (33.1%)
Age, years (mean ± SD)	56.6 ± 12.1
Primary indication for implant	
Syncope	19 (12.6%)
Palpitations/ suspected AF	7 (4.6%)
Cryptogenic stroke	1 (0.7%)
AF ablation monitoring/ AF management	123 (81.5%)
Other	1 (0.7%)
Supraventricular tachycardia	130 (86.1%)
Atrial fibrillation	126 (83.4%)
Paroxysmal	101 (66.9%)
Persistent	27 (17.9%)
Permanent	2 (1.3%)
Atrial flutter/ atrial tachycardia	24 (15.9%)
Stroke/ transient ischemic attach	13 (8.6%)

Values are given as no. (%) unless otherwise indicated
AF: Atrial fibrillation
SD: Standard Deviation

2.3. Slovakia Study

This study enrolled 133 patients (55 ± 9 years at the time of the first catheter ablation of AF; 81% males, 19% female) which were hospitalized from October 2005 to January 2014 at the Department of arrhythmias and pacing of the National Institute of Cardiovascular Diseases in Bratislava. The patients' data was retrieved retrospectively from the hospital information system acquired during hospitalization, from subsequent patient monitoring and the specific interrogation of the ICM device. Out of the 133 patients enrolled, 40 patients had a catheter ablation procedure which consisted of circumferential ablation of pulmonary veins with additional linear lesions when appropriate.

The baseline characteristics of the 40 patients are listed in Table 2.2.

Table 2.2 Baseline demographics of subset of patients enrolled in Slovakia study

Patient Characteristics	Number of subjects (N=40)
Gender	
Male	32 (80%)
Female	8 (20%)
Age, years (mean ± SD)	55.9 ± 9.9
Height, cm (mean ± SD)	175.3 ± 8.1
Weight, kg (mean ± SD)	90.7 ± 16.1
Coronary Risk Profile	
Hypertension	34 (85%)
Heart Failure	2 (5%)
Stroke	4 (10%)
Coronary Artery Disease	7 (18%)
Paroxysmal AF	40 (100%)
History of persistent AF	25 (63%)

Values are given as no. (%) unless otherwise indicated
AF: Atrial fibrillation
SD: Standard Deviation

2.4. Cohort Summary

From the combined cohorts, 191 patients were included in the different analyses performed in this thesis. The individual patient cohorts for the different chapters are shown in Figure 2.1.

For Chapter 3, out of the 191 patients, 132 were found to have available Flashback information to explore the characterization of AF triggers. For Chapter 4, the complete set of 99 patients with pre-ablation data were used to model the atrial fibrillatory rate while for Chapter 5 and Chapter 6, a subsegment of them were used: 54 patient to study the temporal aggregation of AF episodes and 74 patients to predict AF recurrence after catheter ablation. In both cases, 19 patients were excluded due to previous failed ablation. In addition, 26 patients were excluded from Chapter 5 due to model requirements which will be specified in 5.2 and 6 patients were excluded from Chapter 6 due to incomplete medical data.

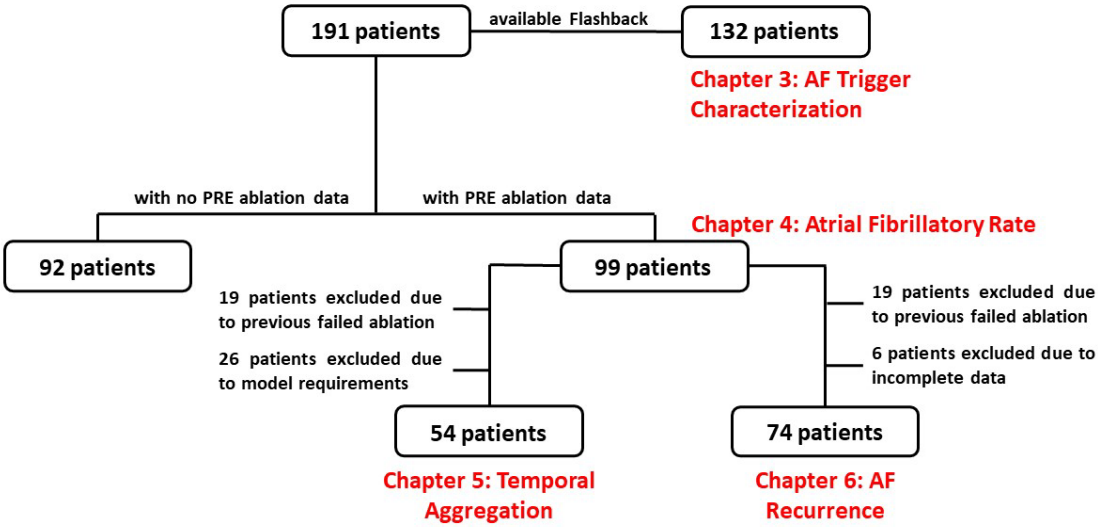

Figure 2.1 Patient distribution for the different chapters included in the thesis.

Chapter 3 AF Trigger Characterization

The publication related to this chapter is:

Saiz-Vivo J, DA Corino VDA, de Melis M, Mainardi LT. **Unsupervised Classification of Atrial Fibrillation Triggers Using Heart Rate Variability Features Extracted from Implantable Cardiac Monitor Data.** Annu Int Conf IEEE Eng Med Biol Soc. 2020 Jul;2020:426-429. doi: 10.1109/EMBC44109.2020.9175369. PMID: 33018019.

3.1. Motivation

Catheter ablation of AF, specifically PVI, is a common treatment for highly symptomatic patients [7]. However, a systematic review study of long-term outcomes of catheter ablation in AF reported single-procedure success rates as low as 66.6% in paroxysmal AF (PAF) patients and 51.9% in non-paroxysmal AF (NPAF) patients [8].

Pokushalov et al. [17] showed an improvement of the success rate, reaching 89%, in a second ablation procedure in patients with a specific AF trigger onset. The data used were provided by an implantable cardiac monitor (ICM) equipped with a highly sensitive AF detection algorithm (96%) [15] which continuously classifies the heart rhythm of a patient by analysing its cardiac cycle. In addition, it stores the trend of 500 ventricular beats preceding the detection marker of the most recent AF episode, hereinafter called “Flashback”. From the Flashback, Pokushalov et al. [17] defined different AF triggers such as atrial tachycardia (AT), atrial flutter, premature atrial contractions (PAC) or spontaneous AF, when the AF started suddenly and was not preceded by any of the previously defined triggers.

Atrial tachycardia is defined as a rapid atrial rhythm, regular, and originating form an unusual location in the upper chambers which causes a fast heart rate (>100 bpm). Similarly, atrial flutter represents very high frequency (240-350bpm) atrial tachycardia with atrial waves that produce continuous activation of the atrial tissue. Premature atrial complexes (PACs) occur when another region of the atria (commonly within the pulmonary veins) depolarizes before the sinoatrial node and triggers a premature heartbeat. Figure 3.1 illustrates the RR intervals of some examples of these onset mechanisms defined in Pokushalov et al’s work and used to guide the ablation strategy.

The success rate shown by the study (89%) was higher than the 78.9% multiple-procedure success rate reported by Ganesan et al. [8] in the systematic review study.

Motivated by Pokushalov et al.’s findings, which used the Flashbacks to guide the ablation strategy once the patients had an already failed ablation, a study using the Flashback to determine the optimum ablation strategy before a first failed ablation attempt was designed. However, the visual annotation of the triggers in the Flashbacks, especially in large populations of patients is far from being a trivial matter. Therefore, an automatic classification of AF triggers is needed.

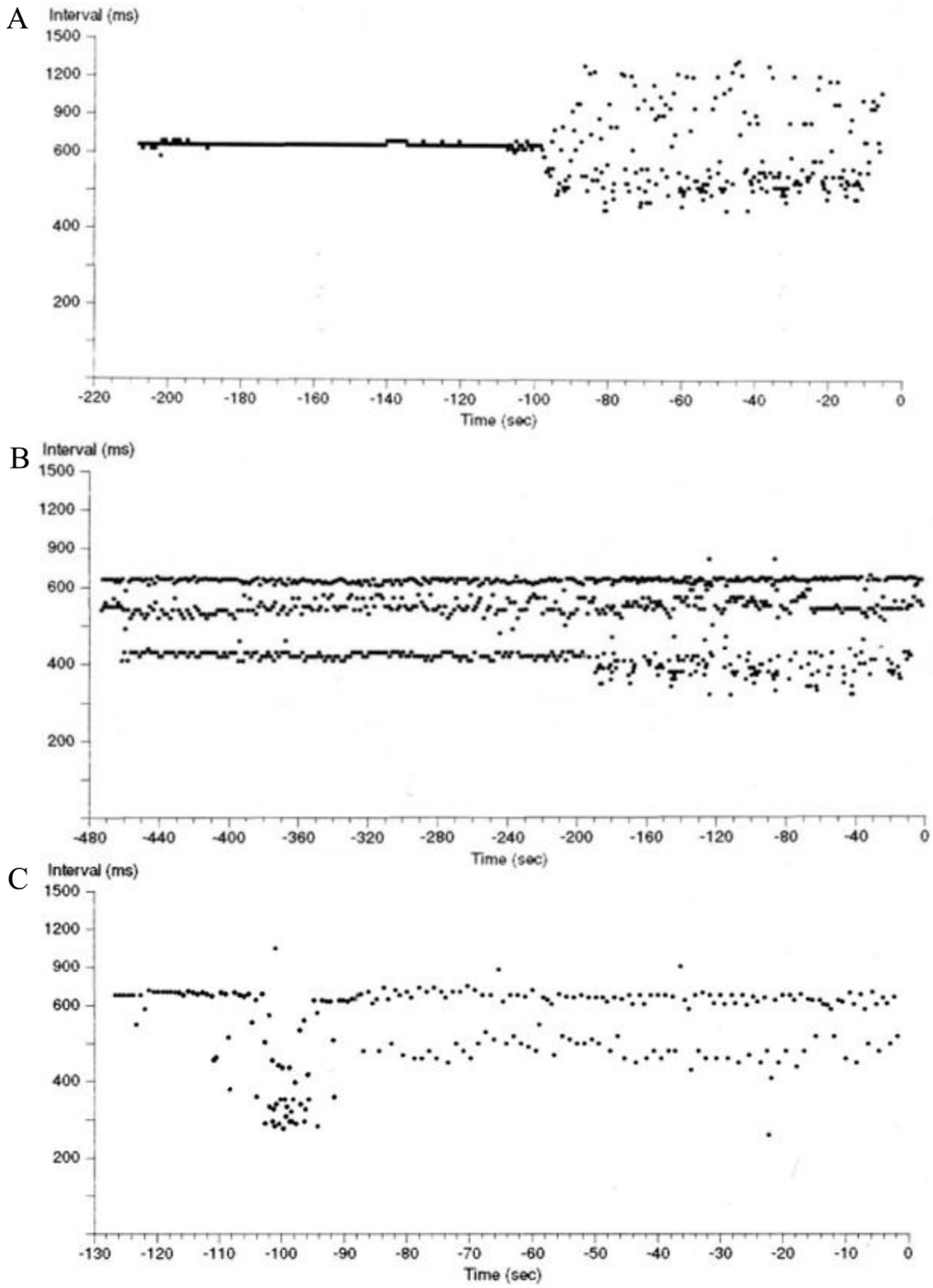

Figure 3.1 Examples of onset mechanisms: (A) sudden onset of AF from SR without a specific trigger; (B) AF triggered by atrial flutter; and (C) AF triggered by premature atrial contractions. From [17].

Supervised classification methods rely on having a sufficiently representative set of training data which is to be manually selected and annotated, which in turn is expensive and time-consuming to obtain, and may introduce bias. Alternatively, unsupervised learning classification methods such as k-means can be applied without the need for training examples (as the centroids of each category are obtained after repeated optimisation starting from randomly selected points) and are a viable solution when dealing with large, unstructured data repositories [121] (hence, the preferred solution for our study.)

The aim of this study was to develop an automatic unsupervised classifier of AF triggers through Heart Rate Variability (HRV) features extracted from the Flashback, as it consists solely of a trend of beats, stored by the Reveal LINQ.

3.2. Materials

Flashbacks (around 500 beats preceding an AF episode) were extracted from the ICM (Reveal LINQ, Medtronic Inc) in a cohort of the 132 patients ($56 \pm 10\ years$) with available Flashback data as introduced in Chapter 2. In total, 528 Flashbacks were obtained ($4\ \pm\ 2\ Flashbacks/patient$, $488\ \pm\ 29\ beats\ long$). The histogram in Figure 3.2 illustrates the distribution of the duration of the Flashbacks considered in the study. In average, the Flashbacks had a duration of $6.7\ \pm\ 1.5$ minutes.

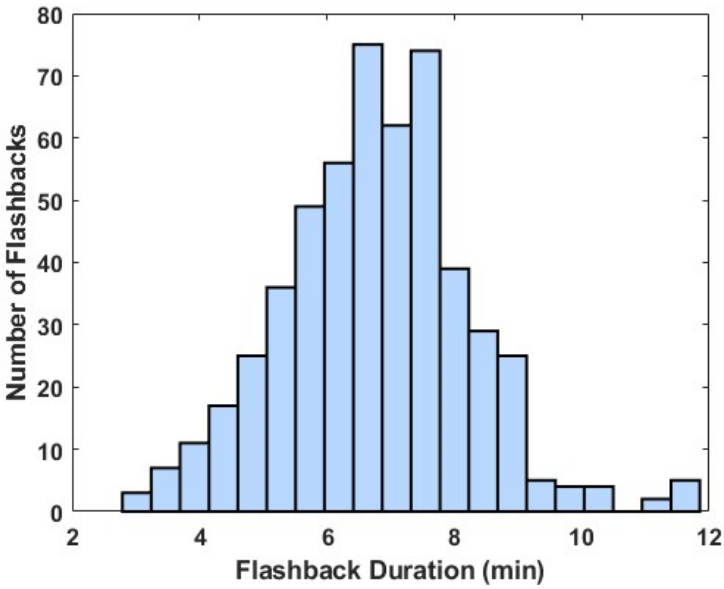

Figure 3.2. Duration in minutes of the Flashbacks extracted from the ICM.

3.3. Methods

3.3.1. Feature Extraction

Features describing variability and irregularity of the RR series were extracted from the Flashbacks. The first feature extracted was the mean of the RR intervals expressed in milliseconds. The percentage of interval differences (ΔRR) of successive RR intervals greater than x ms was also calculated (pNNx, with x = 50 and 20 ms). This metric is derived by computing the ratio between the amount of successive RR intervals, which have a difference greater than x ms, and the total amount of RR intervals. Although pNN50 for interval differences greater than 50 ms is generally used. In [122] it was concluded that using x ms values as low as 20 ms also showed significant discrimination between several normal and pathological conditions and so, pNN20 was also computed. The mean squared differences of successive RR intervals (RMSSD) expressed in milliseconds has been calculated using the expression:

$$RMSSD = \sqrt{\frac{\sum_{i=1}^{N-1}(RR_{i+1} - RR_i)^2}{N-1}} \tag{3.1}$$

where RR_i is the i-th RR interval, RR_{i+1} the successive interval, and N is the total number of RR intervals. The standard deviation of the RR intervals (SDNN) expressed in milliseconds was also computed as:

$$SDNN = \sqrt{\frac{\sum_{i=1}^{N}(RR_i - \overline{RR})^2}{N}} \tag{3.2}$$

where $\overline{RR}$ is the mean RR interval.

An estimation of the irregularity of the RR series was computed using the approximate entropy (ApEn) and the sample entropy (SampEn). The approximate entropy was computed as described in [123] and the sample entropy as described in [124]. In the implementation of the ApEn and SampEn, the input parameters (m,r) must be selected, where m is the length of the template (length of the window of the vectors that are to be compared in the calculation), and r is the noise rejection level (magnitude of noise which barely affects the calculation) [124]. In this study, those parameters were set to $m = 2$ and $r = 0.2 * \sigma$, where σ is the standard deviation as recommended in [124].

Three geometric features were also used and were those derived from the Poincaré Plot: geometric descriptors SD1 and SD2, and the ratio between them (SD1SD2ratio). The Poincaré Plot is a commonly used geometric and non-linear method to assess the dynamics of HRV [125]. It represents the RR time series into a space where each pair of successive RR intervals (RR_i, RR_{i+1}) defines a point in the plot. The descriptors are then computed as:

$$SD1 = \sqrt{var\left(\frac{RR_i + RR_{i+1}}{\sqrt{2}}\right)} \tag{3.3}$$

were var represents the variance, and

$$SD2 = \sqrt{var\left(\frac{RR_i - RR_{i+1}}{\sqrt{2}}\right)} \tag{3.4}$$

where RR_i and RR_{i+1} are vectors defined as $RR_i = (RR_1, RR_2, \dots, RR_{N-1})$ and $RR_{i+1} = (RR_2, RR_3, \dots, RR_N)$ with N again being the total number of RR intervals. SD1 is associated with the standard deviation of the instantaneous (short-term) RR interval variability while SD2 with the standard deviation of the long-term RR interval variability [125]. The SD1SD2ratio was simply calculated by doing the ratio between SD1 and SD2.

3.3.2. Principal Component Analysis

Once the features were extracted, Principal Component Analysis (PCA) was carried out in order to reduce the dimensionality of the data and by doing so, reducing the computational cost of the unsupervised clustering method. PCA reduces the dimensionality of the data by generating new linear combinatorial features from the original features. It maps each example of the dataset present in a d dimensional space to a g dimensional subspace such that $g < d$. The new set of generated dimensions is referred to as the Principal Components (PC). Each PC represents the maximum variance without including the variance which has already been accounted for in all its preceding components. Subsequently, the maximum variance is covered by the first component while the rest of the components cover lesser values of variance. The PC can be represented as:

$$PC = a_1X_1 + a_2X_3 + \cdots a_dX_d \tag{3.5}$$

where PC are the principal components, X_j is the original feature with $j = [1, d]$, and a_j is the loading coefficient for X_j representing the contribution of the original feature to the principal components.

The z-score of the features was applied before the PCA [126]. The normalization of a feature is done by scaling the values in such manner that they fall into a specific range which ensures that features with lower ranges are not outweighed by those with initially larger ranges.

The Z-score normalization for a feature X_j, is based on zero mean and normalized standard deviation (SD):

$$X_j' = \frac{(X_j - \bar{X})}{\sigma_{X_j}} \tag{3.6}$$

where X_j' is the z-scored version of X_j, $\bar{X}$ is the mean of the feature-set $\boldsymbol{X}$, and σ_{X_j} is the standard deviation of X_j.

In this manner, the PCs for the study were represented as:

$$PC = a_1 X'_1 + a_2 X'_3 + \cdots a_d X'_d \tag{3.7}$$

The criteria to choose the number of Principal Components selected was to have an explained variance higher than 0.95, i.e., the PCs contain at least 95% of the information. In addition, loading coefficients, also known as principal component coefficient will be evaluated and only features with a coefficient higher than 0.3 will be considered [127].

3.3.3. Clustering Method

The k-means algorithm was used to perform unsupervised clustering. It aims to partition n observations into k defined clusters, each cluster containing at least one observation and each observation being part of one cluster only.

The clustering is obtained by minimizing the sum, over all clusters, of the within-cluster sums of point-to-cluster-centroid distances. Given a set of randomly initialized k means (centroids) $m_1^{(1)}, \ldots, m_k^{(1)}$, the algorithm alternates between two steps: the assignment and the update step.

In the assignment step every t iteration, each data point x_p is assigned to the i-th cluster $K_i^{(t)}$ with the nearest centroid, i.e., that with the least distance, even if it could be assigned to two or more of them.

Mathematically, x_p is assigned to the cluster $K_i^{(t)}$ which satisfies:

$$K_i^{(t)} = \underset{k}{\operatorname{argmin}}\{d(m_i^{(t)}, x_p)\}, \tag{3.8}$$

for each of the i centroids.

In this study, the distance computed between a given data point x_p and the centroid $m_i^{(t)}$ of their assigned cluster $K_i^{(t)}$ was the Euclidian distance defined as:

$$d(m_i^{(t)}, x_p)^2 = \left(x_{m_i^{(t)}} - x_{x_p}\right)\left(y_{m_i^{(t)}} - y_{x_p}\right)', \tag{3.9}$$

where $(x_{m_i^{(t)}}, y_{m_i^{(t)}})$ and $\left(x_{x_p}, y_{x_p}\right)$ are the coordinates of the centroid and the data point respectively.

In the update step, the centroids are recalculated for the observations assigned in each cluster:

$$m_i^{t+1} = \frac{1}{\left|K_i^{(t)}\right|} \sum_{x_p \in K_i^{(t)}} x_p \tag{3.10}$$

where $\left|K_i^{(t)}\right|$ is the number of points belonging to cluster $K_i^{(t)}$.

The assignment and update steps are repeated until the cluster assignments do not change, or the maximum number of iterations is reached.

The optimum number of clusters was determined using the silhouette coefficient. This coefficient helps define the number of clusters by evaluating how close each point of a given cluster is to the points assigned to the neighbouring clusters [128]. The silhouette coefficient ranges between -1 and 1 with values close to 1 indicating that the points are very distant from neighbouring clusters and therefore, a good clustering.

Assuming the data has been already clustered into k clusters, for data point $x_p \in K_P$ (data point x_p in cluster K_P), let the average inter-cluster distance, i.e., the average distance between each point x_p within a cluster be:

$$a(x_p) = \frac{1}{|K_P| - 1} \sum_{x_j \in K_P,\, x_p \neq x_j} d(x_p, x_j) \tag{3.11}$$

where $|K_P|$ is the number of points belonging to the cluster K_P, and $d(x_p, x_j)$ is the distance between data points x_p and x_j in the cluster K_P. $a(x_p)$ can be interpreted as a measure of how well x_p is assigned to its cluster (the smaller the value, the better the assignment).

Given another cluster K_J (where $K_J \neq K_P$), the mean dissimilarity of point x_p to K_J is defined for each data point $x_p \in K_P$ as:

$$b(x_p) = \min_{J \neq P} \frac{1}{|K_J|} \sum_{x_j \in K_J} d(x_p, x_j) \tag{3.12}$$

to be the smallest mean distance of x_p to all the points in any other clusters, of which x_p is not a member. The silhouette coefficient is then defined for each point x_p as:

$$s(x_p) = \frac{b(x_p) - a(x_p)}{\max\{a(x_p), b(x_p)\}}, \qquad if\ |K_P| > 1 \tag{3.13}$$

For cluster size $|K_P| = 1$, the average inter-cluster distance $a(x_p)$ is not clearly defined, in which case:

$$s(x_p) = 0, \qquad if\ |K_P| = 1. \tag{3.14}$$

This choice is arbitrary, but neutral in the sense that it is at the midpoint of the bounds -1 and 1, and it is the convention when calculating the silhouette coefficient.

For a silhouette coefficient close to 1, i.e., the data is appropriately clustered, we require $a(x_p) \ll b(x_p)$. This is due the fact that $a(x_p)$ measures how dissimilar x_p is from its own cluster, hence a small value means it is well matched, and a large $b(x_p)$ implies the x_p is badly matched to the clusters it's not a member of.

3.3.4. Statistical Analysis

Once the features were extracted and the clustering was performed, the one-way Analysis of Variance Analysis (ANOVA) was computed for the features in the different clusters. The null hypothesis H_0 was defined as: the average value of the dependent variable is the same for all the clusters. The unpaired Student's t-test with Holm's

correction was used to evaluate the one-to-one differences between the features of the different clusters [129].

The feature extraction, PCA, clustering and statistical analysis were conducted using Matlab R2019b (The Mathworks Inc., Natick, Massachusetts).

3.4. Results

The PCA showed that 2 PCs were enough to explain 95.1% of the total variance (PC1: 58.7% and PC2: 36.4%). The k-means algorithm was evaluated for $k \in [2, 20]$ and the optimum number of clusters was chosen as the number of clusters which maximized the silhouette coefficient as shown in Figure 3.3. In this study, the optimum number of clusters selected was 5 (Silhouette coefficient = 0.568).

Figure 3.4 shows the result of the clustering.

The distribution of the observations was the following: Cluster 1 had 31% of the observations, Cluster 2: 4%, Cluster 3: 15%, Cluster 4: 35% and Cluster 5: 15%.

To remove the effect of outliers, clusters containing less than 5% of the total observations were excluded from further analysis hence, Cluster 2 was discarded.

A representative Flashback for each cluster was visually selected and shown in Figure 3.5.

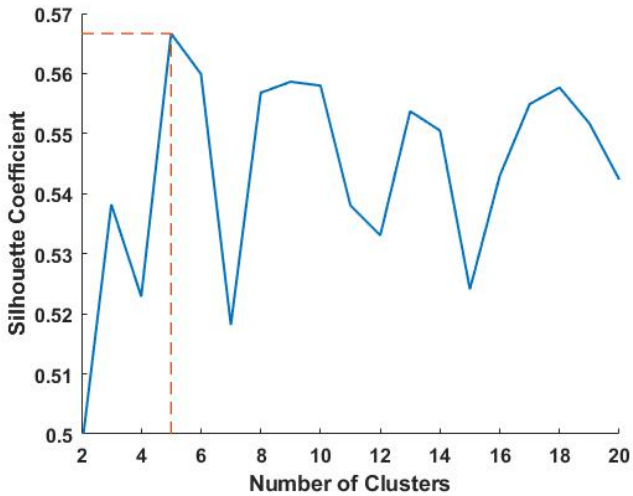

Figure 3.3. Silhouette coefficient for different number of clusters with the maximum value marked.

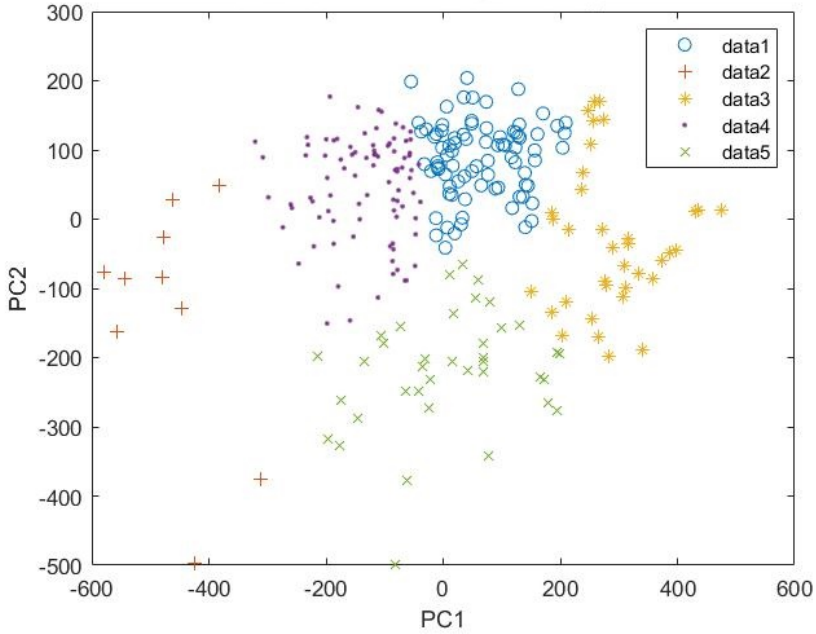

Figure 3.4 k-means clustering for PC1 and PC2 into 5 clusters.

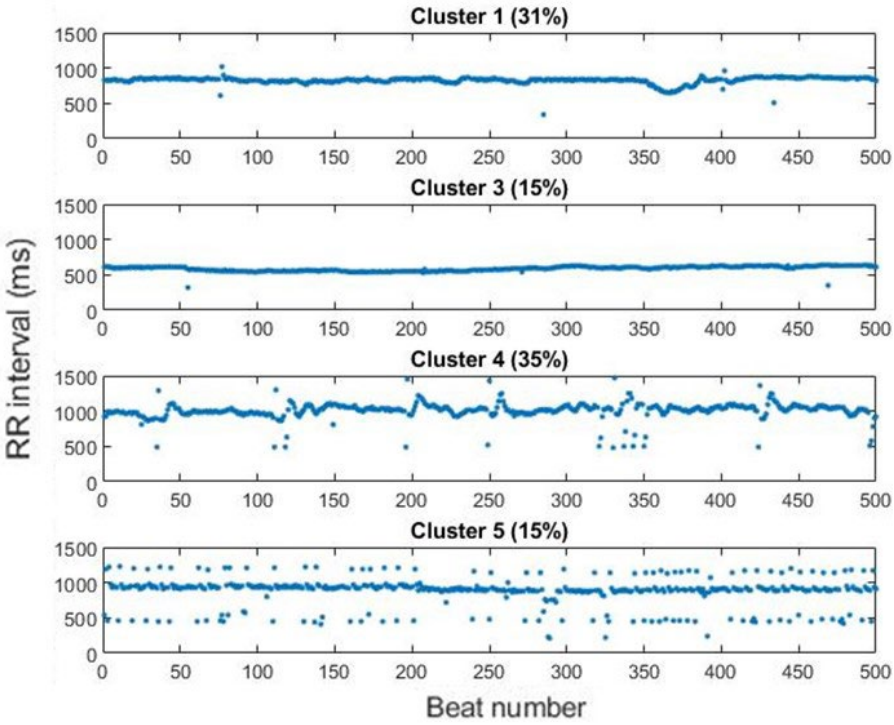

Figure 3.5 Example of the representative flashback for the four selected clusters.

Cluster 1 and Cluster 4 contain a high percentage of the patterns analysed (>30% each) and both have a relatively stable RR interval around 800-1000 ms. Cluster 3 and Cluster 5 contain fewer patterns and while Cluster 3 shows a lower average RR interval around 600 ms, Cluster 5 has a higher RR interval around 100 ms with a high number of ectopic beats.

A further analysis on the features contributing to the PCs was made. Table 3.1 summarizes the loading coefficients for the first 2 principal components.

Table 3.1 Loading coefficients for first 2 principal components (in bold the most relevant parameters)

Features	Loading Coefficients	
	PC1	**PC2**
Mean	**0.982**	-0.162
pNN50	-0.015	0.164
pNN20	0.003	0.144
RMSSD	0.069	**0.619**
SDNN	0.100	**0.423**
TINN	< -0.001	< 0.001
ApEn	-0.001	< 0.001
SamEn	-0.001	0.001
SD1	0.049	**0.438**
SD2	0.132	**0.415**
SD1SD2ratio	< -0.001	0.001

Those features with loading coefficients higher than 0.3 were regarded as contributive. Therefore, for PC1 the feature selected was only the Mean while for PC2, the features selected were RMSSD, SDNN, SD1 and SD2. The rest of the analysis focused on these 5 contributive features.

While the mean RR is the predominant contributor to PC1, the rest of the contributive features have a similar contribution to PC2.

The relationship between the contribute features was also explored and the correlation between them is shown in Table 3.2.

Table 3.2. Correlation between contributive features

Pearson Correlation	Mean	RMSSD	SDNN	SD1	SD2
Mean	1.00				
RMSSD	0.02	1.00			
SDNN	0.15*	0.88*	1.00		
SD1	0.02	1.00*	0.88*	1.00	
SD2	0.21*	0.71*	0.96*	0.71*	1.00

*: pvalue<0.0001

The mean RR, the main contributive feature of PC1, is not strongly correlated with the rest of the contributive features. Looking at the contributive featues for PC2, RMSSD is identical to the non-linear metric SD1, and is moderately correlated with SDNN $(0.88, p < 0.0001)$ and with SD2 $(0.71, p < 0.0001)$. In a similar manner, SDNN is also moderately correlated with both SD1 $(0.88, p < 0.0001)$ while strongly correlated with SD2 $(0.96, p < 0.0001)$. SD1 and SD2 show moderate correlation between them $(0.71, p < 0.0001)$.

Figure 3.6 shows the distribution of the contributive features in each cluster.

The statistical analysis showed that the overall null hypothesis H_0 for every feature was rejected according to the one-way ANOVA $(p - value < 0.05)$. When computing the unpaired Student's t-test with Holm's correction for one-to-one comparison between the different features in the different clusters, features RMSSD (B) and SD1 (C) were statistically significant for every cluster. However, Mean RR (A), SD2 (D) and SDNN (E) were not: Clusters 1 and 4 for the Mean, and Clusters 2 and 3 for SD2 and SDNN had non-significant differences and the null hypothesis H_0 wasn't rejected.

3.5. Discussion

The use of long term ICM devices with robust AF detection will increase our understanding of AF triggers and its progression, and aid clinicians with AF management and treatment strategies.

Pokushalov et al. [17] showed an improvement of the success rate, reaching 89%, in a second ablation procedure in patients with a specific AF trigger onset. The study

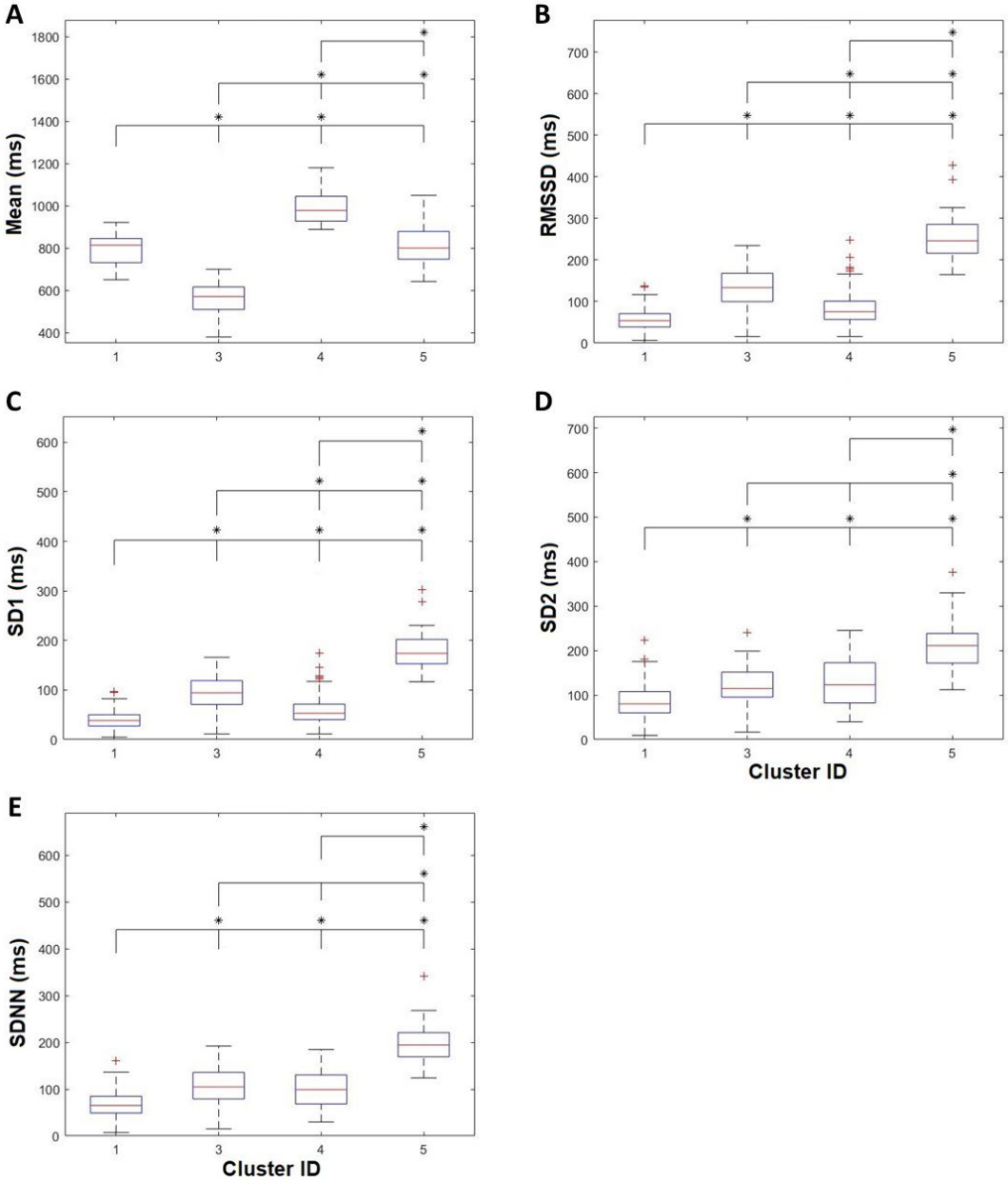

Figure 3.6 Boxplots of (A) Mean RR, (B) RMSSD, (C-D) Poincare descriptors SD1 and SD2, and (E) SDNN distribution in the different clusters. For every feature, the null hypothesis H_0 was rejected as p-value for ANOVA was < 0.05. (*) shows statistically significant differences between the different features in the different clusters according to one-to-one unpaired Student's t-test with Holm's correction.

defined 2 groups which the patients were randomly distributed to, those with no AF trigger study before second AF ablation and those which were treated in accordance with the onset mechanism. 3 different treatment possibilities were adjudicated to the patients based on their trigger. If AF started suddenly, and was not preceded by any other tigger, i.e., patients with spontaneous AF, no reablation was performed and the patients continued with AAD. For those patients where the AF onset was triggered by atrial tachycardia (AT) or atrial flutter, reablation of the supraventricular arrhythmias was performed. Lastly, if PACs triggered the AF, the reablation strategy consisted of PVI. The patients with AF triggered, either by AT, atrial flutter or PAC, which had a second ablation had success rates of 89%. Conversely, those patients with sudden onset which continued with AAD, had 69% of success in AF freedom $(p = 0.003)$ and those patients which were ablated without considering their onset mechanisms only had a success rate of 8% $(p < 0.0001)$. These results address the need of detecting the onset of AF episodes which may provide crucial information to determine the optimal action to take.

Motivated by these findings but considering the drawbacks of manual annotation of AF triggers in larger databases needed to provide reliable supervised classification algorithms, this study proposed an automatic unsupervised classifier of AF triggers through Heart Rate Variability (HRV) features extracted from the Flashback of a continuously monitored cohort. To the best of our knowledge, this is the first study to attempt the classification (unsupervised or otherwise) of AF triggers extracted from a cohort of patients implanted with an ICM.

In this study the Flashbacks, i.e., the 500 beats preceding an AF episode, were studied. From the Flashbacks, HRV parameters were computed and after PCA, unsupervised clustering was performed. Only 2 PCs were enough to explain more than 95% of the total variance. The most important features, i.e., those with loading coefficients > 0.3, were the mean of the RR intervals, features related to the variability (RMSSD and SDNN) and Poincaré descriptors SD1 and SD2.

The relationship between the Poincaré descriptors and the RMSSD and SDNN has been previously described in the literature [125,130]. The RMSSD is identical to SD1 $(1.00, p < 0.0001)$ as they both reflect short-term HRV [131]. Furthermore, the mathematical relationship between them is:

$$SD1 = \frac{1}{\sqrt{2}} * RMSSD \tag{3.15}$$

which can be derived from Equation (3.1) and (3.3).

In addition, SDNN has shown very strong correlation with SD2 $(0.96, p < 0.0001)$. This has also been reported previously in the literature [132]. Even though the features which contributed to PC2 are highly correlated with each other, there is no correlation between those features and the mean RR interval which is the predominant contributive feature for PC1. For this reason, the use of these two principal components is needed to fully explain the variation of our data.

Although five clusters were the optimal selected number, only 4 had more than 5% of the observations and were analysed. Cluster 1 shows normal rhythm with a mean RR interval around 800 ms (75 beats-per-minute) and very few Premature Atrial Contractions (PACs) so this could be an example of spontaneous AF (no trigger). Cluster 3 has a very stable rhythm with mean RR interval lower than 600 ms (over 100 beats-per-minute) so the AF trigger could be atrial tachycardia. Cluster 4 is similar to Cluster 1 but has a higher number of PACs which could indicate that the PACs caused the AF. Lastly, Cluster 5 being a highly unstable rhythm seems to depict atrial flutter as a trigger for AF.

One of the main limitations of this study is the Flashback length. However, while the conventional minimum recording for variability features such as SDNN and RMSSD is 5 minutes [133], researchers have proposed short-term periods from 60s to 240s in the case of SDNN and even shorter periods of 10s and 30s for RMSSD [134,135]. In any case, 88% of the Flashbacks included in the analysis are longer that 5 minutes.

Another limiting factor is the fact that inference of useful clinical information from unsupervised classification of patters has relative reliability. For this reason, future studies including visual inspection and annotation of the Trigger Patterns with their corresponding ECG signal are planned with the support of electrophysiologists to validate the classification process.

Nonetheless, this study shows that there are indeed differences between different types of clusters albeit there is still a need of a clinical validation of the classification. Being the goal of a future study to use the existing differences to discriminate between different treatment strategies or patients, the trigger classification obtained as a black-box process from unsupervised clustering is still clinically relevant.

3.6. Conclusion

Seeing the importance in upcoming years of the understanding of the triggers of AF, this study extracted and analysed classical HRV features of the 500 beats preceding

the onset of AF with the goal of doing an unsupervised clustering of the possible AF triggers. Although validation from a group of electrophysiologists is still needed and it's currently ongoing, the study showed 4 distinct trigger patterns found with the algorithm which could be classified as Spontaneous AF, PAC, Atrial Tachycardia and Atrial Flutter and between which, the differences in their HRV features were statistically significant.

Chapter 4 Atrial Fibrillatory Rate

The publications related to this chapter are:

Saiz-Vivo J, Abdollahpur M, Mainardi LT, Corino VDA, De Melis M and Sandberg F. **Atrial Fibrillatory Rate Characterization Extracted from Implanted Cardiac Monitor Data**, *2021 Computing in Cardiology (CinC)*, 2021, pp. 1-4, doi: 10.23919/CinC53138.2021.9662826.

Saiz-Vivo J, Abdollahpur M, Mainardi LT, Corino VDA, De Melis M, Hatala R and Sandberg F. **Heart Rate Characteristic Based Modelling of Atrial Fibrillatory Rate using Implanted Cardiac Monitor Data**. Submitted to Physiological Measurements. Under review.

4.1. Motivation

The underlying mechanisms of AF are still under investigation and appropriate patient selection for treatment still remains a challenge [136,137]. The opportunity to find additional ways of characterizing atrial electromechanical and anatomical properties and ways of predicting subsequent outcome after therapeutic intervention would favour timely therapy selection. More specifically, AF is related to a compromised atrial function caused by a fast and irregular atrial depolarization which can be characterized from the f-waves in the ECG. There have been many parameters introduced in the literature to characterize f-waves including their amplitude, frequency, morphology [138,139], and atrial organization [140].

The f-wave frequency, often referred to as the atrial fibrillatory rate (AFR) is an AF characteristic which has been subject to considerable clinical attention and has been shown to be a useful tool for monitoring drug effects [141] as well as predict outcomes from clinical procedures such as successful AF cardioversion [142] and early AF recurrence [143].

The correlation of AFR and several well-known HRV features describing the variability and irregularity of RR intervals during AF showed that while it seemed that variability parameters were independent from AFR, the irregularity parameters were significantly correlated with AFR [144]. However, the extrapolation of their findings for all clinical types of AF remains to be determined as the population used in the study included only patients with underlying congestive heart failure. In addition, the analysis didn't account for variations on AFR due to circadian cycles, episode duration or previous ablations.

Circadian variations in the AF frequency within a 24-hour period have been studied using Holter recordings in pursuit of understanding the underlying mechanisms of AF. It was concluded that AFR was significantly lower during night-time than during daytime [145–147]. These studies, however, have a drawback as AFR was computed from sparce measurements with several hours in between estimates. In addition, in one of the studies, two different sets of patients were identified: one which showed an increase (minority) while the other showed a decrease (majority) in nocturnal AFR [145]. A later study used more advanced signal processing techniques and obtained a more robust AF frequency estimate [148]. This study found that circadian variations were present in most of the patients with long-standing persistent AF analysed (13/18). However, both studies have the drawback of having their insight on atrial electrophysiological characteristics during AF constrained to 24-hout long Holter registrations and limited datasets of up to 30 patients. In addition, these studies were all based on persistent and chronic AF patients.

Another study has shown a positive correlation between episode duration and AFR ($R = 0.53, p < 0.05$) [149]. However, this study was conducted in a small dataset with only 31 episodes from 11 paroxysmal AF patients.

The long monitoring periods spanning several months, thus including several episodes per patient, provided by ICMs allow an analysis of the joint effects of HRV derived features and circadian variation, episode duration and previous ablations on AFR.

The estimation of AFR from RR series data would enable wearable based assessment of AFR, e.g., wristband PPG, which would lead to a better characterization of the patient's condition. The aim of this study is to model variations in AFR using RR series features, by correcting for the effect of time of the day of episode onset, episode duration and previous ablations on AFR, in a cohort of AF patients continuously monitored with an ICM. In a previous study regarding AFR and HRV, the analysis was conducted only on patients with underlying congestive heart failure and didn't account for the presence of confounding factors [144]. We used a simple fixed-effect (FE) modelling approach using HRV features and compared it to a more complex mixed-effect (ME) modelling approach to study both the population and patient specific effects of RR series in AFR and another ME modelling approach that allowed correction for the effect of episode duration, previous ablations, and possible circadian variations. In addition, ME modelling will account for the heterogeneity within AF patients.

4.2. Materials

The studied population consisted of a subset of the cohorts of patients presented in Chapter 2. The clinical baseline characteristics of the analysed patients are shown in Table 4.1.

The devices used in the Usability and the Slovakia studies were the Reveal LINQ and Reveal XT (Medtronic Inc, Minneapolis, MN), respectively which were implanted within the fourth intercostal space (V2-V3 electrode orientation) near the apex of the heart. The feasibility of extracting atrial activation from ICM data has been previously explored [150]. Due to memory restrictions, the devices store a single-lead ECG signal of the first 2 minutes of the AF episode detected as well as the ventricular sense, i.e., the positions of the R-peaks. In addition, the devices store the detected episode onset date and time and the total duration of the episode.

Table 4.1Baseline and clinical data of the study population (n = 99).

Patient Characteristics	**Enrolled subjects (N=99)**
Age, years (mean ± SD)	57 ± 12
Coronary Risk Profile	
Paroxysmal AF	73 (74%)
Hypertension	40 (40%)
Diabetes	13 (13%)
Coronary Artery Disease	5 (5%)
Stroke	3 (3%)
Previous Ablation	19 (19%)

Values are given as no. (%) unless otherwise indicated
AF: atrial fibrillation
SD: Standard deviation

This unique database offers the advantage of long monitoring periods and a complete monitorization of patients suffering AF which enables studies way beyond the scope of Holter monitoring.

The 99 patients included in the study had the ICM implanted and were followed-up for 9.2 (0.2-24.3) months as median (min-max). Figure 4.1 illustrates the monitoring period of the patients where 0 represents the ablation time. In this manner, the monitoring days pre-ablation (green) are lower than 0 while the monitoring days after ablation (white for the 3-months blanking period and orange for the rest of the monitoring) are greater than 0. The ablation procedure was performed 5.8 (1.0-14.4) months after the implant. The ablation procedures were either pulmonary vein isolation (PVI) only (76 patients, 77%) or PVI plus extra lesions, which included roof and mitral lines, and ablation of complex fractionated atrial electrograms (23 patients, 23%). AF recurrence was defined as an AF episode detected by the ICM after a 3-month blanking period following catheter ablation and only those episodes outside the blanking period were considered in the analysis.

The blanking period is based on reports describing how early recurrences could be caused by post-ablation inflammation or short-term autonomic imbalance rather than ablation failure [6]. In the analysed cohort, 31 (31%) had AF recurrence, 38 (38%) had no AF recurrence, and 30 patients (30%) left the study before the ending of the 3-months blanking period so there is no available information of their recurrence status. To evaluate the circadian variations of AFR, the episodes occurring during the full monitoring period, except the 3-months blanking period, of the 99 patients included in the study were considered.

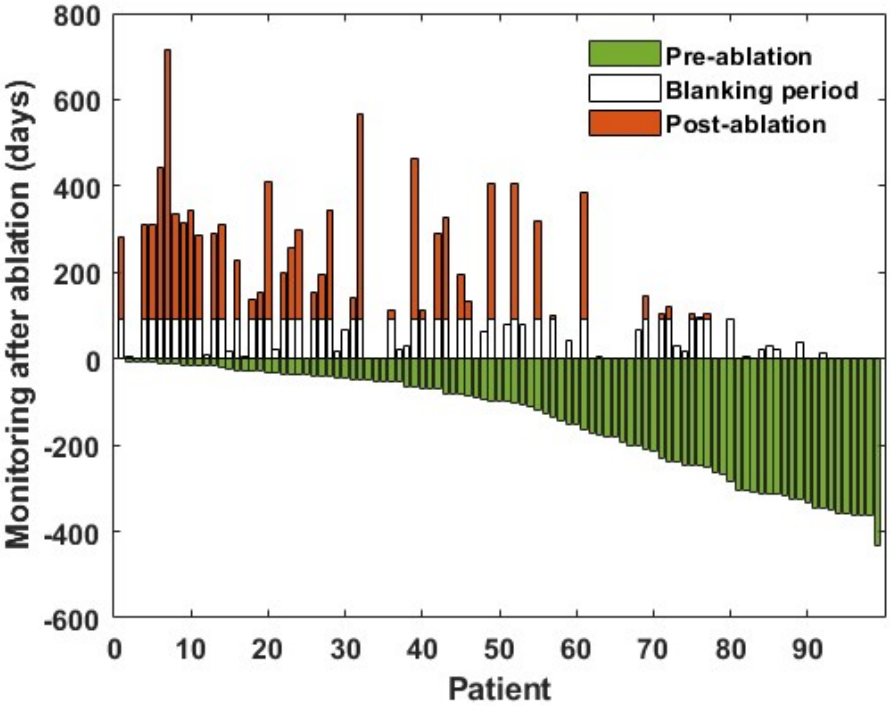

Figure 4.1. Monitoring days of the patients included in the analysis with the baseline being the ablation time. The monitoring time is divided into 3 timeframes: pre-ablation (green), during 3-months blanking period (white) and post-ablation (orange). For reasons of clarity, the patients were sorted based on their pre-ablation monitoring time.

4.3. Methods

4.3.1. Atrial fibrillatory rate

The atrial activity, from which the AFR is computed, is extracted from ECG signals using a QRST cancellation technique included in Cardiolund ECG parser software (www.cardiolund.com). The software removes the ventricular activity form the ECG, producing a residual ECG signal containing the atrial activity.

Once the atrial activity ($x(n)$) having a length of N samples is obtained, a harmonic f-wave model [151] is used to estimate the local f-wave frequency i.e. the AFR. In this model, the f-waves are modelled by a complex signal $s(n; \boldsymbol{\theta})$, defined as the sum of 2 harmonically related, complex exponentials with fundamental frequency f,

$$s(n;\boldsymbol{\theta}) = \sum_{m=1}^{2} A_m e^{j\left(2\pi\frac{f}{f_s}mn + \phi_m\right)}, \tag{4.1}$$

$$\boldsymbol{\theta} = [f \;\; A_1 \;\; \phi_1 \;\; A_2 \;\; \phi_2]^T, \tag{4.2}$$

where A_m and ϕ_m define the amplitude and phase, respectively, of the m-th exponential (first and second), f_s is the sampling frequency and $\boldsymbol{\theta}$, the parameter vector.

The complex values analytic representation $\boldsymbol{x_a}(n)$ of the observed f-wave signal $\boldsymbol{x}(n)$, is assumed to be composed of $s(n,\boldsymbol{\theta})$ and white, complex Gaussian noise $\boldsymbol{e}$,

$$\boldsymbol{x_a}(n) = s(n,\boldsymbol{\theta}) + \boldsymbol{e} = \boldsymbol{Z}(n,\omega_0)\,\boldsymbol{a}(\boldsymbol{\theta}) + \boldsymbol{e}, \tag{4.3}$$

where $\omega_0 = 2\pi\frac{f}{f_s}$, $\boldsymbol{a}(\boldsymbol{\theta})$ is a 2×1 vector containing the amplitude and phase information:

$$\boldsymbol{a}(\boldsymbol{\theta}) = \left[A_1 e^{j\phi_1} \;\; A_2 e^{j\phi_2}\right]^T, \tag{4.4}$$

and $\boldsymbol{Z}(n,\omega_0)$ is an $N \times 2$ Vandermonde matrix defined as:

$$\boldsymbol{Z}(n,\omega_0) = \begin{bmatrix} 1 & 1 \\ e^{j\omega_0} & e^{j2\omega_0} \\ \vdots & \vdots \\ e^{j\omega_0 n} & e^{j\omega_0 n} \\ \vdots & \vdots \\ e^{j\omega_0(N-1)} & e^{j2\omega_0(N-1)} \end{bmatrix}. \tag{4.5}$$

The model is evaluated in 5-s windows by locally fitting the model in K 0.5-s overlapping sub-segments $x_{a,k}, k = 1, \dots, K$ and estimating $\widehat{\boldsymbol{\theta}}$ using a maximum likelihood approach. For each subsegment, the local frequency estimate $\widehat{\omega}_{0,k}$ is determined by:

$$\widehat{\omega}_{0,k} = arg\min\left\|\boldsymbol{x}_{a,k} - \boldsymbol{Z}(\boldsymbol{Z}^H\boldsymbol{Z})^{-1}\boldsymbol{Z}^H\boldsymbol{x}_{a,k}\right\|^2, \tag{4.6}$$

where $Z \equiv Z(\omega_{0,k})$. The local frequency estimates are then averaged over the 5-s windows and the AFR of the segment is determined as:

$$\hat{f} = \sum_{k=1}^{K} \frac{\widehat{\omega}_{0,k} f_s}{2\pi K}, \tag{4.7}$$

The model's fit is evaluated using the model error $\hat{e}(n) = x_a(n) - s(n; \hat{\boldsymbol{\theta}})$ to estimate the signal quality index (SQI):

$$SQI = 1 - \frac{\sigma_{\hat{e}}}{\sigma_{x_a}}, \tag{4.8}$$

where $\sigma_{\hat{e}}$ and σ_{x_a} are the standard deviation of the model error $\hat{e}(n)$ and $x_a(n)$. The SQI is confined between [0,1] with larger values associated to a better fit. A fixed threshold is used to indicate whether f-waves have sufficient quality for the analysis. For this study, the SQI was estimated every 5-second windows and the SQI threshold which determined the usable segments was set to 0.30 as suggested by [151]. Figure 4.2 shows an example of the f-wave extraction process for the AFR estimation illustrating the ECG obtained from the ICM, the atrial activity signal $x(n)$ after QRST cancellation, the signal quality index, and estimated frequency $(\hat{f})$ and estimated f-wave signal $\left(s(n; \hat{\boldsymbol{\theta}})\right)$ with the segment with low SQI represented in light grey.

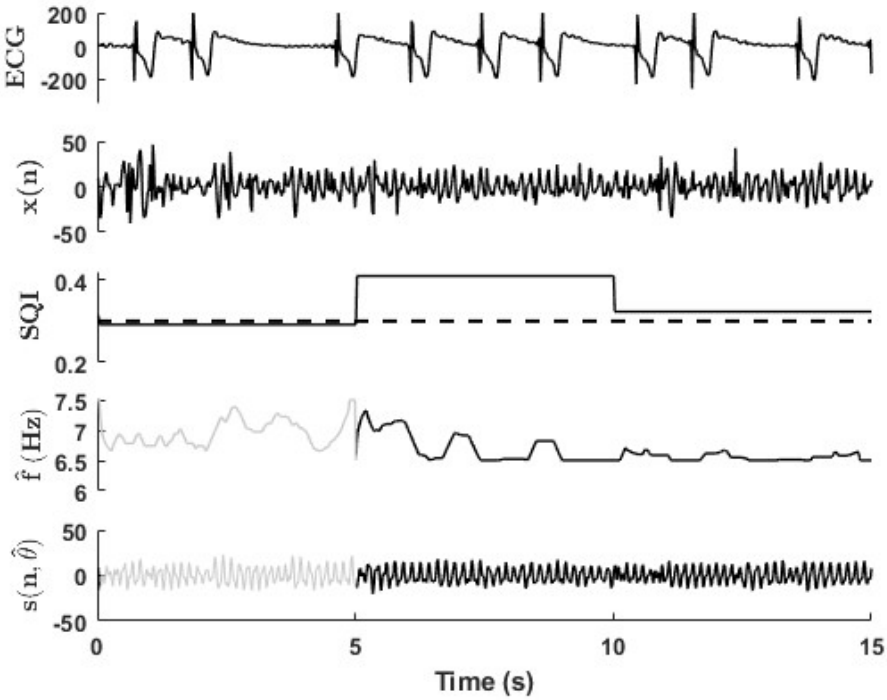

Figure 4.2. Illustration of f-wave extraction for AFR estimation. From top to bottom: ECG signal extracted from ICM, QRST-cancelled signal (x(n)), signal quality index (solid line) with threshold for acceptable signal quality (dashed line), estimated frequency $(\hat{\boldsymbol{f}})$ and estimated f-wave signal $(\boldsymbol{s}(\boldsymbol{n}; \hat{\boldsymbol{\theta}}))$ with signal segment with signal quality below the acceptable threshold marked as light grey.

For further details on the estimation of AFR and the SQI, the reader is referred to [151].

4.3.2. Population-based analysis

As a first approach to evaluate the relationship between AFR and the duration and onset time of the episode, the AFR of episodes extracted from the pre-ablation period were analysed.

In addition to the AFR, the relative AFR was also computed as:

$$relAFR\ (\%) = \frac{AFR}{AFR'} * 100, \tag{4.9}$$

where AFR' is the average AFR for each particular patient.

The episodes were then defined as short (episode duration < 20 minutes) or long (episode duration ≥ 20 minutes), and the onset time defined as night (00:00-06:00) or day (10:00-20:00) as derived from the continuous monitoring of the patients. For this first analysis of episode onset, any episodes outside the definition of night and day were not considered.

4.3.3. Modelling

Fixed-effect (FE) models are statistical models which only contain fixed effects. In contrast, mixed-effect (ME) models contain both fixed effects and random effects, and are useful when dealing with data involving multiple sources of random error such as repeated measures within subjects [152].

In general terms, for the mixed-effect model in this analysis, we consider N patients, with the index i representing the i-th patient ($1 \leq i \leq N$). In general terms, each patient has n_i measurements y_{ij}, with the index j representing the j-th episode ($1 \leq j \leq n_i$). P then is defined as the total number of episodes included in the analysis so that $P = \sum_1^N n_i$. There are M random effects considered, and the patient-specific random effect is represented by b_{im} ($1 \leq m \leq M$). The random effects provide inference on population level information which better accounts for correlated structures and uncertainty. In this thesis, the random effects constitute a set of variables that account for variations in the RR series and the effect of episode

duration, previous ablations, and circadian variations in AFR. The y_{ij} of each episode j in each patient i is assumed to follow a Gaussian distribution, specifically:

$$\left(AFR_{ij}\middle|b_{0i}, b_{1i}, \dots\ b_{Mi}\right) \sim N\left(\mu_{ij}\middle|b_{0i}, b_{1i}, \dots\ b_{Mi},\ \sigma^2\right), \tag{4.10}$$

where $\mu_{ij}|b_{0i}, b_{1i}, \dots\ b_{Mi}$ is the conditional expectation of the observations, in this case the AFR of each episode y_{ij}, given by random vector $\boldsymbol{b_i}$, containing the patient specific random effects $[b_{0i}, b_{1i}, \dots\ b_{Mi}]$, and σ^2 is the dispersion parameter of the distribution.

Linear ME models can be represented as:

$$\boldsymbol{y} = \boldsymbol{X\beta} + \boldsymbol{Zb} + \boldsymbol{e}, \tag{4.11}$$

where $\boldsymbol{y}$ is the set of y_{ij}, $\boldsymbol{X}$ is the design matrix for fixed effects, i.e., not dependent on the patient, $\boldsymbol{Z}$ is the design matrix for random effects, $\boldsymbol{\beta}$ is a vector of fixed effect parameters $[\beta_0, \beta_1, \dots, \beta_M\ ]$, **b** contains the N sets of $\boldsymbol{b_i}$, and $\boldsymbol{e}$ contains the random errors associated with the ij-th observation. The design matrix $\boldsymbol{X}$ $(P \times M + 1)$ is defined by:

$$\boldsymbol{X} = \left[\boldsymbol{x}_{\beta_0}\ \boldsymbol{x}_{\beta_1}\ \boldsymbol{x}_{\beta_2}\ \dots\ \boldsymbol{x}_{\beta_M}\right], \tag{4.12}$$

where $\boldsymbol{x}_{\beta_0}$ is a $P \times 1$ binary vector for patient independent intercept β_0, and $\left[\boldsymbol{x}_{\beta_1}, \boldsymbol{x}_{\beta_2}, \dots, \boldsymbol{x}_{\beta_M}\ \right]$ is a $P \times M$ matrix which contains the values for each of the M features describing the episodes considered in the analysis. Similarly, the design matrix for the random effects $\boldsymbol{Z}$ $(P \times N * (M + 1))$ is defined by:

$$\boldsymbol{Z} = \left[\boldsymbol{Z_{b_0}}\ \boldsymbol{Z_{b_1}}\ \boldsymbol{Z_{b_2}}\ \dots\ \boldsymbol{Z_{b_M}}\right], \tag{4.13}$$

where $\boldsymbol{Z_{b_0}}$ is the $P \times N$ binary matrix for $\boldsymbol{b_0}$, the patient specific intercept vector containing $[b_{01}, b_{02}, \dots, b_{0N}]$ intercepts, and $\left[\boldsymbol{Z_{b_1}}\ \boldsymbol{Z_{b_2}}\ \dots\ \boldsymbol{Z_{b_M}}\right]$ contains the values z_{bm}^{ij} which represent the value of feature m describing the j-th episode of the i-th patient.

The maximum pseudo likelihood method is employed for the parameter estimation. For ME models with observations $\boldsymbol{y}|\boldsymbol{b} \sim N(\boldsymbol{\mu}|\boldsymbol{b}, \boldsymbol{R})$ with $\boldsymbol{b} \sim N(\boldsymbol{0}, \boldsymbol{G})$, being $\boldsymbol{R}$ and $\boldsymbol{G}$, variance matrices for distributions of $\boldsymbol{y}|\boldsymbol{b}$ and $\boldsymbol{b}$ respectively, the log-likelihood equation can be written as [152]:

$$\ln \mathcal{L}(\boldsymbol{y}, \boldsymbol{b}) = -\left(\frac{1}{2}\right)(\boldsymbol{y} - \boldsymbol{X\beta} - \boldsymbol{Zb})'\boldsymbol{R^{-1}}(\boldsymbol{y} - \boldsymbol{X\beta} - \boldsymbol{Zb}) - \left(\frac{1}{2}\right)\boldsymbol{b}'\boldsymbol{G^{-1}}\boldsymbol{b}, \tag{4.14}$$

The estimator is then given by:

$$(\hat{\boldsymbol{y}}, \hat{\boldsymbol{b}}) = arg \max_{(\boldsymbol{y},\boldsymbol{b})} (\ln \mathcal{L}(\boldsymbol{y}, \boldsymbol{b})). \tag{4.15}$$

To solve this estimator, the derivatives $\partial \ell(\boldsymbol{y}, \boldsymbol{b})/\partial \boldsymbol{\beta}'$ and $\partial \ell(\boldsymbol{y}, \boldsymbol{b})/\partial \boldsymbol{b}'$ are set to zero, and the resulting set of equations are solved for $\boldsymbol{\beta}$ and $\boldsymbol{b}$. In the interest of clarity, $\ell(\boldsymbol{y}, \boldsymbol{b}) = \ln \mathcal{L}(\boldsymbol{y}, \boldsymbol{b})$.

The derivatives are, respectively:

$$\frac{\partial[\ell(\boldsymbol{y}, \boldsymbol{b})]}{\partial \boldsymbol{\beta}'} = \boldsymbol{X}'\boldsymbol{R}^{-1}\boldsymbol{y} - \boldsymbol{X}'\boldsymbol{R}^{-1}\boldsymbol{X}\boldsymbol{\beta} - \boldsymbol{Z}'\boldsymbol{R}^{-1}\boldsymbol{X}\boldsymbol{b}, \tag{4.16}$$

$$\frac{\partial[\ell(\boldsymbol{y}, \boldsymbol{b})]}{\partial \boldsymbol{b}'} = \boldsymbol{Z}'\boldsymbol{R}^{-1}\boldsymbol{y} - \boldsymbol{X}'\boldsymbol{R}^{-1}\boldsymbol{Z}\boldsymbol{\beta} - \boldsymbol{Z}'\boldsymbol{R}^{-1}\boldsymbol{Z}\boldsymbol{b} - \boldsymbol{G}^{-1}\boldsymbol{b}. \tag{4.17}$$

Setting equations (4.16) and (4.17) to zero yields the mixed model equation:

$$\begin{bmatrix} \boldsymbol{X}'\boldsymbol{R}^{-1}\boldsymbol{X} & \boldsymbol{X}'\boldsymbol{R}^{-1}\boldsymbol{Z} \\ \boldsymbol{Z}'\boldsymbol{R}^{-1}\boldsymbol{X} & \boldsymbol{Z}'\boldsymbol{R}^{-1}\boldsymbol{Z} + \boldsymbol{G}^{-1} \end{bmatrix} \begin{bmatrix} \boldsymbol{\beta} \\ \boldsymbol{b} \end{bmatrix} = \begin{bmatrix} \boldsymbol{X}'\boldsymbol{R}^{-1}\boldsymbol{y} \\ \boldsymbol{Z}'\boldsymbol{R}^{-1}\boldsymbol{y} \end{bmatrix}. \tag{4.18}$$

From Equation (4.18), the exact estimates of $\boldsymbol{\beta}$ and $\boldsymbol{b}$ can be obtained from a single calculation if components $\boldsymbol{G}$ and $\boldsymbol{R}$ are known. This is rarely the case, meaning that solving Equation (4.18) entails estimating $\boldsymbol{G}$ and $\boldsymbol{R}$ as well. To do so, solving the mixed model equations turns into an iterative process where starting values of $\boldsymbol{G}$ and $\boldsymbol{R}$ enable an initial solution of equation (4.18); the estimates of $\boldsymbol{\beta}$ and $\boldsymbol{b}$ are then used to update $\boldsymbol{G}$ and $\boldsymbol{R}$, and the process continues until convergence, defined as a difference on gradient of the objective function $< 10^{-6}$, or until the maximum number of iterations has been reached (10000).

Fixed-effect models can be represented as in Equation (4.14) but with the random effects coefficient **b** being equal to 0. Hence, the log-likelihood equation can be written as:

$$\ln \mathcal{L}(\boldsymbol{y}) = -\left(\frac{1}{2}\right)(\boldsymbol{y} - \boldsymbol{X}\boldsymbol{\beta})'\boldsymbol{R}^{-1}(\boldsymbol{y} - \boldsymbol{X}\boldsymbol{\beta}) \tag{4.19}$$

and the estimator is given by:

$$(\hat{\boldsymbol{y}}) = arg \max_{(\boldsymbol{y})} (\ln \mathcal{L}(\boldsymbol{y}))\,; \tag{4.20}$$

In this study, a linear FE model is used to evaluate the effects of automimic tone as quantified by RR series characteristics on AFR. In addition, the results obtained will be compared to two ME models which will evaluate both the fixed and random effects of circadian variations, previous ablations, episode duration and RR series

characteristics on AFR. Following the previous formulations, y_{ij} corresponds to the AFR_{ij} of the ij-th episode, $\boldsymbol{X}$ and $\boldsymbol{Z}$ contain the features comprised by time, number of ablations, duration of episode and HRV-derived features, and $\boldsymbol{\beta}$ and $\boldsymbol{b}$ contain the fixed and random effects of the model.

The FE and ME models (described below) were fitted and evaluated using Matlab R2022a (The Mathworks Inc., Natick, Massachusetts). The Akaike Information Criterion (AIC) [153] and the deviance residual, i.e., an index of model fit, where a model with a higher deviance provides a poorer model fit to the data than a model with a lower deviance [154], are used to select the model which fits best the dataset. In addition, to check the goodness of fit of the models, the fitted values of AFR are compared to the observed values of AFR, and the coefficients of determination (R^2) [155] are computed.

Fixed-effect model of AFR

From the ventricular sense of the AF episode stored in the ICM, HRV derived features are computed to represent the variability and irregularity of the episode. For this study, the parameters extracted were the mean RR intervals (mean interval between ventricular senses in milliseconds), the mean squared differences of successive RR intervals (RMSSD) expressed in milliseconds and calculated with Equation (3.1), and the sample entropy (SampEn). SampEn estimates the irregularity of the RR series and was computed as described in 3.3.1 [124].

The $\boldsymbol{FE}$ **model** assumes fixed (population) effects of RR mean, RR variability and RR irregularity on AFR (Mean RR, RMSSD and SampEn) hence an estimate of AFR ($\widehat{AFR}_{ij}$), for patient i and episode j, is given by:

$$\widehat{AFR}_{ij} = \beta_0 + \beta_1 \times MeanRR_{ij} + \beta_2 \times RMSSD_{ij} + \beta_3 \times SampEn_{ij}, \qquad (4.21)$$

where β_0 is the intercept estimate for the fixed effect. In a similar way, β_1, β_2 and $\beta_3$represent the fixed effects of the Mean RR, RMSSD and SampEn respectively, in Model FE.

Mixed-effect model of AFR

In order to account for the heterogeneity between patients, an ME model is used. The $\boldsymbol{ME}$ **model** assumes both the fixed and random effects of changes in RR series on AFR by introducing the patient-specific random effects to Equation (4.21):

$$\widehat{AFR}_{ij} = \beta_0 + b_{0i} + (\beta_1 + b_{1i}) \times MeanRR_{ij} + (\beta_2 + b_{2i}) \times RMSSD_{ij} + (\beta_3 + b_{3i}) \times SampEn_{ij}, \qquad (4.22)$$

where b_{0i} represents the intercept estimate for the patient-specific random effect, and b_{1i}, b_{2i} and b_{3i} represent the patient-specific random effect of Mean RR, RMSSD and SampEn respectively.

Mixed-effect model of AFR and correct for confounding factors

There are several variables that could affect AFR and need to be accounted for. In this study, the effect of circadian variations quantified by the episode onset time, the effect of multiple ablations, the effect of the long monitoring periods quantified by the time since ICM implant, and the effect of episode duration will be used to correct the ME model.

The circadian variations of AFR were modelled by considering the time of the day of the onset of each AF episode with sufficient SQI stored in the ICM. In order to relate AFR with circadian variation which has a cyclical nature, the time onset parameter was transformed into a sinusoid where -1 represents the middle of the day (12:00) and 1 represents the middle of the night (00:00) using the following expression:

$$Time = \cos\left(2\pi \frac{Time_{24h}}{24}\right), \tag{4.23}$$

where $Time_{24h}$ represents the 24-hour based AF onset and $Time$ the modified AF onset used in the analysis.

Furthermore, the patients of this cohort have undergone one or two ablation procedures. The *"nAblations"* parameter represents the number of ablations undergone by the patient at the time of the episode onset. This parameter can either be 0 for patients with no previous ablations in episodes occurring before their first ablation, 1 for patients after their first ablation or before their second ablation, or 2 for patients with a previously failed ablation and after their second ablation. This parameter will correct for the effect on AFR of episodes occurring pre- and post-ablation as well as for patients with previously failed ablation procedures with compromised atria.

In addition, the patients of this cohort have been followed up for long monitoring periods, so the feature *"DaysSinceImplant"* represents the period between the episode onset date and the date the patients were implanted with the ICM. This parameter will correct for the effects of the long monitoring periods on AFR; the change in *"DaysSinceImplant"* provides a common timescale for the episodes included in the analysis.

Lastly, the Reveal LINQ also stores the total duration of the episode in minutes: *"Duration"*.

The complete $\boldsymbol{ME'}$ **model** assumes the fixed and random effects of changes in the RR series, and corrects for circadian variation, number of ablations and episode duration:

$$\begin{aligned} A\hat{F}R_{ij} = \; & \beta'_0 + b'_{0i} + (\beta'_1 + b'_{1i}) \times MeanRR_{ij} + (\beta'_2 + b'_{2i}) \times RMSSD_{ij} \\ & + (\beta'_3 + b'_{3i}) \times SampEn_{ij} + (\beta'_4 + b'_{4i}) \times Time_{ij} \\ & + (\beta'_5 + b'_{5i}) \times nAblations_{ij} \\ & + (\beta'_6 + b'_{6i}) \times DaysSinceImplant_{ij} \\ & + (\beta'_7 + b'_{7i}) \times Duration_{ij}, \end{aligned} \tag{4.24}$$

where β'_4, β'_5, β'_6 and β'_7 represent the fixed effects of the circadian variations, number of ablations, period between implant date and onset and episode duration respectively, and b'_{4i}, b'_{5i}, b'_{6i} and b'_{7i} represent the patient-specific random effects. β'_0, b'_{0i}, β'_1, b'_{1i}, β'_2, b'_{2i}, β'_3 and b'_{3i} correspond to the fixed and patient-specific random effects introduced in Equation (4.21) and (4.22) but for the ME' model.

4.3.4. Statistical Analysis

Continuous data are presented as mean ± standard deviation if the null hypothesis H_0 of the Kolmogorov–Smirnov test (H_0: data is normally distributed) was not rejected. Otherwise, continuous data are presented as median (min-max). Categorical data are presented as absolute frequency (relative frequency in percentage). The null hypothesis was rejected when $p < 0.05$, then set as the level of significance. The relationship between the features was studied using the patient-average of the features. This average was defined as the mean for those normally distributed (such as AFR, Mean RR and SampEn) and the median for those not normally distributed (such as onset time and episode duration). The normality of the feature was determined by analysing the complete set of episodes.

The statistical analysis was performed using Matlab R2022a (The Mathworks Inc., Natick, Massachusetts).

4.4. Results

The distribution of 5-s segments available for analysis after elimination of insufficient quality segments is shown in Figure 4.3.

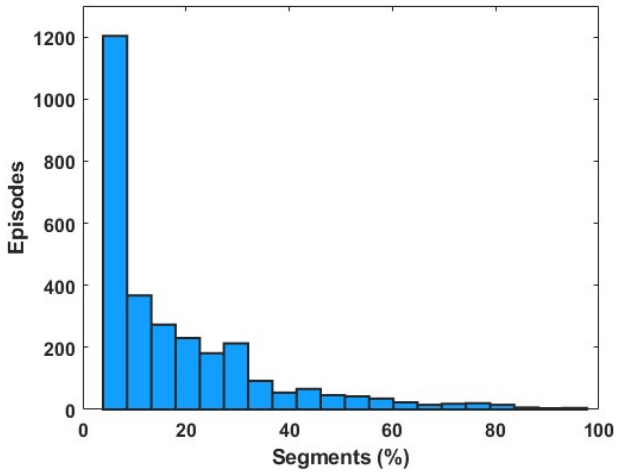

Figure 4.3. Number of episodes with percentage of analyzable 5-s segments after application of the SQI (SQI>0.3).

During the monitoring period, the ICMs stored 3739 episodes out of which 2908 (77%) episodes contained at least one 5-s segment of sufficient signal quality for estimation of AFR.

Out of the episodes included in the analysis, 1796 (62%) occurred before ablation, 657 (23%) occurred after ablation and 455 (15%) occurred during the 3-months blanking period and were excluded from the analysis. Each patient had a median (min-max) of 20.5 (2-114) episodes with 16 (0-77) episodes pre-ablation, and for those patients which had AF recurrence, 10 (1-61) episodes post-ablation per patient. Figure 4.4 illustrates the number of episodes each patient had in the defined timeframes, i.e., pre-ablation, during 3-month blanking period and post-ablation.

The mean AFR of at least one acceptable 5-s segment was considered to be representative of the whole segment under the assumption that the AFR was stable within 2 minutes of AF. The stability of AFR within the episodes was studied by selecting the 24 episodes where more than 80% of the episode had acceptable levels of SQI and iteratively computing the mean AFR for decreasing percentages of the signal and evaluating the relative absolute error between the mean AFR of the reduced signal segments and the mean AFR of the whole acceptable signal. Figure 4.5 shows the evolution of the relative error (%) for varying percentages of signal.

The stability analysis showed a maximum relative error of 7.2 (4.4) % so AFR was assumed to be stable within the AF episodes.

The distribution of the AFR extracted from the episodes with at least one acceptable 5-s segment for each patient is shown in Figure 4.6.

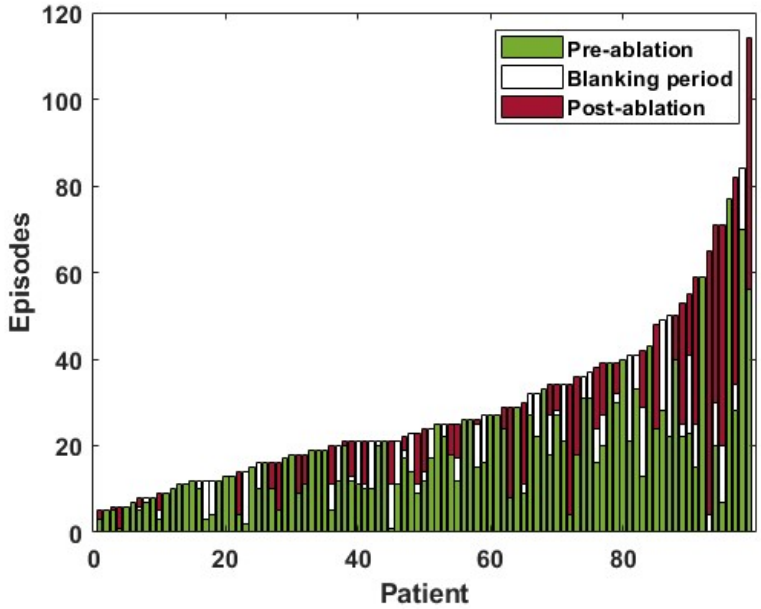

Figure 4.4. Number of episodes occurring pre-ablation, during blanking period and post-ablation. Data sorted in ascending number of episodes.

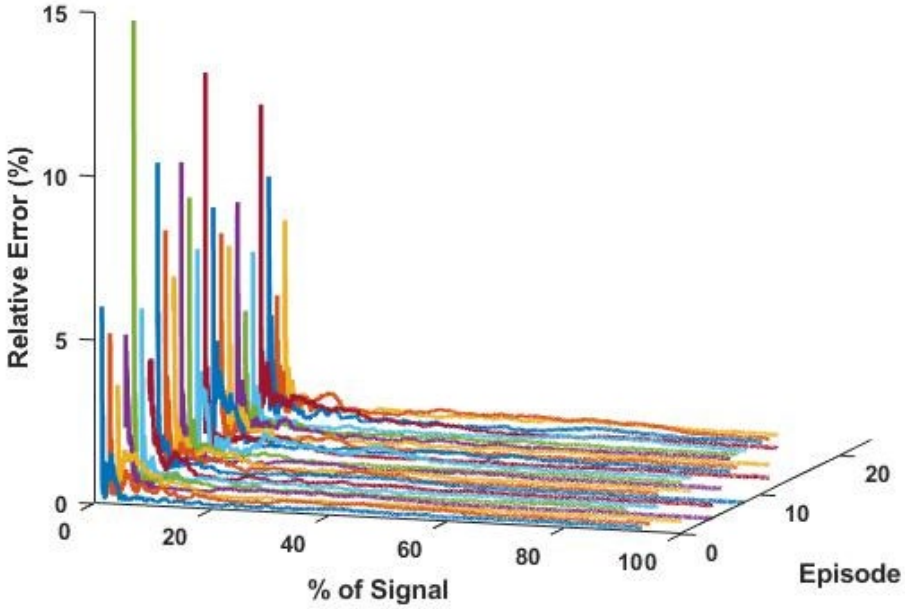

Figure 4.5. Relative error evolution with percentage of signal analyzed for those episodes containing more than 80% of acceptable segments.

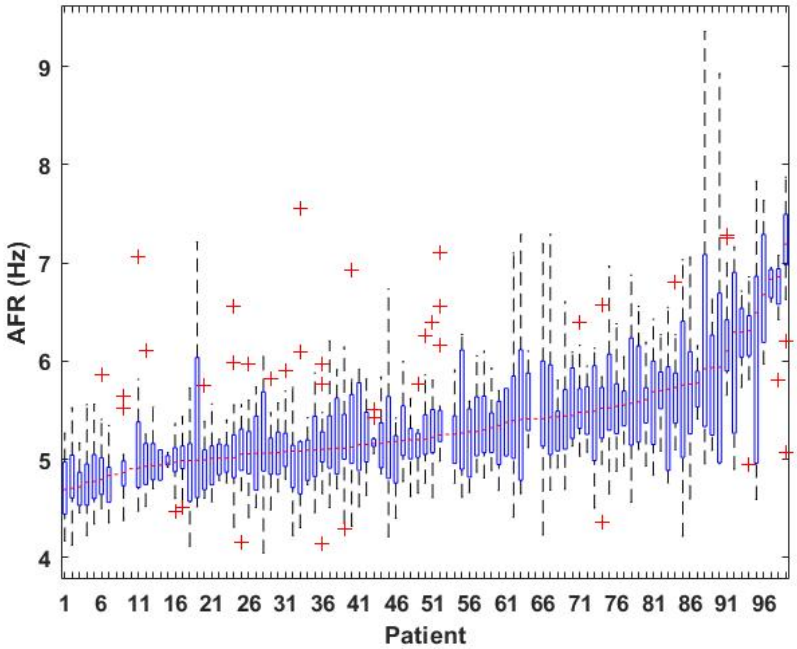

Figure 4.6. Distribution of AFR in each patient of the episodes included in the analysis displayed as median, interquartile range and 10/90th percentiles. Data sorted in ascending order of median AFR.

The figure shows that a high proportion (85%) of the AFR extracted from the episodes considered in the analysis were comprised between 4 and 6 Hz.

4.4.1. Population-based analysis

For the population-based analysis, the AFRs estimated from the 1796 episodes pre-ablation were included. 897 (50%) episodes were considered to be short, i.e., duration less than 20 minutes, and 899 (50%) episodes were considered to be long. Exploring the onset times: 840 (47%) episodes occurred during the day, 557 (31%) episodes occurred during the night and 399 (22%) occurred outside the defined onset and were therefore excluded.

The relationship between both AFR and relative AFR with episode length and episode onset was analysed and their distribution shown in Figure 4.7.

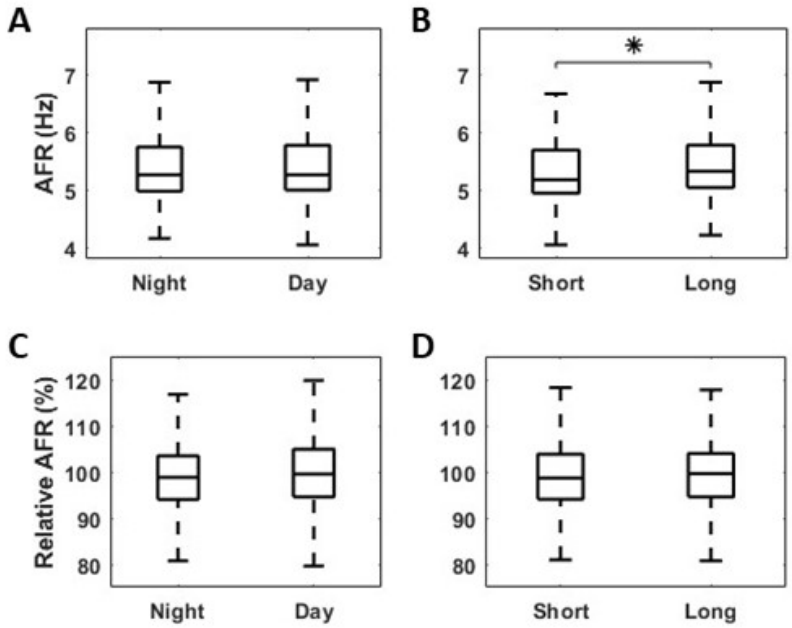

*Figure 4.7. Relationship between (A) AFR and episode onset, (B) AFR and episode duration, (C) relative AFR and episode onset, and (D) relative AFR and episode duration. Statistical significance (p-value < 0.05) is shown as *.*

AFR was significantly higher ($p < 0.05$, Mann-Whitney U test) in long episodes (≥ 20 mins) than in short episodes (< 20 mins) where the AFR in long episodes was 5.32 (0.73) Hz while in short episodes, the AFR was 5.17 (0.75).

4.4.2. Modelling

For the FE and ME models, the complete set of episodes was used taking into consideration the different patients and the number of ablations the patient went through.

Figure 4.8 shows the AFR of the episodes based on their modified onset time for each patient color-coded depending on if the episode onset was before or after their first ablation procedure, or before or after their second ablation procedure. As described in 4.2, the patients were monitored through only one ablation procedure. Therefore, patients either had no previous ablations (labelled as Before 1st Ablation) and had

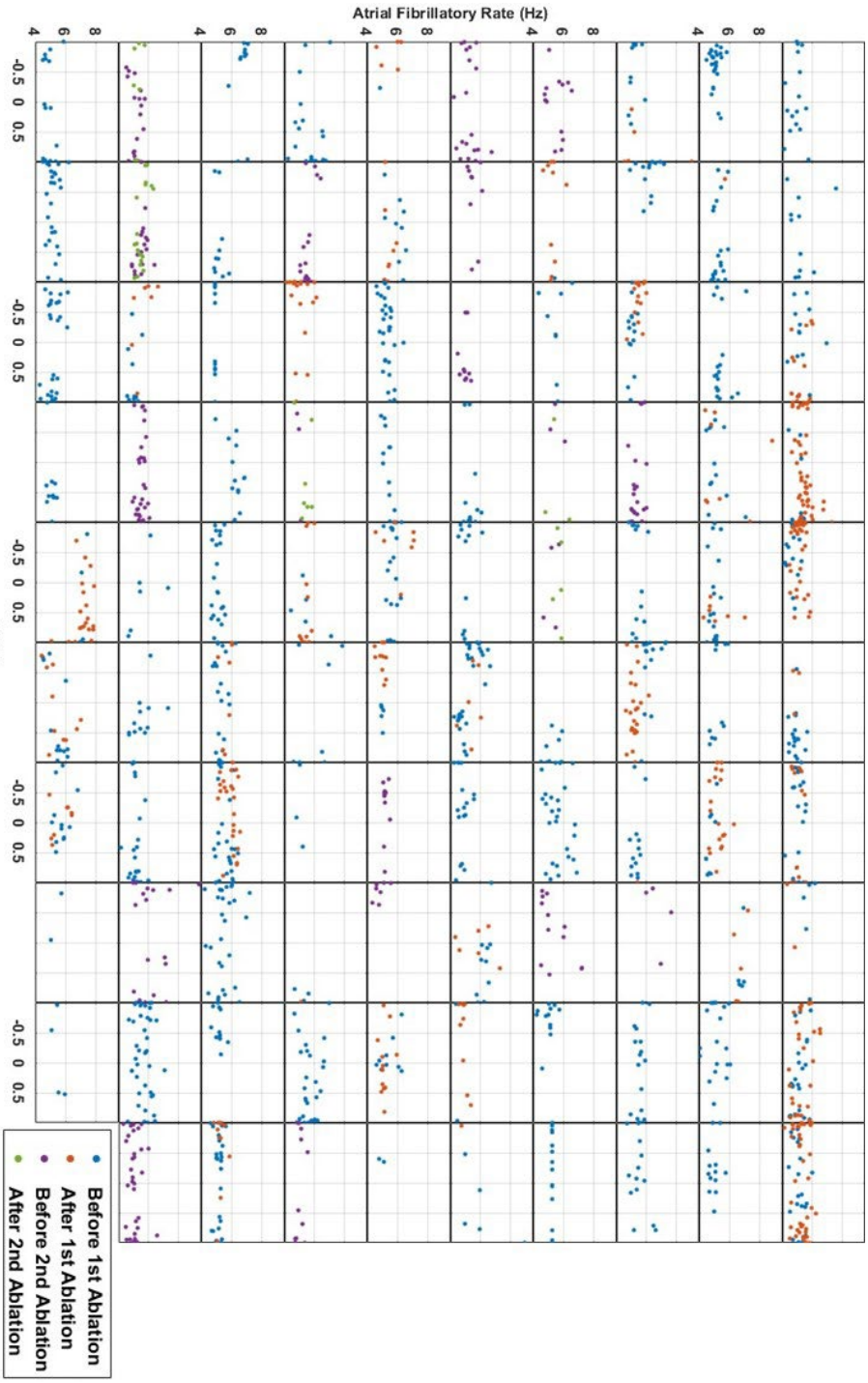

Figure 4.8. Atrial Fibrillatory Rate of AF episodes with their onset for each patient included in the study. Color-coded as before and after first ablation, and before and after second ablation.

their first ablation during the monitoring time (After 1st Ablation) or have had 1 previous ablation (Before 2nd Ablation) and underwent their second ablation during the monitoring time (After 2nd Ablation). The episodes are evenly distributed through the day with 75 (76%) patients having episodes both during Night and Day times, defined as between 00:00-06:00 and between 10:00 and 20:00 respectively [156].

The scatter plots of the average AFR, modified time of AF onset, duration of AF episode (in log scale), and HRV derived parameters, Mean RR, RMSSD and SampEn, for each patient are shown in Figure 4.9.

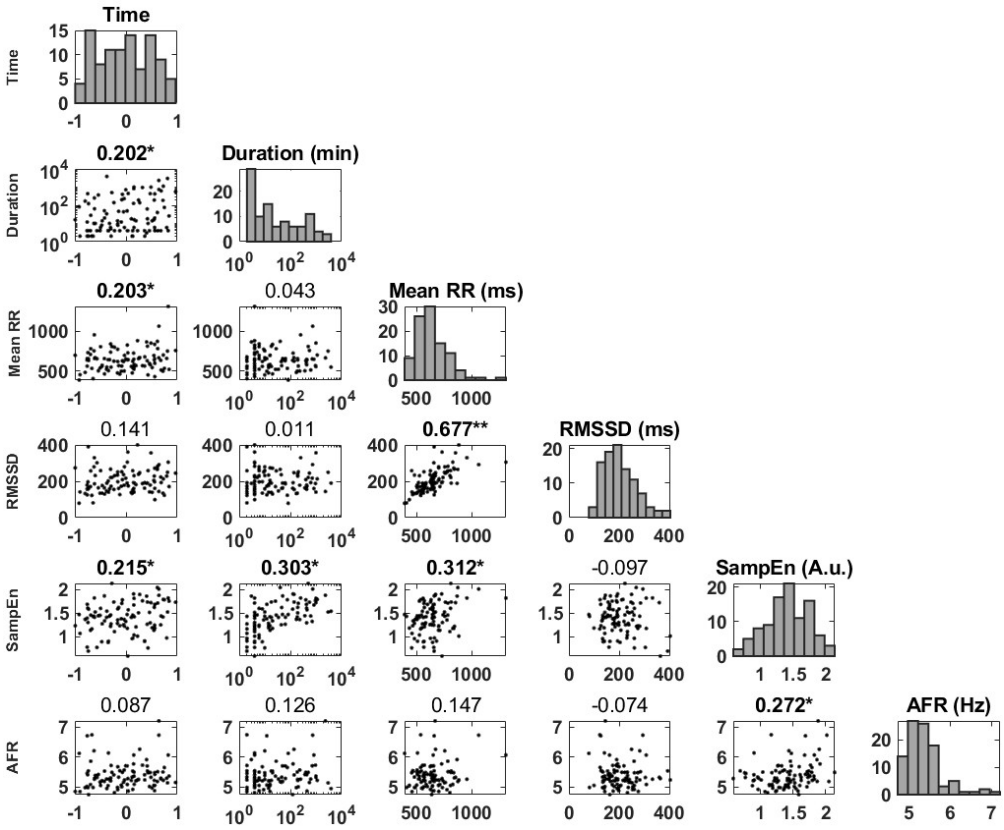

Figure 4.9. The correlation analysis between the studied parameters and the Atrial Fibrillatory Rate (AFR). The diagonal shows the histogram of the parameters while the lower triangular area displays the distribution of the parameter values by the scatter plots with their title showing the correlation coefficient between parameters, and (, p<0.05) and (**, p<0.001) representing the statistical significance. For reasons of clarity, the Duration is plotted in a log scale.*

The average AFR for each patient shows a mild significant correlation with the average SampEn ($R = 0.27, p < 0.05$).

In addition, the frequency distribution histograms of the average per patient of the features studied are also aligned diagonally on the subpanels of Figure 4.9. The

patient averaged AFR shows a mild significant correlation with the SampEn ($R = 0.27, p < 0.05$). Mean RR has a moderate significant correlation with the RMSSD ($R = 0.68, p < 0.001$).

In this study, no correlation between the average AFR and the average modified AF onset time was found. This frequency distribution histograms show that the patient-average of the AF episode duration is predominantly short episodes with 54 patients (55%) having an average episode duration shorter than 20 minutes.

Overall, the duration of the episodes had a median of 14 minutes with the minimum duration being the detection threshold, i.e., 2 minutes, and the maximum duration spanning 62.7 days.

The results of the different models are summarized in Table 4.2, and the fitted values of AFR were plotted against the true values and illustrated in Figure 4.10.

Table 4.2. Results comparison between the different models.

Model	Input Variable	AIC	Deviance	R^2
FE model	Mean RR RMSSD SampEn	5699	5689	0.04
ME model	Mean RR RMSSD SampEn	4424	4394	0.49
ME' model	Mean RR RMSSD SampEn Time nAblations DaysSinceImplant Duration	4298	4208	0.56

AIC: Akaike Information Criterion
R^2: coefficient of determination
nAblations: number of Ablations
RMSSD: Root mean square of standard deviation
SampEn: Sample entropy

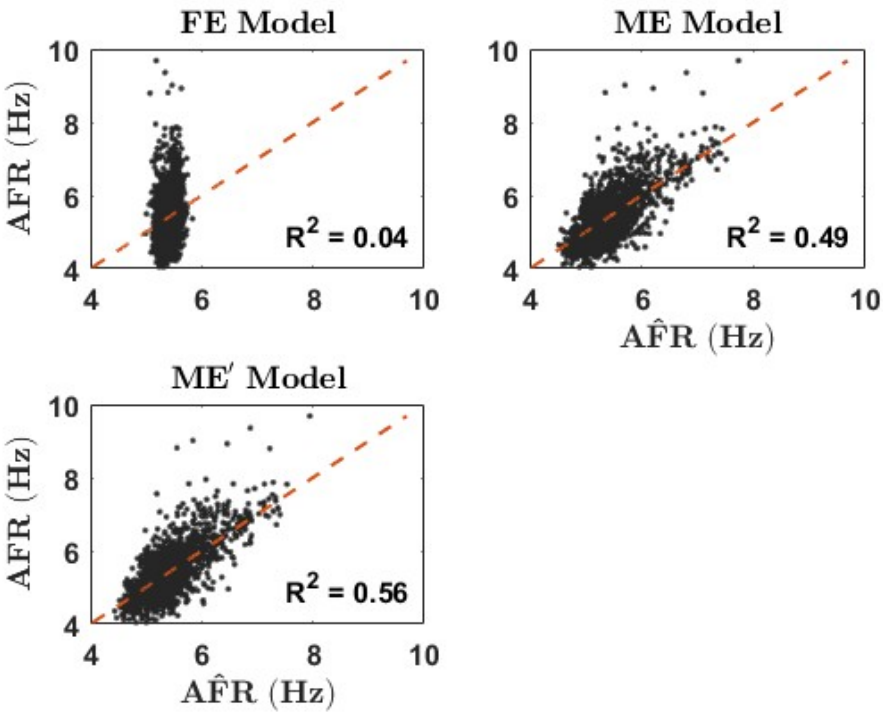

Figure 4.10. True (AFR_{ij}) vs estimated ($\hat{AFR}_{ij}$) values for the different models with their coefficient of determination (R^2). The dashed line represents the perfect fit.

The FE model, which only included the fixed effect of changes in RR series had the lowest complexity but had also the largest AIC value. When also considering the random effects in the ME model, the values of AIC and the deviance decreased. Lastly, when accounting for the circadian variation, the duration of the episode, the number of ablations before the episode and correcting for the monitoring period as in the ME' model, the deviance and AIC value is minimum suggesting that the ME' model outweighs the other models also when accounting for the increased model complexity. The coefficients of determination (R^2) also corroborate that the ME' model has the better fit as its coefficient is the highest ($R^2 = 0.56$).

The irregularity in RR intervals has a significant effect on the AFR ($\beta_3' = 0.105$, $p < 0.05$) with higher AFR for higher irregularity. The number of prior ablations also has a significant effect on the AFR ($\beta_5' = 0.168, \mathrm{p} < 0.05$) with higher AFR after multiple ablations, and so does the episode duration ($\beta_7' = 1.182 \times 10^{-5}$, $p < 0.05$) with AFR being higher for longer episodes.

The maximum pseudo likelihood method is employed for the parameter estimation and the results for the fixed effect coefficients for the ME' model are summarized in Table 4.3.

Table 4.3. Fixed effect coefficients for the ME' model.

Parameter	Associated to:	Estimate	SE	p-value
β_0'	Intercept	4.979	0.100	<0.001**
β_1'	Mean RR	8.853×10^{-5}	2.289×10^{-4}	0.698
β_2'	RMSSD	5.453×10^{-4}	4.040×10^{-4}	0.177
β_3'	SampEn	0.105	0.047	0.031*
β_4'	Time	-0.021	0.034	0.521
β_5'	Number of Ablations	0.168	0.073	0.022*
β_6'	Days Since Implant	-5.323×10^{-5}	2.440×10^{-4}	0.827
β_7'	Duration	1.182×10^{-5}	3.721×10^{-6}	0.002*

(*, p<0.05) and (**, p<0.001) representing statistical significance
SE: Standard Error of the coefficient

The irregularity in RR intervals has a significant effect on the AFR ($\beta_3' = 0.105$, p<0.05) with higher AFR for higher irregularity. The number of prior ablations also has a significant effect on the AFR ($\beta_5' = 0.168, \mathrm{p} < 0.05$) with higher AFR after multiple ablations, and so does the episode duration ($\beta_7' = 1.182 \times 10^{-5}$, p<0.05) with AFR being higher for longer episodes.

4.5. Discussion

The rapidly increasing use of continuous monitoring devices for patients diagnosed with AF [157] offers the chance of a more detailed characterization and a better understanding of the patients' condition in order to select the most appropriate therapy but above all the right timing in order to avoid disease deterioration. Continuous assessment of AFR extracted from ECG strips is a non-trivial matter. However, the estimation of AFR from RR series data would enable wearable based assessment of AFR, e.g., wristband PPG. The aim of the study was to model variations in AFR based on changes of RR series characteristics (mean RR interval, RMSSD and sample entropy). After a first attempt using FE modelling approach (FE model), the

results were compared to a more complex ME modelling approaches: considering both population and specific effects of RR series (ME model) and allowing correction for the effect of episode duration, previous ablations, and possible circadian variations (ME' model). In addition, ME modelling would account for the heterogeneity within AF patients. In order to apply the different models, the AFR stability within the first 2 minutes of the AF episodes was evaluated. In the 24 episodes with enough data to run the analysis we found that for different percentages of signal, the error between the mean AFR of the signal and the mean AFR on the remaining segments was 7.2 (4.4) %. With this result in mind, AFR was considered stable and the mean AFR calculated on a single segment (5 seconds) was considered representative of the whole signal.

The correlation between AFR and HRV features describing the variability and irregularity of RR intervals has been explored before in a cohort of patients with underlying congestive heart failure [144]. However, to the best of our knowledge, this is the first study to assess the variation of AFR in AF patients without congestive heart failure which were continuously monitored over several months. It is also the first study to model AFR variations using mixed-effect models which account for the heterogeneity of the patient population and confounding factors.

The model's parameters showed a significant effect of RR irregularity quantified by SampEn ($\beta_3' = 0.105$, $p < 0.05$), number of ablations ($\beta_5' = 0.168, \mathrm{p} < 0.05$), and episode duration ($\beta_7' = 1.182 \times 10^{-5}$, $p < 0.05$) on AFR. Due to the heterogeneity between patients, the mixed-effect model developed with correction for the confounding factors (ME' model) was able to better fit the data compared to the FE model, the fixed-effect modelling approach, ($R^2 = 0.56$ vs $R^2 = 0.04$).

The fact that average SampEn is correlated with average AFR ($R = 0.27, p < 0.05$) and that has a significant effect on AFR when evaluating the ME model, is in line with a previous study [144] which evaluated the relationship between AFR and HRV derived features. In the aforementioned study, the regularity statistic quantifying the unpredictability of fluctuations in a time series used was the approximate entropy (ApEn) and was shown to have a Pearson's correlation of $R = 0.26, p < 0.05$, indicating that the higher the AFR, the less organized the RR series. In our study, the effect the regularity of the RR series has in modelling AFR was further evaluated in the ME' model showing a significant effect ($\beta_3' = 0.105, p < 0.05$). Previous studies have shown that the RR irregularity during AF change in response to changes in autonomic tone induced by drugs [158–160] and tilt-test [161]. However, it should be noted that increased RR irregularity may also be a direct effect of changes in atrial electrical activity as quantified by an increased AFR or variations in the atrioventricular node conduction [162].

Out of the 99 patients included, 19 (19%) had a previous ablation so the information available corresponds to the episodes before and after (if had AF recurrence) their second ablation while for the remaining patients, the information available consists of the episodes before and after their first ablation. Evidence of negative correlation between the percentage of fibrotic tissue in the left atria with the fibrillatory frequency have been reported [163]. However, our study suggests that the number of ablations has a positive significant effect on AFR ($\beta_5' = 0.168, \mathrm{p} < 0.05$) with patients having gone through a higher number of ablations, having higher AFR. Though further investigation with mapping and electrogram recordings is needed, this result suggests that creating lesions in the atria reduces macro-reentrant pathways but at the same time, promotes micro-reentrant circuits and/or faster, smaller rotors which would increase the fibrillatory rate of the atria.

Trying to understand AF behaviour, the link between AF episode duration and AFR had been previously studied showing a positive correlation between them ($R = 0.53, p < 0.05$) [149] where having a higher AFR at the start of the AF episode could predict longer episodes. However, this study was conducted in a small dataset with only 31 episodes from 11 paroxysmal AF patients and the correlation was describing the whole database without explicitly considering intra- and inter-patient effects. The results of the present study confirm Bollmann's results as the episode duration had a significant effect on the AFR in the ME' model ($\beta_7' = 1.182 \times 10^{-5}, p < 0.05$). Finding of longer episodes of AF having higher AFR could be explained by an increase of sympathetic drive with longer duration of arrhythmia [164].

In several studies, circadian dynamics of AFR were observed in patients using Holter monitoring [145–147]. In these studies, AFR showed a decrease at night and an increase during the morning hours, with a peak during the afternoon. In one of those studies, two different sets of patients were identified: one which showed an increase (minority) while the other showed a decrease (majority) in nocturnal AFR [145]. However, the insight in circadian behaviour of atrial electrophysiological characteristics during AF was constrained to 24-hour long Holter registrations and limited datasets of up to 30 patients. Circadian variation in the AFR is caused by autonomic modulation in the atrial electrical activity and could potentially be used to guide clinical strategies such as time of the day medication should be administered, or which patient would benefit the most from a catheter ablation procedure. Hence, as a secondary objective, we wanted to assess the effect of circadian variation on AFR. The present study is also based on a larger study population (99 patients) and longer monitoring periods ($0.2 - 24.3$ months) than the previous studies. Three additional ME models were evaluated: Model 1C modelled the circadian variations in AFR, Model 2C corrected Model 1C for the effect of previous ablations and Model 3C corrected Model 2C for the effect of episode

duration. None of the models showed significant fixed effect of the onset time (quantifying the circadian variations) when modelling the AFR. When analysing the patient specific random effects of time in Model 1C, 9 (9%) of the patients in the cohort showed circadian variations of AFR. This aligns with the literature describing circadian variations only on a subset of patients [148].

When studying the association between the average of the features extracted from each patient, only the average SampEn ($R = 0.27, p < 0.05$) showed a mild significant correlation with the AFR. However, when taking into account the repeated measures in the ME model both episode duration and number of ablations showed to also have a significant effect on AFR. For this cohort, longer and more irregular episodes after multiple ablations showed to have a higher fibrillatory frequency.

Currently, there is still uncertainty about the optimal selection for catheter ablation and overall, the challenges to define clear patients' phenotypes for appropriate AF management are still prominent [165,166]. Our study suggests that continuous assessment of AFR has the potential to estimate the impact of therapies and so to help the stratification of patients towards AF ablation especially when it can help the physician decide when, whether or not to recommend ablation therapy and persist in drug treatment.

To assess the importance of including patient specific dependencies on RR series characteristics in the model, the results were compared to an ME model that only considered $\boldsymbol{b_0}$. This model had a better performance compared to the FE model ($R^2 = 0.37$; $AIC = 4727$ vs $R^2 = 0.05$; $AIC = 5699$) but had a worse fit to the data than the ME model ($R^2 = 0.49$; $AIC = 4424$). This shows that the patients still have a high heterogeneity not being addressed by the model but some of it is found in their RR characteristics.

This retrospective study combining 2 different cohorts with limited clinical baseline data, is based on a patient population implanted with the Reveal LINQ based on clinical indications including suspected AF, AF ablation monitoring or AF management. Although this unique database offers the advantage of long monitoring periods and a complete monitorization of patients suffering AF, some limitations should be noted. The patient population included in the study is relatively young ($57 \pm 12\ years$) compared to the general AF population and with a low degree of cardiovascular risk. Due to the retrospective nature of the study, the medication administered to each patient during the monitoring period and the ablation technique in those patients with a previous failed ablation were not available. Hence, possible influence of medication and scar tissue from previous ablations on AFR is modelled as a patient specific random effect. The ICM evaluates

the rhythm and detects AF episodes based on 2 minutes ECG data. Hence, episodes longer than 30s, defined as AF episodes by the guidelines [6], but shorter than 2 minutes remained undetected. Furthermore, due to the limited memory of the device, ECG data was only stored for a subset of the detected episodes; 57840 episodes were detected by the device out of which ECG data from 3739 (6.5%) were stored. The number of episodes detected but not stored is not only linked to the number of episodes suffered by the patient but also to the frequency of visits to the hospital as the data was downloaded and saved each time the patient had a check-up. Overall, the patients had a median (min-max) of 130 (1-4564) episodes detected pre-ablation out of which 43.4 (1.9-100)% were stored. Post-ablation, the device detected 1 (0-4245) episodes out of which 60.2 (2.9-100)% were stored. Another limitation of the study is that the Reveal device only stores the first 2 minutes of ECG, which may not be representative of the whole episode; results from a previous study suggest that AFR may accelerate during the first 3-4 hours [150]. In addition, the harmonic f-wave model used for AFR estimation was originally developed for surface ECG, and the characteristics of the f-waves in the ECG recorded by the ICM may differ from these since the electrodes are placed next to the apex of the heart. However, our results indicate that the model fit was sufficient in most cases; 2908 of the 3739 detected AF episodes in our 99-patient cohort had sufficient signal quality to be analysed.

4.6. Conclusion

Fixed and mixed effects modelling approaches were used to investigate the effect of changes in RR series characteristics corrected for episode onset and duration, previous ablations, and onset date, on variations in AFR in a study population of 99 patients monitored for 9.2 (0.2-24.3) months as median (min-max). The ME modelling approach was shown to be superior to the FE modelling approach due to the heterogeneity of the patient population and the presence of confounding factors. The fixed effects extracted from the ME' model showed that AFR is slightly higher in episodes with less organized RR series and of longer duration and is affected by catheter ablations. The use of ME models combined with long term monitoring of patients offers the chance of continuously estimating the AFR from RR series and episode-based characteristic and will lead to a more detailed characterization and a better understanding of the patients' condition which could potentially aid the clinicians in their decision-making process.

Chapter 5 Temporal Aggregation

The publication related to this chapter is:

Saiz-Vivo J, Corino VDA, Martín-Yebra A, Mainardi LT, Hatala R, Sörnmo L. **Atrial fibrillation episode patterns as predictor of clinical outcome of catheter ablation**. Medical & Biological Engineering & Computing. 2022 Nov. DOI: 10.1007/s11517-022-02713-x. PMID: 36409405.

5.1. Motivation

With the development of long-term monitoring devices, the binary approach, i.e., whether AF is present or absent, is slowly being replaced by an approach involving features such as AF burden, i.e., the percentage of time in AF [167] which has been found to be a significant predictor of patients at risk of ischemic stroke [168]. Nonetheless, this measure does not describe whether AF episodes are clustered or distributed evenly throughout the monitoring period despite that characterization of the episode pattern may be relevant for better understanding of AF progression and risk assessment of AF recurrence post-ablation.

Characterization of AF patterns has mainly focused on statistical analysis of either interepisode intervals, i.e., the interval between consecutive AF episodes [169–171] or inter-detection intervals, i.e., the interval between the onset of consecutive AF episodes [172], without accounting for episode history in the analysis. While these descriptive studies speculated that the information on episode patterns could be useful to predict AF recurrence [173], the clinical significance was never established.

Recently, the alternating bivariate Hawkes model, a novel statistical approach to characterize AF episode patterns was proposed where episodes are assumed to be history-dependent [174]. In this chapter, the performance of a subset of the model parameters is evaluated to predict the risk of AF recurrence. In addition, the performance of AF burden and AF density, being one of the very few parameters proposed for characterizing the temporal aggregation of the daily AF burden in patients using an ICM [175], is evaluated. To the best of our knowledge, there have been no studies using this or any other episode pattern characterization method as AF recurrence risk predictor.

5.2. Methods and Materials

5.2.1. Alternating bivariate Hawkes model

A statistical approach to characterizing episode patterns in paroxysmal AF (PAF) is based on history-dependent point process modelling of the transition times from sinus rhythm (SR) to AF and vice versa [174]. With the bivariate Hawkes model, the episode pattern is modelled by two alternating point processes $\{N_1(t), N_2(t), t > 0\}$ which describe the number of transitions that have occurred up to t: one accounting

for transitions from SR to AF occurring at times (points) $t_{1,1}, t_{1,2}, \ldots$, and another for transitions from AF to SR occurring at times $t_{2,1}, t_{2,2}, \ldots$; the first subscript describes the type of transition (SR-to-AF AF-to-SR are denoted 1 and 2, respectively) and the second, the transition number. For simplicity in this study, SR and AF are assumed to be the alternating rhythms with only AF interrupting a SR rhythm and vice versa, while, in practice, a non-AF rhythm may very well replace SR.

The counting processes $N_1(t)$ and $N_2(t)$ are defined by two conditional intensity functions of the form [176]:

$$\lambda_m(t) = \mu_m + \sum_{n=1}^{2} \sum_{\{k:t>t_{n,k}\}} \alpha_{m,n} e^{-\beta_{m,n}(t-t_{n,k})} \tag{5.1}$$

where $\mu_m > 0$, $\alpha_{m,n} \geq 0$ and $\beta_{m,n} \geq 0$ for $m, n = 1, 2$.

The main characteristic of the model is that the conditional intensity function $\lambda_1(t)$ increases by $\alpha_{1,1}$ immediately after an SR-to-AF transition (self-excitation) and then decreases exponentially, defined by the decay parameter $\beta_{1,1}$, to the base intensity μ_1 reflecting the mean rate of SR-to-AF transitions. The conditional intensity function $\lambda_2(t)$ characterizes AF-to-SR transitions and behaves similarly to $\lambda_1(t)$, defined by the excitation parameter $\alpha_{2,2}$, the decay parameter $\beta_{2,2}$, and the base intensity μ_2. As the probability of additional transitions increases immediately after a transition, the process can account for clustering behaviour by modelling the chance of a transition occurring after a previous transition. In addition to the self-excitation, both $\lambda_1(t)$ and $\lambda_2(t)$ contain additional terms, defined by $\alpha_{1,2}$ and $\beta_{1,2}$ in the case of $\lambda_1(t)$, and by $\alpha_{2,1}$ and $\beta_{2,1}$ in the case of $\lambda_2(t)$, which lets the counting processes influence each other (cross-excitation).

The bivariate Hawkes model in its original formulation does not impose alternating transitions, i.e., an SR-to-AF transition is not necessarily followed by an AF-to-SR transition, while from the physiological point of view this constrain is required. This is obtained by multiplying $\lambda_1(t)$ and $\lambda_2(t)$ with a binary "occurrence" function:

$$o_1(t) = \begin{cases} 1, & N_1(t) = N_2(t - d_2), \\ 0, & otherwise, \end{cases} \tag{5.2}$$

and

$$o_2(t) = \begin{cases} 1, & N_2(t) \neq N_1(t - d_1), \\ 0, & otherwise, \end{cases} \tag{5.3}$$

which ensures that AF occurs after SR, and that SR occurs after AF, respectively.

The parameters d_1 and d_2 define the minimum duration of AF and SR, respectively.

Finally, the conditional intensity functions for the alternating, bivariate Hawkes process are given by:

$$\tilde{\lambda}_m(t) = \lambda_m(t) o_m(t), \qquad m = 1, 2. \tag{5.4}$$

The structure of $\tilde{\lambda}_m(t)$ is identical to that of the bivariate Hawkes process $\lambda_m(t)$, except that a SR-to-AF transition can, once a certain time d_1 has elapsed, only be followed by an AF-to-SR transition, and so on. Figure 5.1 shows an AF episode pattern, the transition times corresponding to the two alternating point processes and the conditional intensity functions associated to those point processes.

The model parameters, defining the conditional intensity functions, can be estimated using the maximum likelihood (ML) method. For a bivariate process, the likelihood function is given by [177]:

$$\ln \mathcal{L}(\boldsymbol{\theta}; \boldsymbol{t}) = \sum_{m=1}^{2} \sum_{k=1}^{N_m(T)} \ln \lambda_m(t_{m,k}; \boldsymbol{\theta}) - \sum_{m=1}^{2} \int_0^T \lambda_m(t; \boldsymbol{\theta}) dt \tag{5.5}$$

where the vector $\boldsymbol{t}$ contains the transition times in the observation interval [0, T] and the vector $\boldsymbol{\theta}$ collects all the model parameters, i.e., $\boldsymbol{\theta} = [\mu_1, \mu_2, \alpha_{1,1}, \beta_{1,1}, \alpha_{1,2}, \beta_{1,2}, \alpha_{2,1}, \beta_{2,1}, \alpha_{2,2}, \beta_{2,2}]$.

The ML estimator is then given by:

$$\widehat{\boldsymbol{\theta}} = \arg\max_{\theta} (\ln \mathcal{L}(\boldsymbol{\theta}; \boldsymbol{t})); \tag{5.6}$$

see [17] for details of the ML estimator.

Due to the alternating nature of the Hawkes model brought by the occurrence function $o_m(t)$, only the cross-excitation part of the conditional intensity functions ($\beta_{1,2}$ and $\beta_{2,1}$) are relevant for the modelling.

The conditional intensity functions for the alternating, bivariate Hawkes process ($\tilde{\lambda}_1$ and $\tilde{\lambda}_2$) will only be active after an AF-to-SR transition or a SR-to-AF transition, respectively. To illustrate: SR-to-AF transitions are modelled by $\tilde{\lambda}_1$ which will equal λ_1 after an AF-to-SR transition and will be governed by $\beta_{1,2}$. On the other hand, after a SR-to-AF transition, $\tilde{\lambda}_1$ will equal to 0, as there cannot be another SR-to-AF transition before an AF-to-SR transition, thereby rendering $\beta_{1,1}$ irrelevant for the

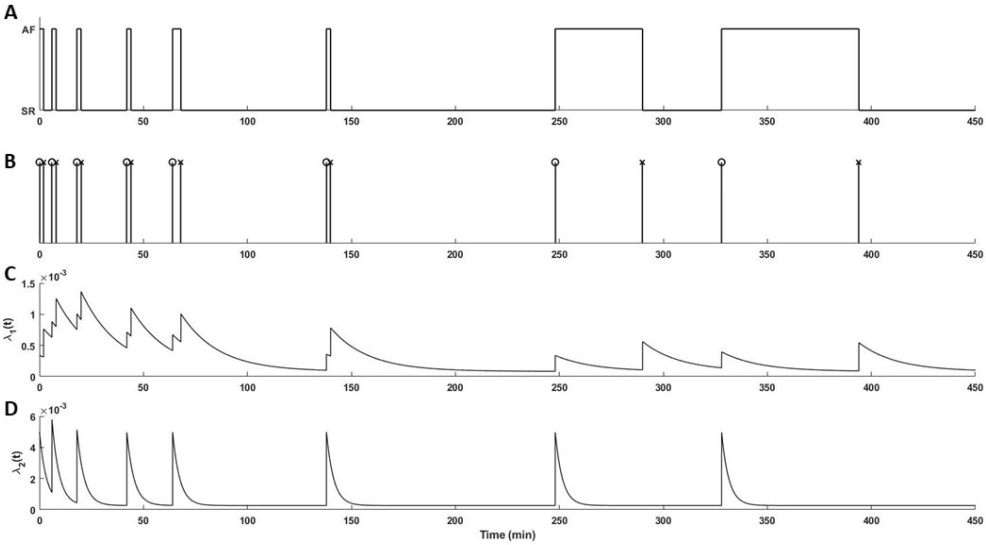

Figure 5.1 (A) Example of real AF episode pattern. (B) Transition times for the episode pattern in (A). The marks "o" and "x" indicate SR-to-AF and AF-to-SR transitions, respectively. (C-D) The conditional intensity function of SR-to-AF transitions and of AF-to-SR transitions. For reasons of clarity, $\lambda_1(t)$ and $\lambda_2(t)$ are displayed rather than $\tilde{\lambda}_1(t)$ and $\tilde{\lambda}_2(t)$.

monitoring. The same happens to $\beta_{2,1}$ and $\beta_{2,2}$ when modelling AF-to-SR transitions through $\tilde{\lambda}_2$. It is then assumed that $\beta_{1,1} = \beta_{1,2} = \beta_1$ and $\beta_{2,1} = \beta_{2,2} = \beta_2$. Hence, the conditional intensity functions are defined by a relatively small number of parameters and therefore suitable for statistical inference. Note that in the example shown in Figure 5.1, $\lambda_2(t)$, i.e., the probability of a SR-to-AF transition, doesn't increase whenever there is a SR-to-AF transition having an $\alpha_{2,2} = 0$. Nonetheless, as explained above, $\tilde{\lambda}_2 = 0$ for the instance after a SR-to-AF transition, and similarly for $\tilde{\lambda}_1$ after an AF-to-SR transition, so neither $\alpha_{2,2}$ nor $\alpha_{1,1}$ affect the model. The onset of the first AF episode and the end of the last AF episode are assumed to be entirely contained in the observation interval. Thus, the first transition for analysis is from SR-to-AF and the last from AF-to-SR.

The base intensity ratio is defined as:

$$\mu = \frac{\mu_1}{\mu_2} \tag{5.7}$$

and provides information on the dominating rhythm of the analysed segment: $\mu > 1$ indicates dominance of AF (Figure 5.2 (A and D)) and $\mu < 1$ dominance of SR (Figure 5.2 (B and C)). In the present study, the natural logarithm of μ ($\log(\mu)$) is

used instead of μ as μ is a ratio, and, therefore, $\log(\mu)$ exhibits a more linear behaviour.

The decay parameter β_1, empirically restricted to a range between 0 and 0.3 [174], describes the degree of episode clustering, where a value of β_1 close to 0.3 reflects few clusters. This is illustrated in Figure 5.2 (A and C) where the episodes are spread out throughout the monitoring period, although the time span differs considerably (A in minutes and C in days). Conversely, a value of β_1 close to 0 reflects high episode clustering as illustrated in Figure 5.2 (B and D). In this study, β_2 is not considered for prediction as β_1 is deemed to play the main role with regard to AF episode clustering as it determines the rate at which the probability of a new AF episode onset decreases.

The Hawkes model requires a minimum number of episodes to produce adequate parameter estimates, here set to 10, i.e., 20 transitions, as suggested in [174].

For further details on the alternating bivariate Hawkes model and the estimation of μ_1, μ_2 and β_1, the reader is referred to [174].

The Hawkes model was computed using the particle swarm optimization algorithm in Matlab R2019b (The Mathworks Inc., Natick, Massachusetts) with the default function tolerance equal to 10^{-6} and the maximum number of iterations set to 3500.

5.2.2. AF Density

AF density is defined as the ratio of the cumulative deviation of the patient's actual AF burden level from a hypothetical uniform burden level, to that of the hypothetical maximum burden aggregation [175].

For a patient with a total AF burden b (expressed as the proportion of the observed time T in which a patient is in AF), the patient's AF burden level corresponds to:

$$F(p;b) = \frac{T(p;b)}{T} \tag{5.8}$$

with $T(p;b)$ denoted as the minimum continuous period required for the development of a proportion p of the patient's total observed burden (b). This was computed by determining what was the minimum continuous time period needed for the patient to develop 5-95% (with 5% increments) of their total observed burden.

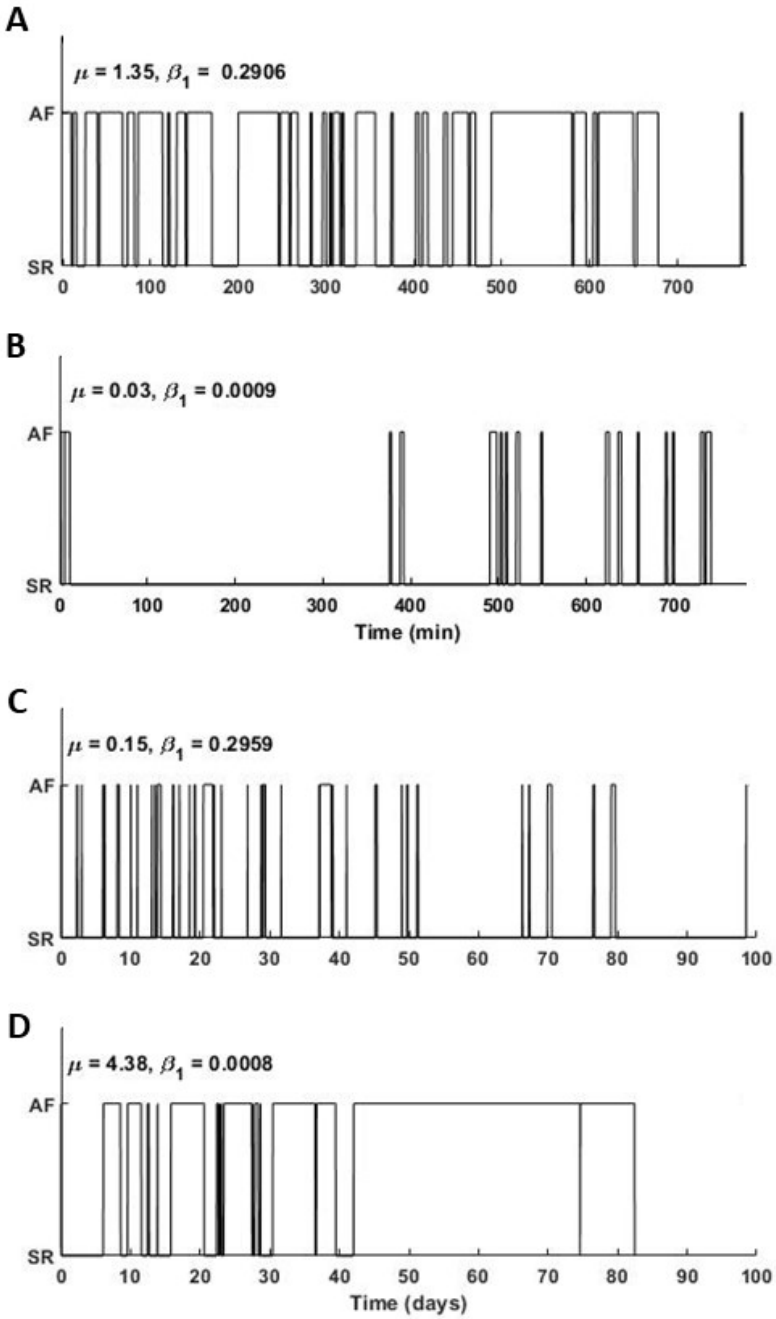

Figure 5.2. Episode patterns and the estimated Hawkes model parameters μ and β_1. (A) and (B) are short segments around 800 minutes with (A) episode pattern dominated by AF with a lower degree of clustering ($\beta_1 \approx 0.3$) and (B) episode pattern dominated by SR with a higher degree of clustering ($\beta_1 \approx 0$). (C) and (D) are long segments up to 100 days with (C) episode pattern dominated by SR and a lower degree of clustering and (D) episode pattern dominated by AF and a higher degree of clustering.

The cumulative deviation of the patient's actual burden from a hypothetical uniform burden level can be evaluated as:

$$\int_0^1 |F'(p;b) - p|\, dp, \tag{5.9}$$

where $F'(p;b)$ is the patient's actual burden, and $F(p;b) = p$ corresponds to the hypothetical uniform burden level defined by the burden evenly distributed throughout the monitoring period.

Conversely, the hypothetical maximum burden aggregation is defined by the total burden comprised in one continuous episode and equation (5.9) can be simplified to:

$$\frac{(1-b)}{2}. \tag{5.10}$$

Finally, the AF density is defined as:

$$AF\ density = 2\frac{\int_0^1 |F(p;b) - p|\, dp}{1-b}, \tag{5.11}$$

and assumes values on the interval [0,1], where a value close to 0 indicates a homogeneous distribution of AF burden, whereas a value close to 1 indicates that AF burden is confined to an interval much shorter than the monitored period. Figure 5.3 shows examples of temporal aggregation for two patients with similar levels of AF burden and monitoring time, with low and high temporal aggregation.

5.2.3. Cohort

Out of the 99 patients which had available pre-ablation data introduced in Chapter 2, 19 were excluded due to previously failed ablation and 26 had less than 10 episodes before catheter ablation (the minimum number of episodes required by the model). Therefore, the analysis included 54 patients (age 56±11 years; 67% men) with a documented history of AF (74% PAF, the remaining being persistent AF), and ablation candidates.

The baseline and clinical characteristics of the study cohort are shown in Table 5.1.

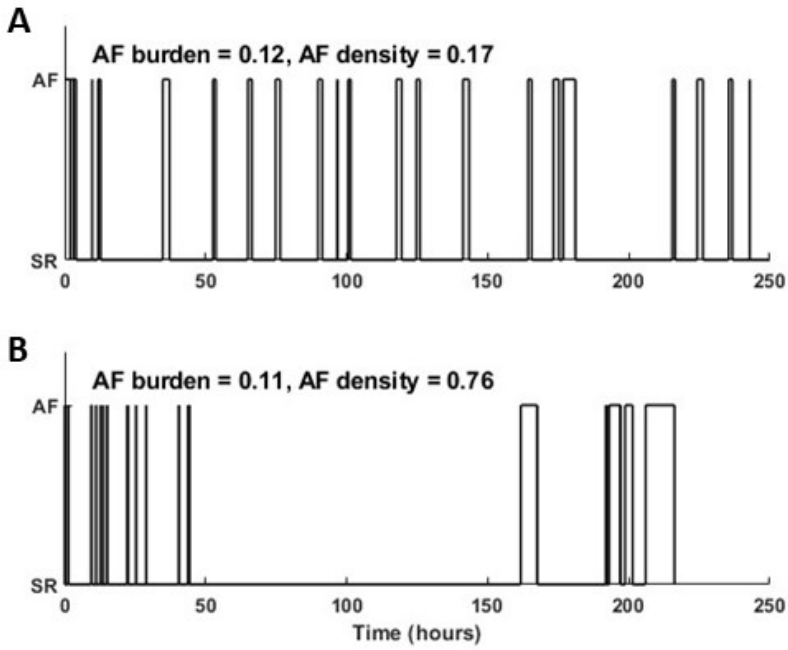

Figure 5.3. Patients with different types of temporal aggregation but with similar AF burden (≈ 0.12) with (A) low aggregation (AF density = 0.17) and (B) high aggregation (AF density = 0.76).

Table 5.1. Baseline and clinical data of the study population.

Feature	**Patient (N = 54)**
Age, years (mean ± SD)	56 ± 11
Coronary Risk Profile:	
Paroxysmal AF	40 (74%)
Hypertension	21 (39%)
Diabetes	7 (13%)
Coronary Artery Disease	3 (5%)
Stroke	3 (6%)

Values are given as no. (%) unless otherwise indicated
AF: Atrial fibrillation
SD: Standard deviation

5.2.4. Data Collection

The ICM was implanted for an average period of 2.7 (1–15) months, median (min-max), before the ablation procedure and the patients had 10.9 (3–4) months, median (min-max), follow-up for AF recurrence detection. AF recurrence was defined as an AF episode detected by the ICM after a 3-month blanking period following catheter ablation. The blanking period is based on reports on the efficacy of catheter ablation describing how early recurrences could be caused by post-ablation inflammation or short-term autonomic imbalance rather than ablation failure [83].

The devices and the AF detection algorithm used in this study have been introduced in 1.5.2. The detection algorithm makes a rhythm classification every 2 minutes [117]. This provides us the values for d_1 and d_2, the minimum duration of AF and SR, respectively. Due to memory restrictions described in 1.5.2, only data from the last 30 episodes before each data download were available. Nonetheless, several downloads could be grouped together if temporal continuity existed between them, increasing the number of episodes available for characterization.

In addition to the onset and duration of each AF episode, the device stored the daily AF burden in minutes for the entire monitoring period. An example of data extracted from the device is presented in Figure 5.4 with the ablation date and the end of the 3-month blanking period marked by dashed lines. It also shows the rhythm condition (either SR or AF) of the patient extracted from each session (color-coded) where the onset and duration of the episodes can be derived, and the daily AF burden stored for the entire monitoring period highlighting AF burden during the stored sessions. Figure 5.5 shows the rhythm condition of the last session before catheter ablation and its daily AF burden corresponding to the second session (orange) shown in Figure 5.4.

5.2.5. Statistical Analysis

The four parameters $\log(\mu)$, β_1, AF burden and AF density were computed using the episode information of the last available session, i.e., the last information download done by the clinician, before catheter ablation. Continuous data are presented as mean ± standard deviation if the null hypothesis H_0 of the Kolmogorov–Smirnov test (H_0: data is normally distributed) was not rejected. Otherwise, continuous data are presented as median (min-max). Categorical data are presented as absolute frequency (relative frequency in percentage). The primary endpoint (time to AF

recurrence) was analysed using the Kaplan–Meier method and the null hypothesis was tested by means of the log-rank test. The hazard ratio (HR) and its confidence intervals were computed using Cox's proportional hazards models. This study aimed at evaluating the risk stratification capabilities of the computed parameters on their own and in combination which would account for both AF prevalence ($\log(\mu)$ or AF burden) and AF episode aggregation (β_1 or AF density).

The combinations analysed were the Hawkes combination ($\log(\mu)$ and β_1) and the combination of AF burden and AF density. For the one-parameter prediction, the patients were dichotomized into high- and low-risk groups based on the optimal cut-off value chosen to maximize the separation between groups. This was accomplished by evaluating the Cox proportional hazard regression in the different groups of patients divided by a threshold that varied from quantile 25-75% with 5% increments. The regression with the lowest p-value was selected as the optimum separation cut-off. In case of β_1, the parameter was found to be bimodal so the cut-off was selected as the average between the lower limit ($\beta_1 \approx 0$) and the upper limit ($\beta_1 \approx 0.3$). In the two-parameter prediction, a linear combination of the selected parameters and the corresponding regression coefficients in the Cox model was computed and high- and low-risk groups were defined, based on the median of the combination. The Hawkes combination, defined by log(μ) and β_1, provides information on dominating rhythm (AF or SR) and episode clustering. Similarly, the combination of AF burden and AF density provides information on dominating rhythm and episode aggregation. The null hypothesis was rejected when $p < 0.05$, then set as the level of significance. The statistical analysis was performed using Matlab R2019b (The Mathworks Inc., Natick, Massachusetts).

5.3. Results

During the monitoring period before ablation, the patients had between 1 and 4 data downloads with 96 (20–188) days between scheduled appointments. For the present analysis, the focus was set on the last data download before ablation which in 43 (80%) patients occurred 1 month before ablation (75% during the last week) and contained 29 (10–37) AF episodes within a monitoring period of 9.8 (23.3) days, ranging from 2.6 h to 7 months.

The relationship between the parameters was explored and out of the considered variables, only AF burden showed high correlation with $\log(\mu)$ ($r = 0.78$; $p < 0.001$). Even though both β_1 and AF density reflect different aspects of episode aggregation,

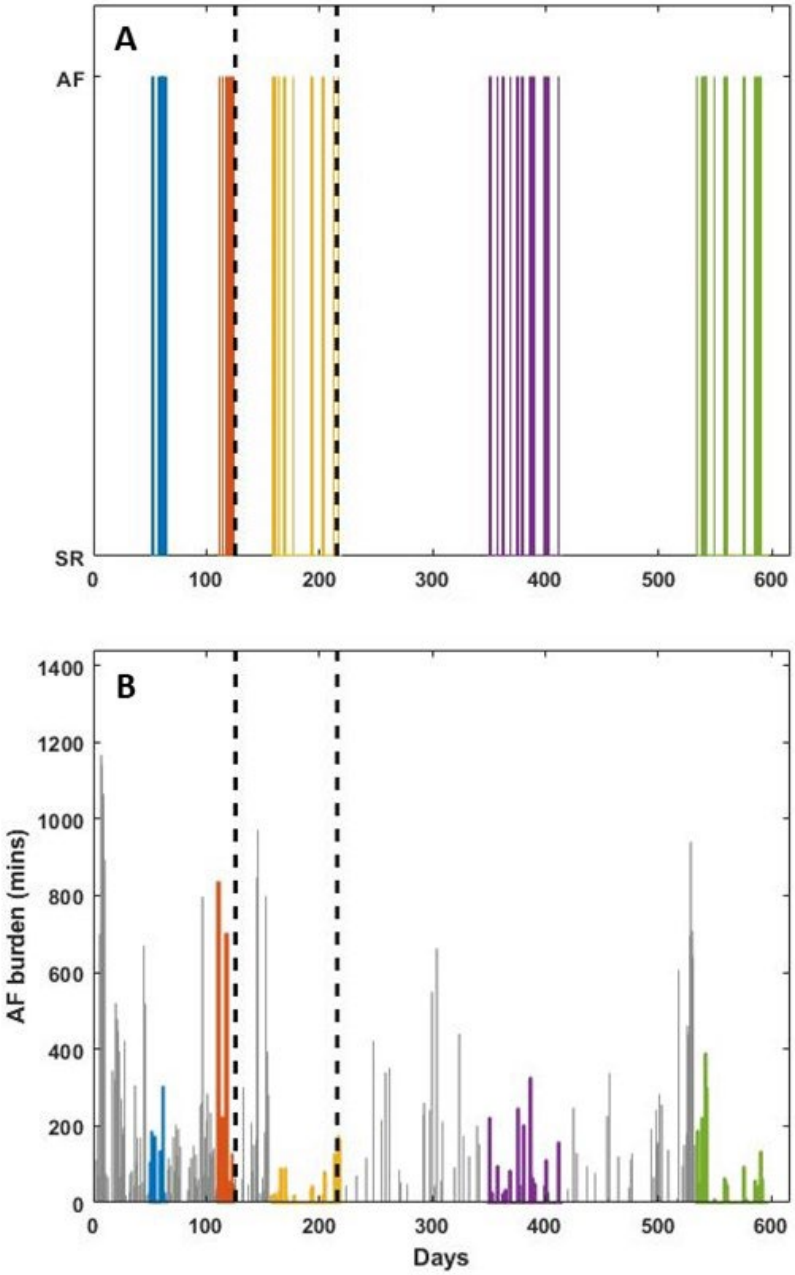

Figure 5.4. Example of data extracted from Reveal LINQ presented as a function of days of monitoring; the leftmost dashed line marks the catheter ablation and the following dashed line the end of the 3-month blanking period. (A) Episodes with onset and duration. (B) Daily AF burden detected in minutes (grey) with highlights on the days where the episodes have onset and duration information (color-coded as in (A)).

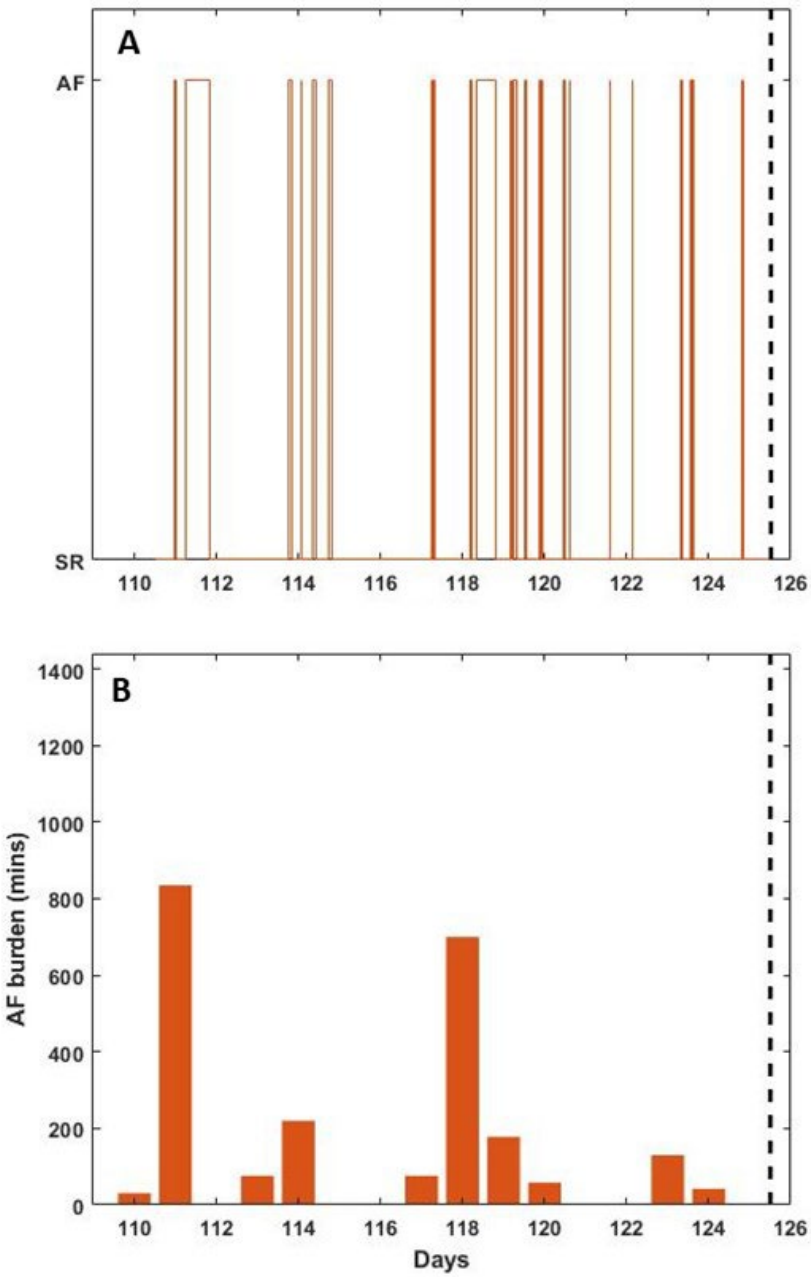

Figure 5.5.(A) Episodes with onset and duration downloaded from the last session before catheter ablation (second session in Figure 5.4. and (B) daily AF burden detected in minutes during the last session before catheter ablation.

they were found to be weakly correlated (r = -0.07; p = 0.63), and, therefore, may provide complementary information. When studying the distribution of β_1, it was

found to be bimodal showing that AF episodes were either highly clustered or uniformly distributed throughout the monitoring period.

In the analysed cohort, 41 patients (76%) had AF recurrence within 15 months following catheter ablation and the overall estimated event-free rate at 1 month after the blanking period (4 months after catheter ablation) was 39%. The statistical analysis of the parameters extracted from the last data download shows that there are no statistical differences between patients having had AF recurrence and those not having (p > 0.05 for all parameters).

The one-parameter analysis showed no significant differences (log-rank p > 0.05) between high- and low-risk groups for the selected parameters (Figure 5.6).

In two-parameter Cox analysis, AF burden and AF density were linearly combined and weighted with their respective Cox coefficient (0.03 for AF burden and -0.02 for AF density). The positive coefficient indicates a positive effect of the covariate AF burden to the risk of AF recurrence, meaning that more AF would increase the risk of AF recurrence. Conversely, a negative coefficient for AF density indicates that a higher AF density, i.e., a higher episode aggregation, reduces the risk of AF recurrence.

The combination of AF burden and AF density (Figure 5.7 (A)) is related to a 1.09 (95% CI, 0.60–2.01; p = 0.77) higher risk of early recurrence between the high- and low-risk groups (defined by the median value of the combination); however, the results are non-significant for this combination.

The parameters $\log(\mu)$ and β_1 were also linearly combined and weighted with their respective Cox coefficient (0.23 for $\log(\mu)$ and -0.36 for β_1). The positive effect of the covariate $\log(\mu)$ to the AF recurrence risk indicates that a higher AF dominance would increase the risk of AF recurrence, while a negative coefficient for β_1 indicates that a higher β_1, i.e., less episode clustering, reduces the risk of AF recurrence. In this case, the combination of $\log(\mu)$ and β_1 is associated with a higher risk of early AF recurrence with an HR of 1.95 (95% CI, 1.03–3.70; p < 0.05) (Figure 5.7 (B)). The estimated event-free rates at 1 month after the blanking period were 31% for high-risk patients and 49% for low-risk patients. In addition, 21 (78%) patients at high risk had AF recurrence, while 20 (74%) patients at low risk had AF recurrence (chi-squared p = 0.31). Even though both groups had similar proportions of AF recurrence, the survival times for the patients at high risk which had AF recurrence was less than 10 months while for those in the low-risk group was 14 months.

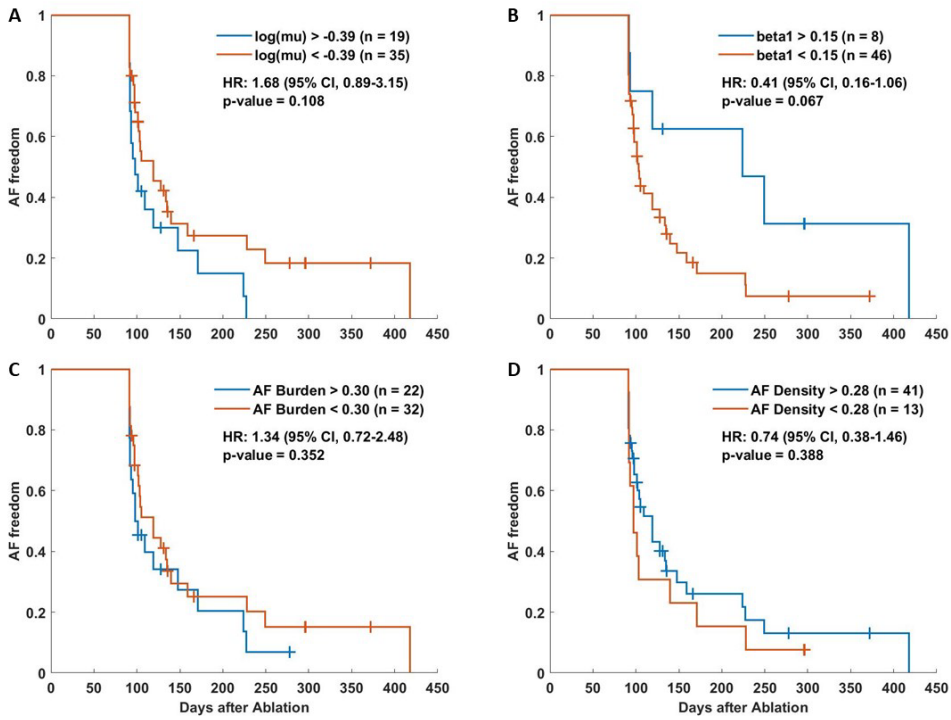

Figure 5.6. Kaplan-Meier curves for AF freedom after catheter ablation using each parameter as a risk predictor: (A) $log(\mu)$, (B) β_1, (C) AF burden and (D) AF density. The legend of each panel shows the threshold used and the number of patients in each group, and the panels show the hazard ratio (HR) and the 95% confidence intervals with their significance levels. (+) symbolize the censored patients.

5.4. Discussion

ICMs with high AF detection accuracy offer the unique advantage of long-term monitoring periods spanning several months which can lead to a more detailed characterization of AF behaviour. With the rapidly increasing use these continuous monitoring devices for patients diagnosed with AF [157] and the relatively high recurrence rates post-catheter ablation [83], the need for a method to characterize AF episode patterns to evaluate the risk of recurrence is increasingly important. To the best of our knowledge, there have been no studies using episode pattern characterization method as AF recurrence risk predictor. Our approach is also the first one comparing different parameters to determine the risk of AF recurrence in a cohort of continuously monitored AF patients outside of the restrictions 24-hour Holter devices entail. The main finding of this study is that the combination of

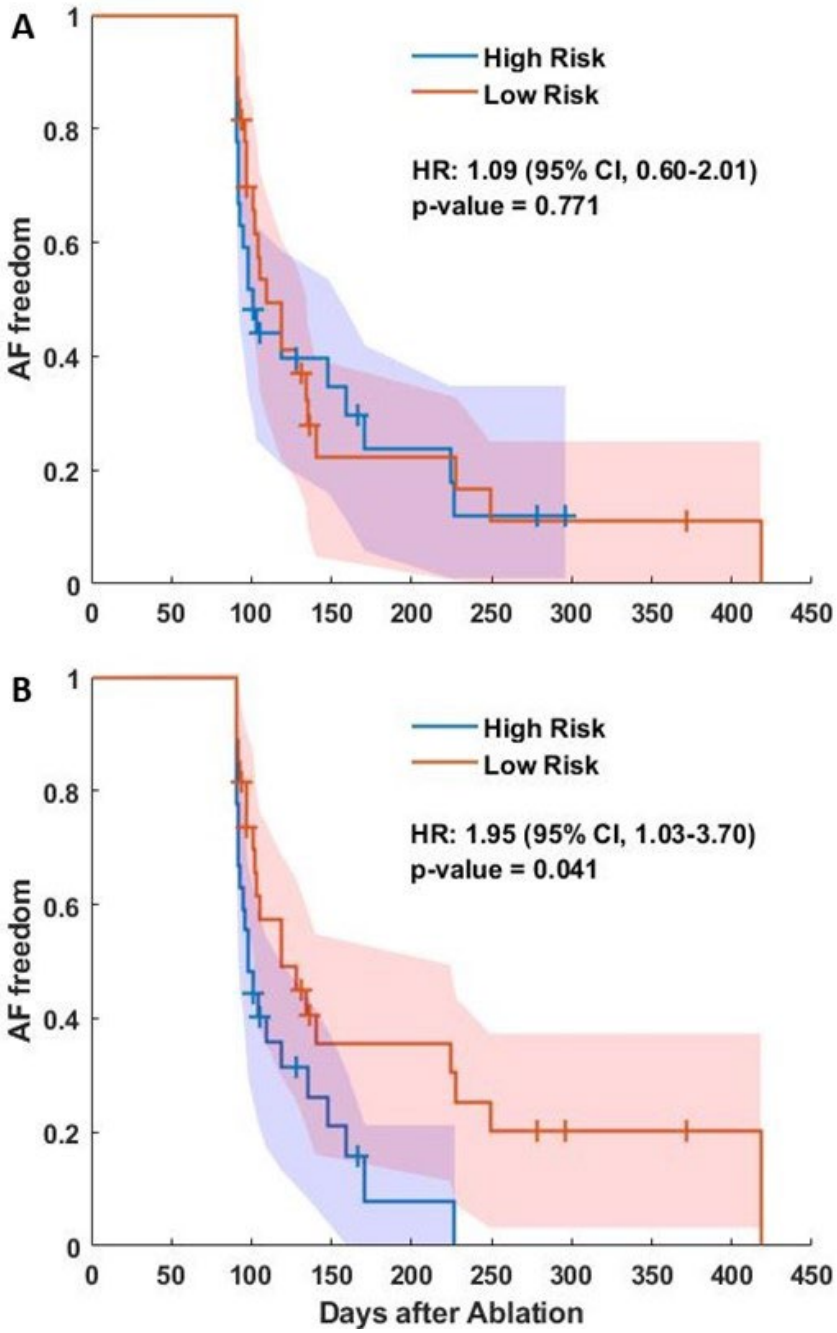

Figure 5.7. Kaplan-Meier and 95% confidence intervals curves for AF freedom after catheter ablation combining (A) AF burden and AF density, and (B) the Hawkes parameters. The panels show the hazard ratio (HR) and the 95% confidence intervals with their significance levels. (+) symbolize the censored patients.

$\log(\mu)$ and β_1 can significantly divide patients into groups of low and high risk of AF recurrence.

In recent years the problem of how to characterize episode patterns has received certain attention. However, it has been mainly focused on statistical analysis of either interepisode intervals, i.e. the interval between consecutive AF episodes [169–171] or inter-detection intervals, i.e. the intervals between onset of consecutive AF episodes [172]. The main drawback of this type of analysis is that it resides on the assumption that episodes are statistically independent, which may be questioned since AF episodes tend to cluster [170].

The alternating, bivariate Hawkes model was developed to provide a model-based, statistical approach to characterizing the dynamics of episode patterns [174]. While that work conjectured that the episode pattern could offer insight into AF and the degree of atrial electrical and structural remodelling, the clinical significance of $\log(\mu)$ and β_1 has not been established previously.

Numerous risk factors have been linked to recurrent AF after ablation, including thromboembolic risk predictors like $CHADS_2$ or CHA_2DS_2-VASc [10] and other specific rhythm outcome predictors such as APPLE [11], SUCCESS [12] and MB-LATER [13]. These scores have shown limited risk evaluation capability and have the drawback of relying on the detection of AF recurrence in patients using conventional Holter devices and the need of image-based parameters such as ejection fraction or left atrial diameter. In particular, MB-LATER uses early recurrence of AF as a feature and therefore cannot be used to evaluate the risk of AF recurrence before attempting the catheter ablation procedure. Conversely, the proposed method uses a subset of parameters estimated from a model-based approach which characterizes AF episode patterns in a continuously monitored cohort of patients.

In the analysis of the recurrence predictors, no statistical differences were found between the Recurrence and No Recurrence groups. However, when studying β_1, we found that a higher proportion of patients with AF recurrence had more clustered episodes, i.e., β_1 close to 0 (90% vs 69%, chi-squared p = 0.724). Although this gives us a first indication that patients with more episode clustering may have a higher risk of AF recurrence, the overall proportion of patients with more clustering is also high (85%) and the population is biased towards patients with AF recurrence.

Unsurprisingly, when evaluating the relationships between covariates, $\log(\mu)$ and AF burden had significant correlation ($r = 0.78$; $p < 0.001$) as both parameters provide information on AF dominance ($\log(\mu) > 0$ and AF burden > 0.5). However, β_1 was weakly correlated with AF density, and, while both features describe the degree of

episode aggregation, β_1 extracted from a statistical model and AF density being an ad hoc parameter, these parameters may provide complementary information.

The parameters studied were estimated from the episodes stored from the last session available before catheter ablation containing episodes with durations from 2.6 hours to 7 months. To produce a more homogeneous results and taking advantage of the long monitoring periods of the Reveal, the multivariate analysis was also computed for the last 4 weeks before the ablation. A monitoring period of 4 weeks was chosen as it was the minimum pre-ablation period common for the cohort. In this case, only AF burden and AF density were computed due to that while the Reveal stores the daily AF suffered by the patient, the onset and duration of the individual episodes were unavailable. The combination of AF burden and AF density showed a non-significant HR of 1.00 (95% CI 0.55–1.84; p = 0.99). This result, combined with the non-significant result of the Cox analysis for AF burden and AF density estimated over the last session, suggests that both AF burden and AF density do not convey significant information for assessing the risk of AF recurrence in this cohort. While AF density has not been used to assess risk of AF recurrence before, AF burden levels were shown to be able to predict the risk of AF recurrence [178]. The study found a lower risk of AF recurrence with a lower pre-ablation AF burden in AF patients. However, a significant difference in risk was found between those patients with less than 1% AF burden and those with higher levels of AF burden. Our patient population has relatively higher AF burden levels as our cut-off threshold between high and low burden groups was defined as 30%.

The risk of AF recurrence for was found to have an HR of 1.95 (95% CI, 1.03–3.70; $p < 0.05$). The combination showed that the risk was significantly higher for patients with a higher AF prevalence and associated with more episode clustering.

The $\log(\mu)$ and β_1 parameters of episode clustering may represent an early sign of transition from paroxysmal to persistent AF. The observed increased risk of arrhythmia recurrence once the novel criteria are present would be well in line with lower catheter ablation efficacy in patients with persistent forms of AF. If confirmed, this could be used as an early triaging mechanism pointing towards the need of accelerated referral for ablation.

The retrospective analysis carries certain limitations as, for example, it was based on a limited patient population from 2 different cohorts implanted with the Reveal LINQ ICM, which automatically detects AF episodes longer than 2 minutes. Therefore, episodes longer than 30 s, defined as AF episodes by the guidelines [6], but shorter than 2 minutes were undetected by the ICM. Furthermore, due to memory restrictions, only the onset and duration of the last 30 episodes detected by the ICM before each data download are stored. The 96 (41) days between scheduled

appointments (and therefore between data downloads) potentially resulted in a loss of AF episodes that could have been used to better characterize the episode patterns. In addition, due to the retrospective nature of the study, the medication administered to each patient during the monitoring period was not available. Despite these drawbacks, the advantage of having continuous monitoring of the patients before and after ablation greatly outweighs the disadvantages of possible information loss due the device resolution or memory restrictions. Using the Hawkes model, at least 10 episodes, i.e., 20 transitions, should be available to produce adequate results [174]; hence, with 30 stored episodes, the requirement is fulfilled.

5.5. Conclusion

The clinical relevance of AF episode pattern characterization using the alternating, bivariate Hawkes model is evidenced by its capability to predict AF recurrence post-catheter ablation. The proposed parameter combination is related to increased risk of AF recurrence within 1 year of the procedure for patients with more dominant AF and more episode clustering. This approach represents a preliminary step to demonstrate the clinical significance of AF episode pattern characterization as well as to popularize pre-ablation risk assessment which could be used in a more effective patient triage and reduce the economic and personal burden associated with the procedure.

Chapter 6 AF Recurrence Prediction

The publication related to this chapter is:

Saiz-Vivo J, Corino VDA, Hatala R, de Melis M, Mainardi LT**. Heart Rate Variability and Clinical Features as Predictors of Atrial Fibrillation Recurrence After Catheter Ablation: A Pilot Study.** Front Physiol. 2021;12:672896. Published 2021 May 25. doi:10.3389/fphys.2021.672896

6.1. Motivation

Long-term outcomes of catheter ablation in AF reported relatively low success rates[8]. Several well-established scoring systems aimed at predicting rhythm outcome after catheter ablation, including thromboembolic risk predictors like $CHADS_2$ or CHA_2DS_2-VASc, have shown modest prediction capabilities [10]. Other specific rhythm outcome predictors such as APPLE [11], SUCCESS [12], and MB-LATER [13] have achieved better results. However, most studies done so far have the drawback of relying on 24-hour Holter monitoring to detect AF recurrences, which was shown to have a rather poor detection rate for subclinical AF of 5.5% [14].

Heart Rate Variability (HRV) features have been proven to be predictors of chronic AF recurrence after electrical cardioversion [179,180] and extensive work has been done in describing the changes in HRV before and after ablation [181–184].

This chapter proposed the use of common HRV derived features in conjunction with clinical data to predict recurrences within the first 12 months after catheter ablation in a continuously monitored patient population. To accomplish this, the work evaluated several single classification methods including Support Vector Machines (SVM), with linear [185], polynomial (SVMp) and Gaussian (SVMg) kernels [186], Classification and Regression Trees (CART) and K-Nearest Neighbor (KNN) algorithms. In addition, the capabilities of ensemble learning methods [187] in which a weighted combination of the single classifiers is used as the predictor of AF recurrence was explored.

6.2. Materials

This retrospective study included patients introduced in Chapter 2. Out of the 99 patients with available pre-ablation data, 19 were excluded due to previously failed ablation and 6 due to incomplete data such as no medical and/or ablation records. The selected 74 patients ($57 \pm 12\ years$; $26\%\ NPAF$) were divided into two classes: those with AF recurrence ($R = 42\ patients$; $57\%\ of\ the\ total$) and those with no AF recurrence ($NR = 32$; 43%). AF recurrence was defined as presence of an AF episode longer that 2 minutes recorded by the ICM after a 3-month blanking period following catheter ablation. The blanking period of 3 months is used as suggested by the 2012 Consensus Statement of Catheter and Surgical Ablation of Atrial Fibrillation to report the efficacy of the ablation as early recurrences could be caused by post-ablation inflammation or short-term autonomic imbalance [188].

Both cohorts had more than 12 months follow-up for AF recurrence after catheter ablation.

The ICM was implanted 5.9 ± 3.8 months before the ablation procedures, which were classified as pulmonary vein isolation (PVI) or PVI plus Extra Lesions. These long monitoring periods ensure the detection of the AF onset of both paroxysmal and non-paroxysmal patients. The devices used in the Usability and the Slovakia studies were the Reveal LINQ and Reveal XT (Medtronic Inc, Minneapolis, MN), respectively and to optimize memory slots, store the R-peak timestamps and the ECG of the first 2 minutes of the AF episodes. For the last AF episode recorded, the device also stores the timestamps of the beats preceding the AF onset (Flashback). For the analysis, the first beats of the last recorded AF episode (477 ± 71 beats) before the catheter ablation and its Flashback (483 ± 33 beats) were extracted (D and A in Figure 6.1). The last AF episodes occurred between 1 and 183 days before the ablation.

6.3. Methods

6.3.1. Data Collection and Feature Extraction

From these two types of signals (Flashback and last AF episode) 4 different areas of interest (AoI) were defined: the whole Flashback (A), the first 300 beats of the Flashback (B), the last 100 beats of the Flashback (C), and the first beats of the AF episode (D) as shown in Figure 6.1.

Classical HRV derived features describing the variability and irregularity of the RR intervals were computed from the different AoIs and then categorized into 4 groups: whole Flashback (FB, AoI: A), Last 100 beats of Flashback (L100, AoI: C), Delta and First beats of AF episode (AF, AoI: D). Delta was defined as the percentage difference between the first 300 beats of the Flashback (AoI: B) and the last 100 beats of the Flashback (AoI: C) and was computed as:

$$Delta(f) = \frac{First300(f) - Last100(f)}{First300(f)} * 100 \tag{6.1}$$

with the aim of studying the changes occurring within the Flashback itself.

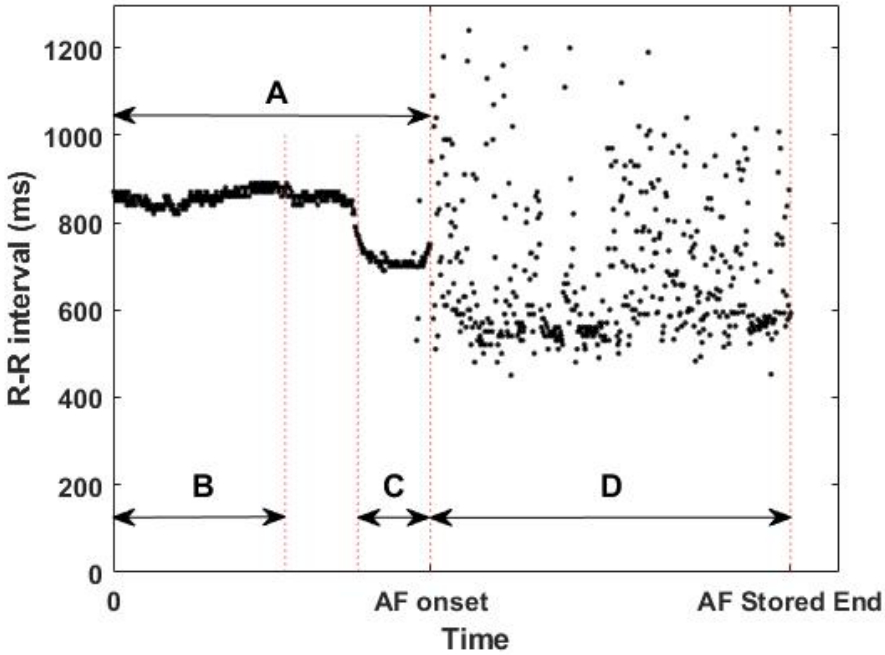

Figure 6.1. Example of available ICM data: A: Whole Flashback, B: First 300 beats of the Flashback, C: Last 100 beats of the Flashback, D: First two minutes of the last Atrial Fibrillation (AF) episode recorded before Catheter Ablation, illustrating short term changes in the RR intervals (ms) prior to the AF onset and the differences in RR intervals between the Flashback (A) and the AF episode (D).

The classical HRV derived features were Mean RR, pNN50, pNN20, RMSSD, SDNN, TINN, ApEn, SampEn and Poincare descriptors SD1, SD2 and SD1SD2ratio and were computed as described in Chapter 3**.** For this section, the triangular index (TRI), i.e., the integral of the density distribution of RR intervals [189] , and α1 and α2, the scaling components of short- and long- term fluctuations of the RR intervals from the detrended fluctuation analysis (DFA) [190], were also computed.

In addition to variability and irregularity features, clinical information such as the Age, AF type (Paroxysmal or Non-paroxysmal), Hypertension presence and Ablation type (PVI or PVI plus Extra lesions) were included in the analysis. 14 RR interval variability and irregularity features were computed for the 4 areas of interest, except pNN50 and pNN20 for Delta as the values for the First 300 beats of these features where 0 for some patients and the relative change could not be computed. A total of 58 features were considered per patient including the 4 clinical features, and the variability and irregularity features.

6.3.2. Classification

Based on the extracted features, 8 classification algorithms were evaluated to predict AF recurrence after a 3-months blanking period. As a first step, a test set was randomly selected, containing 22% of the data (8 patients with recurrence and 8 with no recurrence), which was used to evaluate the performance of the classifiers on never-before-seen data. The remaining 78% of the observations were processed by the classification algorithm, using 2/3 of the data to train the classification model (the training set) and 1/3 to validate the trained model (validation set) as illustrated in Figure 6.2.

The classification algorithm included the feature selection and the model training out of which the validation performance metrics were computed.

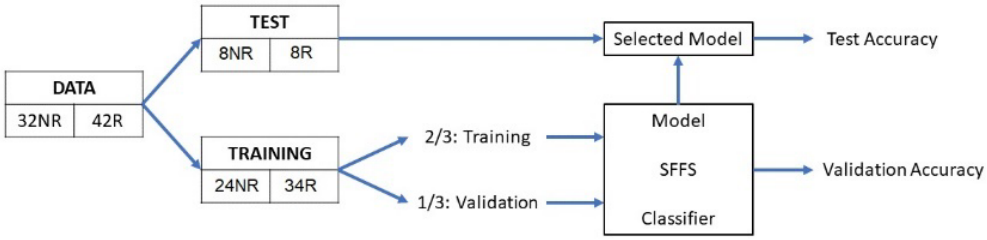

Figure 6.2 Schematic representation of the overall method. NR: No Recurrence; R: Recurrence; SFFS: Sequential Forward Floating Search

As a feature selection tool, the sequential forward floating search (SFFS) algorithm, was used. This algorithm considers and analyses subsets with different number of features by iteratively selecting the features that increase the overall accuracy of the model [191]. Briefly, starting from an empty set of features (S_k), the feature f_i that maximizes the objective function (accuracy) when combined with S_k, is added. After the forward step is repeated and a minimum of 3 features are already added, SFFS performs backward steps in which the feature that makes the objective function increase when removed from S_k, is removed [191].

A schematic representation of the algorithm is shown in Figure 6.3 which depicts an example of the forward and backward steps once 3 features are selected and the accuracy $Acc(3)$ is computed.

The trained model was evaluated on the test set, on which the performance metrics were computed.

The classification was performed using 2 types of classifiers: single classifiers and ensemble classifiers. The single classifiers were Support Vector Machines (SVM), Classification and Regression Trees (CART), and K-nearest neighbour (KNN); the ensemble classifiers were Mean Voting (MV), Accuracy Weighted Voting (AWV), and Optimum Weighted Voting (OWV).

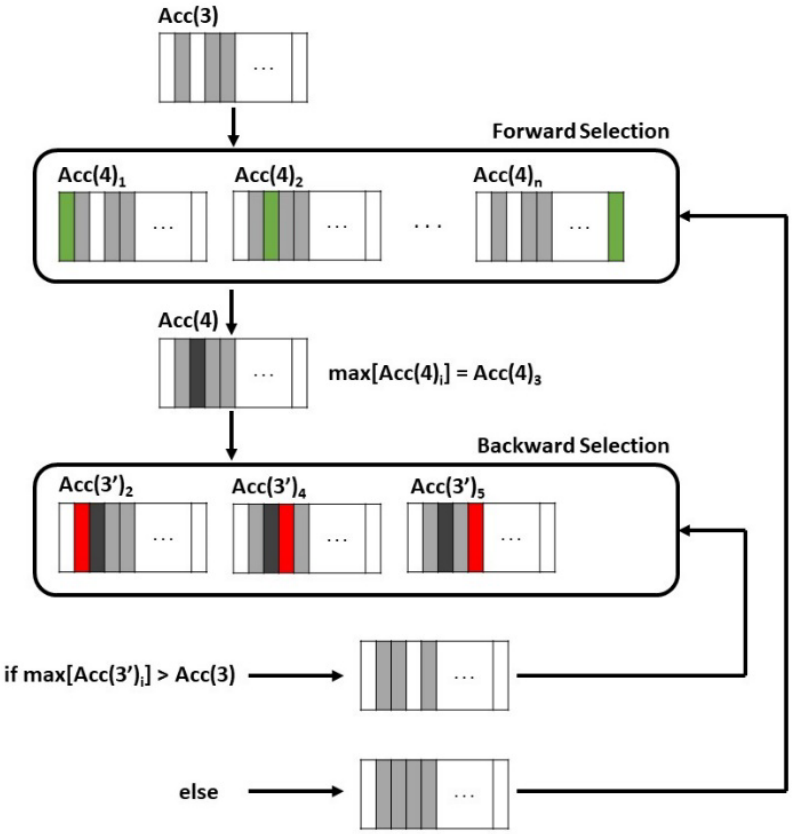

Figure 6.3 Schematic representation of the SFFS algorithm, as an example starting with three features already selected. The top rectangle represents the current set of 3 chosen features (grey lines) along with the unchosen features (white lines) which have an $Acc(3)$. In the Forward Selection step, each of the remaining features are iteratively added (green line) and the new accuracy $Acc(4)_i$ computed. Once the feature producing the maximum accuracy is selected and included in the selected set (black line), the Backward Selection step takes place. Each of the selected features, except the newly selected one, are removed from the selected feature set (red line) and the new accuracy $Acc(3')_i$ computed. If the maximum $Acc(3')_i$ is higher than the previous $Acc(3)$, the feature is removed from the selected features set and the Backward Selection is repeated, otherwise the algorithm goes to Forward selection where $Acc(5)_i$ are evaluated. Modified from [192].

The aim of SVM techniques is to devise a computationally efficient way of finding separating hyperplanes in an N-dimensional space that will minimize the generalization error, those which have the largest distance to the nearest training-

data point of any class (so-called functional margin) [185]. Support vectors are data points that are closer to a given hyperplane. This technique was originally designed to solve linear problems, however SVM can be adapted to work as a non-linear classifier by using non-linear kernels. In this study, in addition to linear SVM (SVM), 2 different non-linear kernels will be evaluated: Polynomial kernel (SVMp) with polynomial order equal to 3, and radial basis function or Gaussian kernel (SVMg) [186].

The CART technique classifies the observations into different groups of objects, a.k.a. branches, using decision rules learned from the pattern of features in the training data set. The split criterion used in this study was cross entropy which maximized the reduction of deviance in the new child branches. The cross-entropy function was defined as:

$$CrossEn = -\sum_{i} p(i) \log_2 p(i)\,, \tag{6.2}$$

where the sum is over the classes i at the node, and $p(i)$ is the observed fraction of classes with class i that reach the node. A node with just one class, i.e., a pure node has cross entropy 0; otherwise, the cross entropy is positive. The branches are iteratively created until every branch contains a single observation or the stopping criteria is met. No stopping criteria was used in this study.

The last single classifier used was KNN. This algorithm classifies the input features based on the classification of its K neighbours (K=3 in this study) [193]. To find the nearest neighbours the Euclidean distance was computed between the input and all the previously classified data points. Given an mx-by-n data matrix $\boldsymbol{X}$, which is treated as mx (1-by-n) row vectors $x_1, x_2, \dots, x_{mx}$, and an my-by-n data matrix $\boldsymbol{Y}$, which is treated as my (1-by-n) row vectors $y_1, y_2, \dots, y_{my}$, the Euclidean distances between the vectors x_s and y_t are computed as:

$$d_{st}^2 = (x_s - y_t)(x_s - y_t)' \tag{6.3}$$

After the distances are calculated and the K-neighbours selected, the classification of the input is made based on similarities between the input and its K-neighbours [187].

For the ensemble classifiers, the 5 classifications of the single classifiers were weighed and combined to classify a given observation x: $C(x)$, which is the result of the scalar product between the weight vector ($\boldsymbol{W}$) and the voting vector ($\boldsymbol{V}(x)$):

$$C(x) = \begin{cases} 1 \; if \; \boldsymbol{W} \cdot \boldsymbol{V}(x)^{\boldsymbol{T}} > 0.5 \\ 0 \; if \; \boldsymbol{W} \cdot \boldsymbol{V}(x)^{\boldsymbol{T}} \leq 0.5 \end{cases} \tag{6.4}$$

where the weight vector:

$$\boldsymbol{W} = [w_{SVM}, w_{SVMp}, w_{SVMg}, w_{CART}, w_{KNN}] \tag{6.5}$$

contains the weights for the single classifiers ($w_i \epsilon [0,1], \sum w_i = 1$), and the voting vector:

$$\boldsymbol{V}(x) = [v_{SVM}(x), v_{SVMp}(x), v_{SVMg}(x), v_{CART}(x), v_{KNN}(x)] \tag{6.6}$$

is the binary classification of the observation x made by the single classifiers.

Each ensemble algorithm had a different weight configuration. The MV algorithm was defined as the average of all the classifications, thus the single classifiers have the same weight:

$$w_{SVM} = w_{SVMp} = w_{SVMg} = w_{CART} = w_{KNN} = 0.2. \tag{6.7}$$

In the AWV method, the weights are proportional to the accuracy on the validation set of the single classifiers, thus being:

$$w_i = \frac{Accuracy_i}{\sum Accuracy_i} \tag{6.8}$$

with $i = \{'SVM', 'SVMp', 'SVMg', 'CART', 'KNN'\}$.

Finally, for the OWV method, all possible weight combinations (considering step of 0.1 for each weight) were iteratively evaluated and the set of weights that maximizes the overall accuracy of the validation set was selected.

The schematic in Figure 6.4 illustrates the general iterative process. Starting with an empty dataset with $Acc(0)$, each of the N features $[f_1, f_2, \dots, f_N]$ is evaluated. For each feature, the maximum accuracy from the different weight configurations $[\boldsymbol{W}_1, \boldsymbol{W}_2, \dots, \boldsymbol{W}_M]$ is chosen as $Acc(1)_n$. As shown previously in Figure 6.3, once the number of features is higher than 3, the Backward selection step takes place. The algorithm finishes when an optimum weight configuration and feature set are obtained for the N number of features.

Leave-p-out cross-validation (where p is 1/3 of the data) was performed with 100 bootstrap repetitions, i.e., all the above steps were repeated 100 times, randomizing the patient selection, allowing patients with both AF recurrence and without to be part of the training and validation phases.

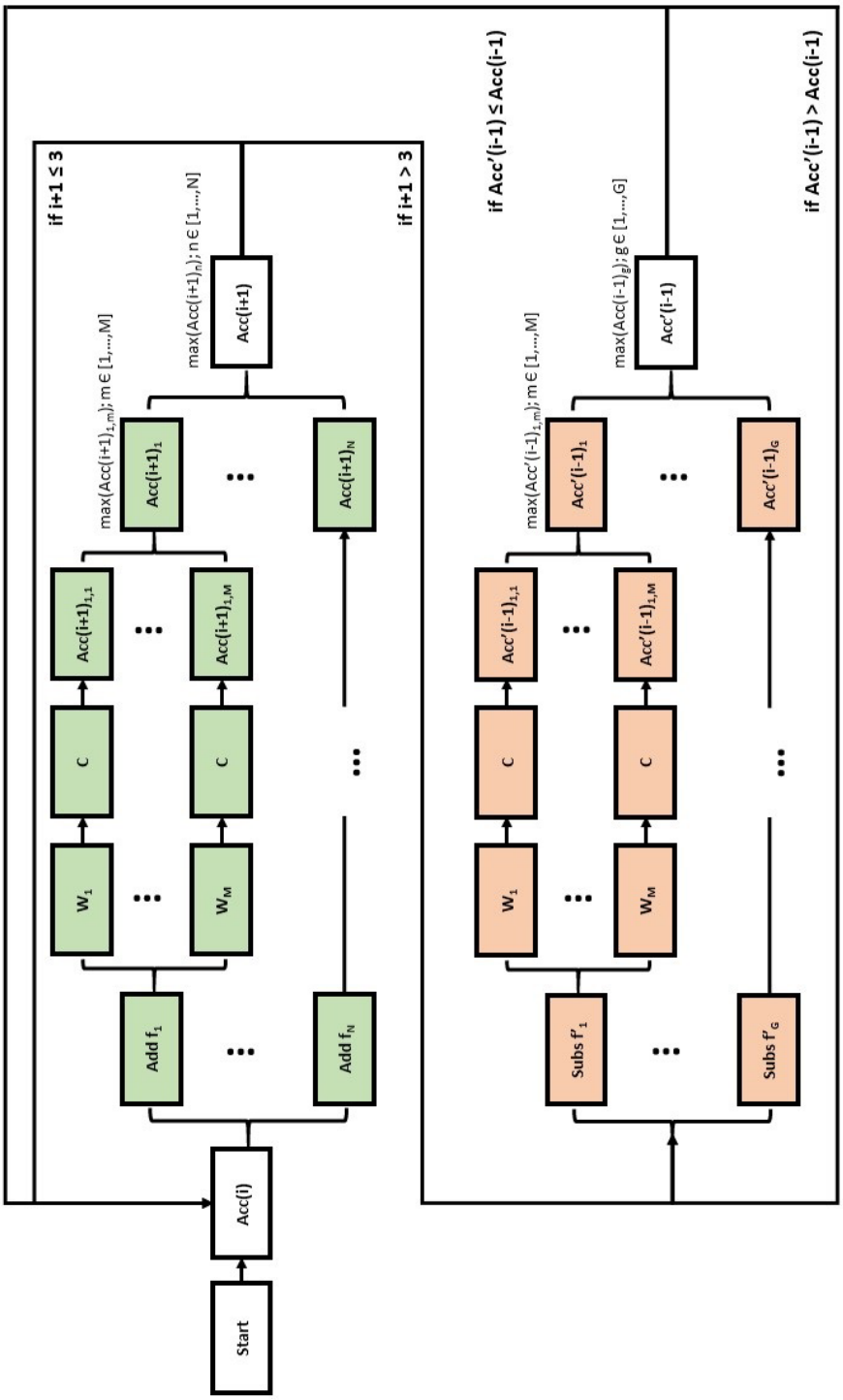

Figure 6.4. General schematic of the selection algorithm. The Forward selection stage is shown in green, and the Backward selection stage is shown in orange.

Performance metrics such as accuracy (Acc), sensitivity ($Sens$) and specificity ($Spec$) were then averaged over the repetitions while $F1\text{-}score$ was computed from the averaged confusion matrix, and were computed as:

$$Acc = \frac{TP + TN}{TP + TN + FP + FN} \tag{6.9}$$

$$Sens = \frac{TP}{TP + FN} \tag{6.10}$$

$$Spec = \frac{TN}{TN + FP} \tag{6.11}$$

$$F1\text{-}score = 2 \cdot \frac{PPV \cdot Sens}{PPV + Sens} = \frac{2TP}{2TP + FP + FN} \tag{6.12}$$

where TP is True Positive, TN is True Negative, FP is False Positive, FN is False Negative, and PPV is Positive Predictive Value. The feature extraction, selection and classification were conducted using Matlab R2019b (The Mathworks Inc., Natick, Massachusetts).

The statistic properties of the optimum set of features used by the classification method with the highest accuracy were analysed. Continuous data are presented as mean ± SD if the null hypothesis H_0 of the Shapiro-Wilk test (H_0: data is normally distributed) was not rejected and were compared with the unpaired Student's t-test. Otherwise, continuous data are presented as median (IQR), being IQR the interquartile range, and compared using the Mann-Whitney U test. Conversely, categorical data is presented as absolute frequency (relative frequency in percentage) and were compared with the Pearson Chi-Squared method. A p-value < 0.05 was considered for the rejection of the null hypothesis and set as the level of significance. All statistical analyses were conducted using SPSS version 23 (SPSS Inc., Chicago, Illinois).

6.4. Results

The available clinical baseline characteristics of the patients are shown in Table 6.1. Even though there are no statistically significant differences between the clinical baseline characteristics used in the analysis of the patients with and without recurrences (Age, Paroxysmal AF, Hypertension and Extra Lesions), patients with AF recurrence were in average 3.6 years older than those without.

Table 6.1 Clinical baseline characteristics of the patients that had No Recurrence and those who did.

Features	Patient (N = 74)		p
	No Recurrence (NR = 32, 43%)	**Recurrence (R = 42, 57%)**	
Age, years	56 ± 13	59 ± 12	0.20
PAF	26 (81%)	29 (69%)	0.18
Hypertension	19 (59%)	26 (62%)	0.83
Diabetes	1 (3%)	5 (12%)	<0.001
CAD	0	5 (12%)	<0.001
Stroke	3 (9%)	2 (5%)	<0.001
Pre-CA time, months	8.1 ± 3.7	4.3 ± 2.9	<0.001
Extra Lesions	5 (16%)	10 (24%)	0.39

PAF: Paroxysmal AF, CAD: Coronary Artery Disease, Pre-CA: Pre-Catheter Ablation

There was also a higher proportion of paroxysmal AF patients and a lower proportion of arterial hypertension patients among those who did not have AF recurrences. Diabetes, Coronary Artery Disease (CAD) and Stroke were excluded from the analysis as these features were heavily underrepresented.

The HRV derived features for each group of interest are shown in Appendix A as mean ± standard deviation for normally distributed data and as median (IQR) for non-normally distributed data. Only pNN20 for the whole Flashback (FB), delta triangular index (TRI), and Sample Entropy in the AF episode have a statistically significant difference between patients with and without AF recurrences.

6.4.1. Single Classifiers

Firstly, the single classifiers were evaluated by computing the accuracy on the validation set for subsets with an increasing number of features, as selected by the SFFS. Figure 6.5(A) shows the mean accuracies on the validation set of the single classifiers as a function of the number of selected features. It can be observed that all the classifiers reach a maximum of accuracy for the validation set with a subset containing less than 10 features except KNN (number of features = 18).

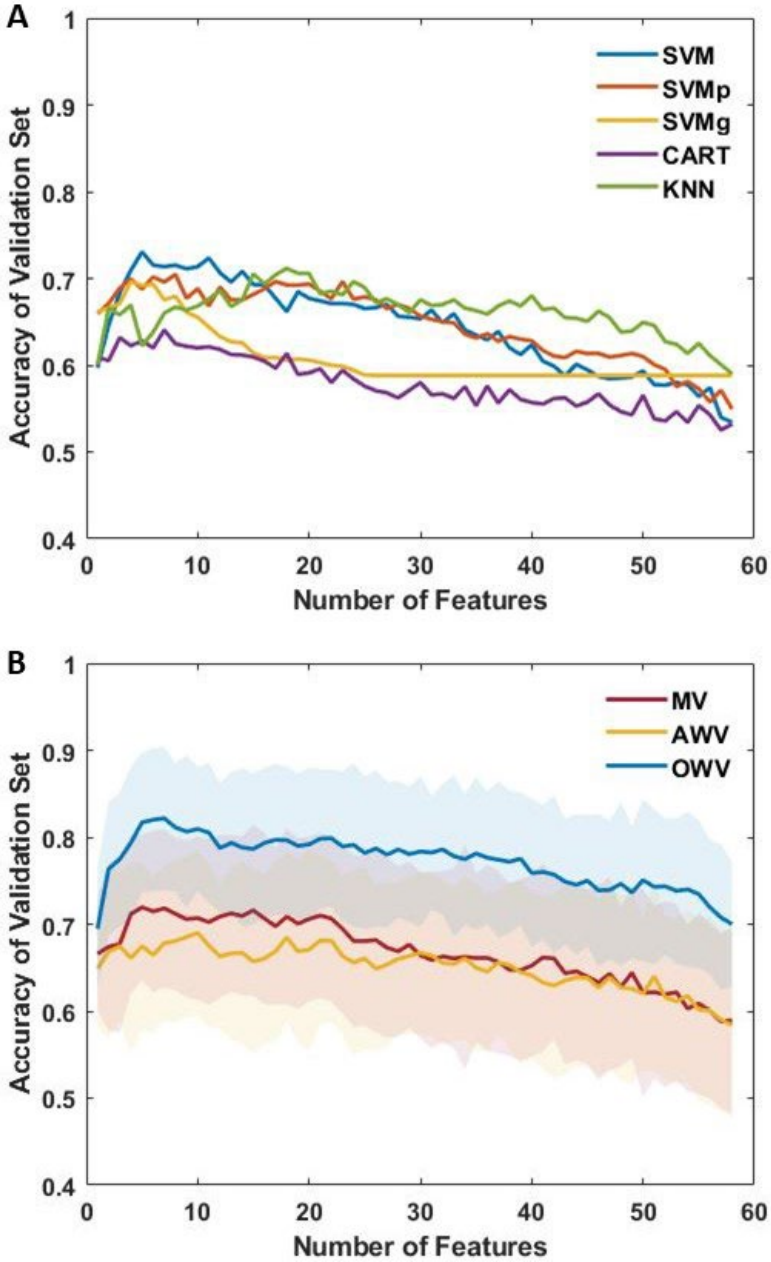

Figure 6.5 (A) Mean accuracy of the single classifiers on the validation set, plotted as a function of the number of selected features. (B) Mean and standard deviation of the accuracy of the multiple classifiers (line and colored area, respectively) for each subset of features on the validation set. AWV: Accuracy Weighted Voting; CART: Classification and Regression Trees; KNN: K-Nearest Neighbours; OWV: Optimum Weighted Voting; SVM: Support Vector Machine; SVMg: Support Vector Machine Gaussian kernel; SVMp: Support Vector Machine polynomial kernel.

For each single classifier, the feature subset that maximizes the validation accuracy is selected as the Optimum Feature set, which is used to evaluate the test using the trained model The performance evaluators for the test set were then computed in every iteration and Figure 6.6 depicts the mean and standard deviation. The F1-score, however, was computed from the averaged confusion matrix (also shown in Figure 6.6) as only the average score was of interest to compare different classifiers.

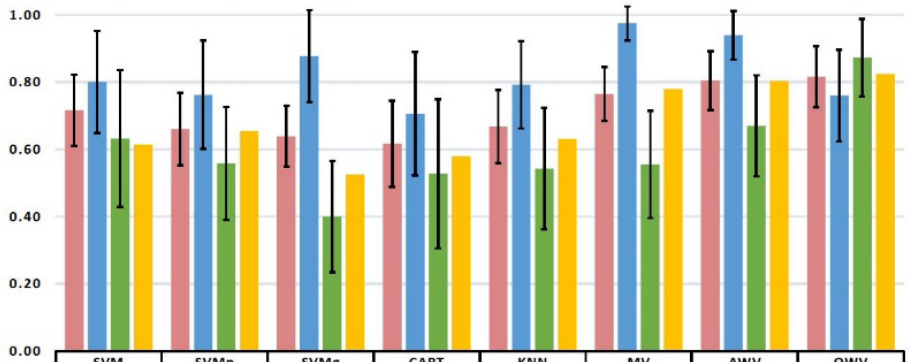

	SVM	SVMp	SVMg	CART	KNN	MV	AWV	OWV
Accuracy	0.72	0.66	0.64	0.62	0.67	0.77	0.81	0.82
Sensitivity	0.80	0.76	0.88	0.71	0.79	0.98	0.94	0.76
Specificity	0.63	0.56	0.40	0.53	0.54	0.56	0.67	0.87
F1-score	0.61	0.65	0.53	0.58	0.63	0.78	0.80	0.82

Figure 6.6 Mean and standard deviation of the performance metrics on the test set of the different classification methods. Table shows the mean values. AWV: Accuracy Weighted Voting; CART: Classification and Regression Trees; KNN: K-Nearest Neighbours; OWV: Optimum Weighted Voting; SVM: Support Vector Machine; SVMg: Support Vector Machine Gaussian kernel; SVMp: Support Vector Machine polynomial kernel.

When working with never-seen data, SVM had the highest accuracy (0.72 ± 0.11) and specificity (0.63 ± 0.20) while, SVMg had the highest sensitivity (0.88 ± 0.14). The highest F1-score (0.65) was obtained by SVMp.

6.4.2. Ensemble Classifiers

The single classifiers were then combined in an ensemble classifier in which a weighted combination of the single classification is used to compute the final classification. Figure 6.5(B) shows the mean (bold line) and the standard deviation (shaded area) of the accuracy of the validation set for the different ensemble classifiers. Similar to the single classifiers, the maximum accuracy was reached with less than 10 features. The optimum feature set was determined as the subset that maximized the accuracy on the validation set and the results for the ensemble classifiers comparison are shown in Figure 6.6.

The best overall classifier with the highest F1-score (0.82) is the OWV method in which the weights used to combine the different single classifiers are evaluated in each iteration. This method also has the highest accuracy (0.82 ± 0.09) and specificity (0.87 ± 0.12) on the test set while MV has the highest sensitivity (0.98 ± 0.05).

This OWV method of classification used a set of 7 features combining geometric delta features ("delta SD1SD2ratio") with complexity delta features ("delta ApEn"), statistical delta features ("delta RMSSD"), geometric AF features ("SD2 AF"), statistical AF features ("pNN20 AF"), statistical Flashback features ("pNN20") and clinical features ("Extra Lesions").

To provide added information and insight on the performance of the different classification models, the Receiver Operating Characteristic (ROC) curves from the single and the ensemble classifiers are shown in Figure 6.7 alongside their Area Under the Curve (AUC) values. SVM had the highest AUC value (0.75) of the single classifiers while AWV and OWV both obtained the highest overall AUC value (0.85).

The frequency of use of each of the feature groups, i.e. FB: Flashback, L100: Last 100, Delta, AF and Clinical by the different classification methods was also analysed. Figure 6.8 shows the percentage of each feature group used by the different methods.

Features from feature group Delta were the most frequently used by the different classifiers. In average, the classifiers used features from Delta group for 31% of their selected features, reaching 63% of the selected features for the SVMp method. However, it is worth noting that every classifier took at least "Extra Lesions" as one of the optimum features in their feature list and classifiers such as SVM, and SVMg had features from the Clinical group comprising more than 25% of their features, being SVMg the classifier with the highest percentage of use (40%).

6.5. Discussion

The main finding of this study is that a reduced set of HRV and clinical features extracted from an ICM can be used by an ensemble classifier to predict AF recurrence with a mean accuracy higher than 0.8 in patients that underwent single-procedure catheter ablation. If confirmed by future studies, these findings are potentially of significant clinical relevance for several reasons: first, catheter ablation of AF substrate is a procedure with high economic and personal burden; secondly, due to the epidemic character of AF prevalence, these interventions cannot be offered (even in countries with developed health-care systems) to all patients and third, the

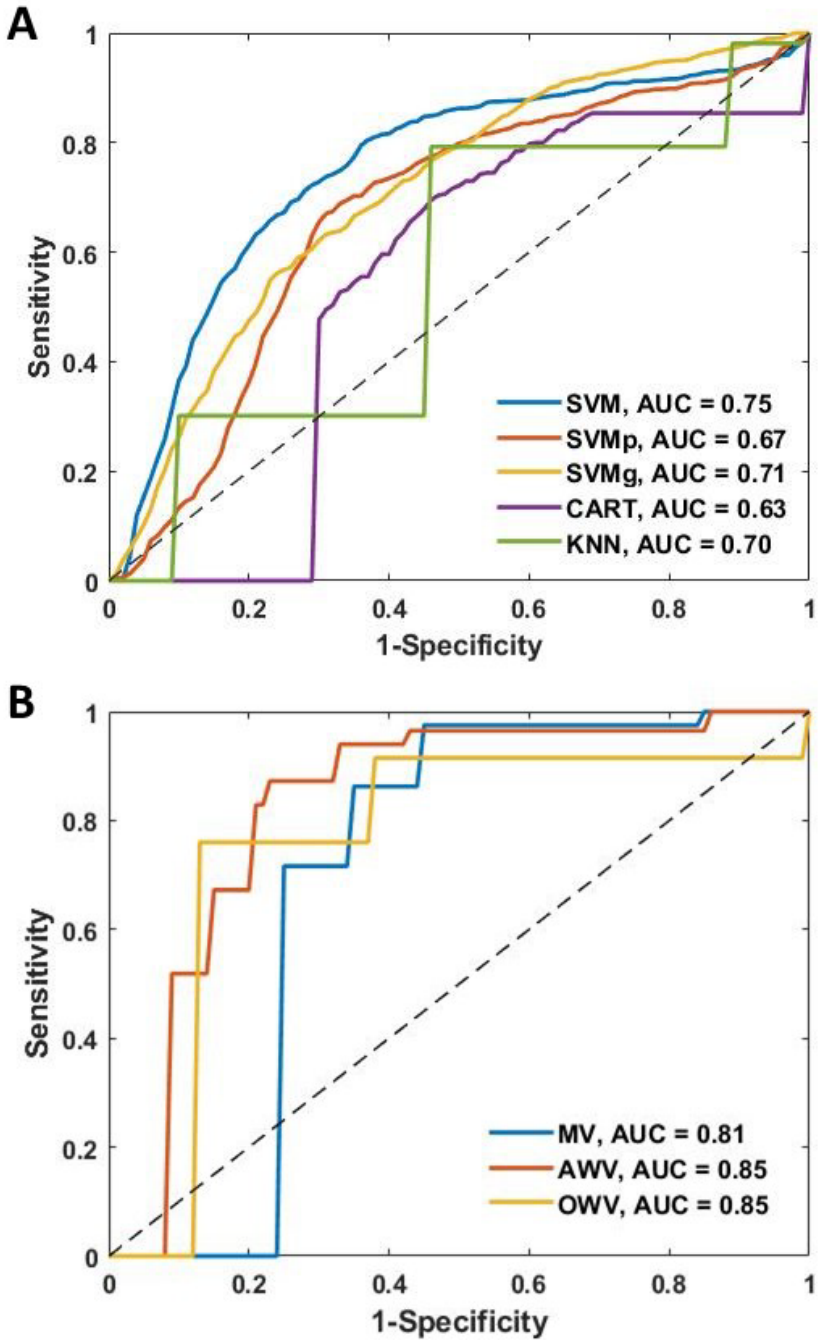

Figure 6.7 (A) Receiver Operating Characteristic (ROC) curves of the single classifiers and the Area Under the Curve (AUC). (B) Receiver Operating Characteristic (ROC) curves of the ensemble classifiers and the Area Under the Curve (AUC). AWV: Accuracy Weighted Voting; CART: Classification and Regression Trees; KNN: K-Nearest Neighbours; OWV: Optimum Weighted Voting; SVM: Support Vector Machine; SVMg: Support Vector Machine Gaussian kernel; SVMp: Support Vector Machine polynomial kernel.

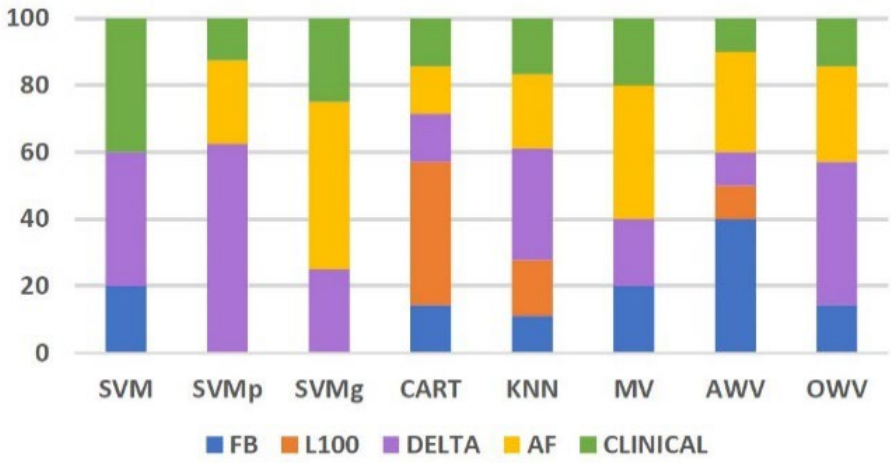

Figure 6.8 Percentage of features from each feature group used by the different classification methods. AF: Atrial Fibrillation; AWV: Accuracy Weighted Voting; CART: Classification and Regression Trees; FB: Flashback; KNN: K-Nearest Neighbours; L100: Last 100 beats; OWV: Optimum Weighted Voting; SVM: Support Vector Machine; SVMg: Support Vector Machine Gaussian kernel; SVMp: Support Vector Machine polynomial kernel.

selection of patients with higher probability of long-term elimination of AF has high priority. Until now, the various clinical scoring systems based on phenotypic biomarkers used to this aim generate a rather poor prediction of limited clinical usefulness.

HRV has been extensively studied with respect to procedural outcome by analysing the changes in HRV features before and after ablation [181–184]. However, these studies mainly describe the effect of ablation on HRV and use non-continuous Holter monitoring of the patients.

To the best of our knowledge, this is the first study that reports the combination of classical HRV and clinical features to predict AF recurrence in a continuously monitored ablation cohort using a variety of classification methods.

Although all the different HRV and clinical features were initially introduced in the algorithm, SFFS iteratively selected the optimum set and only 1 of the 8 different methods used had the peak performance with more than 10 features and OWV only used 7: delta SD1SD2 ratio, delta ApEn, delta RMSSD, pNN20 AF, SD2 AF and Extra lesions. Out of the 7 features found as optimum, only 1 was a clinical feature while the others were classical HRV features extracted from 3 different feature groups: delta, Flashback and AF. RMSSD and Poincare descriptor SD1SD2ratio both describe the variability of the RR intervals and so, when analysing the correlation between the features, it was not surprising to observe that they had an $R = 0.51, p < 0.01$ in

the 2-tailed Pearson correlation test. The rest of the features had weak correlation between them.

The most used feature group appeared to be Delta with an average use of 31% in the different classifiers and a maximum of 63% in SVMp which shows the importance of studying the onset of the AF contained within the Flashback.

Several studies have investigated different methods of AF recurrence prediction by analysing the impact of different clinical scores. While thromboembolic risk predictors like $CHADS_2$ or CHA_2DS_2-VASc showed relatively modest prediction [10], other specific rhythm outcome predictors such as APPLE [11], SUCCESS[12], and MB-LATER [13] have been introduced yielding better results. The APPLE score (one point for Age > 65 years, Persistent AF, imPaired estimated glomerular filtration rate (eGFR) < 60 ml/min/1.73 m2, Left atrial (LA) diameter ≥ 43 mm and Ejection Fraction (EF) < 50%) was originally developed to predict AF recurrences after first ablation with area under the receiver operating characteristic curve (AUC) of 0.634 [11] but has also been tested predicting recurrence in repeated ablations with AUC 0.617 [82]. Based on this score, the SUCCESS score was created by adding one point for each preciously performed ablation and although it did demonstrate an improvement over APPLE (AUC 0.657 vs 0.620), the findings were not significant in the study [12]. The MB-LATER score (Male, Bundle branch block, Left atrium ≥ 47 mm, Type of AF [paroxysmal, persistent or long-standing persistent], and ER-AF = early recurrent AF) was associated with patients who will develop very late AF recurrence i.e. recurrence documented more than 12 months after the ablation procedure (AUC 0.782) [13] and was also proven to predict late AF recurrence (AUC 0.62) [194]. However, this score has the drawback that it uses early recurrence of AF as a feature, and it cannot be used as a baseline predictor. All these scoring systems have the disadvantage of relying on conventional Holter devices to detect AF recurrence in the patients and the need of image-based parameters such as LA diameter or EF while the proposed method uses easily obtainable clinical information and classical HRV features extracted from a ICM which continuously monitors the patient.

In the review of AF recurrence predictors developed by Balk et al. the relationship between success of ablation for AF and clinical features was systematically evaluated [195]. The multivariable analyses showed that neither age, AF type nor hypertension showed significant association to ablation success. However, in the case of age, Balk et al. suggested that this result was due to the limitations of the existing literature rather than a true lack of association as only relatively young patients were included in the analyses (40-70 years). The patient population analysed in this study was relatively young $(57 \pm 12\, years)$ and this could be the reason why age was not

included in the final feature set. Even though the multivariate analyses performed by Balk et al. failed to show significant association between AF type and ablation success, the univariate analysis found that patients with NPAF had a 60% increased risk of AF recurrence compared to those with PAF and it was hypothesized that it would be a good clinical indicator of the likelihood of AF recurrence. In this study, AF type was chosen by only 2 of the 8 classification methods and while one was AWV, that had the second highest F1-score, the other one was SVMp, that had one of the lowest. This could be explained by the under-representation in the patient population of non-paroxysmal patients (25.7%) which translated into 18.8% of those which did not have AF recurrence and 31.0% of those who did. Ablation type was the only feature used by every method: from these preliminary results, patients that had extra lesions had also higher chance of having AF recurrence. Although there are some confounding factors to consider, i.e., the need of extra lesions may be due to a more advanced AF with a higher presence of fibrotic tissue in the atria, the extra scar tissue could be the foci of new re-entry circuits that could develop and sustain AF. Nonetheless, this feature was also heavily biased as most of the patients underwent PVI ablations and only 15 patients (20.3%) had also extra lesions so further work would have to confirm this.

This retrospective study was made using a limited patient population from 2 different cohorts with different clinical information, which limited the clinical features that could be used to those which were collected in both studies. Furthermore, the features that were included such as AF type and Ablation type were heavily biased as Persistent patients (26% of the total number of patients) and ablation strategies with extra lesions (20%) were underrepresented. However, the main part of this study was focused on HRV features and even though the use of the clinical features increased the accuracy and future work should be done to understand their impact, the presented classification method and the results are still clinically relevant. The sample size for this study is very limited, also when considering the partitions needed for the training, validation, and test set. This prevented us from using more complex classification approaches such as deep learning neural networks due to the risk of overfitting the data. The number of features extracted from the database was also concerning and could have increased the risk of overfitting the data. For this reason, the SFFS algorithm was used to minimize the number of features hence, minimizing the risk of overfitting. In addition, due to the retrospective nature of the study, the medication administered to each patient during the monitoring period was not available and the possible influence of medication on AF recurrence was not studied. The data were extracted from the Reveal LINQ ICM which automatically detected AF episodes longer than 2 minutes and, due to memory restrictions, stored the RR intervals of the episodes detected and their Flashbacks. Therefore, episodes longer than 30s, which are

defined as AF episodes by the guidelines, but shorter than 2 minutes were undetected by the ICM. The lack of stored ECG signals also limited the number of features that could be extracted and restricted the analysis to HRV derived features that could be extracted from the RR intervals. Despite these drawbacks, the advantage of having continuous monitoring of the patients before and after the ablation greatly outweighs the disadvantages of possible information loss due to device resolution or memory restrictions. Although the study shows promising results and serves as proof of the feasibility of the method described, being a pilot study, results should need to be validated on an external database.

6.6. Conclusion

Recurrence of AF after ablation can be predicted with varying degrees of accuracy using simple classification methods and an iteratively selected feature set of easily obtainable HRV and clinical features. The best approach is an optimally weighted combination of single classifiers which uses HRV (Poincare descriptors SD1SD2ratio, pNN20 Approximate Entropy, RMSSD and Triangular index) and clinical (extra PVI lesions) features. This could be a first step into a more effective pre-ablation patient triage that could reduce economic and personal burden of the procedure by increasing the success rate of first catheter ablation to achieve long-term AF termination.

Chapter 7 Conclusions and Future Work

7.1. Summary and main conclusions

The objective of this thesis was to propose methodological advancements for the characterization of the AF triggers and AF episodes detected by ICMs in cohorts of continuously monitored patients, to attain a better understanding of AF and its mechanisms. This may lead to improvement in clinical decisions, as those related to catheter ablation strategies which could lead to a more effective patient triage that could reduce the economic and personal burden of the ablation procedure by increasing the success rate of long-term AF termination. These methods have been evaluated in clinical conditions.

First, the AF triggers found in the last 500 beats preceding an AF episode extracted from ICMs on a cohort of continuously monitored patients were characterized using HRV features. In addition, an automatic unsupervised classification based on the linear combination of a subset of the extracted features was evaluated. This approach allowed us to find which HRV features were the most representative for the different triggers and showed that distinct patterns could be found in the different clusters.

Then, the AF episodes stored in the ICM were characterized by studying the circadian variations of their f-wave frequency, and their temporal aggregation. The circadian variations were analysed by modelling the AFR as a function of time of onset using a mixed-effect modelling approach. This enabled us to correct the model for the effect of episode duration, previous ablations, and changes is autonomic tone quantified by RR series characteristics as well as dealing with repeated measures within subjects. The temporal aggregation of the AF episodes detected by the ICM was achieved using the alternating bivariate Hawkes model. This model outputs the AF dominance and the temporal clustering of episodes during the monitoring period. This approach allowed us to prove that the risk of AF recurrence within 1 year after the catheter ablation procedure was higher for patients with high AF dominance and high episode clustering and may be used for pre-ablation risk assessment.

Finally, a new algorithm was designed for catheter ablation outcome prediction based on clinical and HRV features extracted from both the last AF trigger and the AF episode before the procedure. The results obtained from this method suggest the importance of appropriate characterization of both the AF trigger and the AF episode to enable a more effective pre-ablation patient triage strategy that could reduce economic and personal burden of the procedure by increasing the success rate of first catheter ablation to achieve long-term AF termination.

7.1.1. Trigger Characterization

Catheter ablation of atrial fibrillation (AF), specifically pulmonary vein isolation (PVI), is a common treatment for highly symptomatic patients [7]. However, a systematic review study of long-term outcomes of catheter ablation in AF reported single-procedure success rates as low as 66.6% in paroxysmal AF (PAF) patients and 51.9% in non-paroxysmal AF (NPAF) patients [8].

Pokushalov et al. [17] showed an improvement of the success rate, reaching 89%, in a second ablation procedure in patients with a specific AF trigger onset. Motivated by Pokushalov et al.'s findings, a study using the Flashback to determine the optimum ablation strategy before a first failed ablation attempt was designed. However, the visual annotation of the triggers in the Flashbacks, especially in large populations of patients is a far from trivial matter. Therefore, an automatic classification of AF triggers is needed.

Supervised classification methods rely on having a sufficiently representative set of training data which is to be manually selected and annotated, which in turn is expensive and time-consuming to obtain, and may introduce bias.

In this thesis, the data used was provided by an implantable cardiac monitor (ICM) equipped with a highly sensitive AF detection algorithm (96%) [15] which continuously classifies the heart rhythm of a patient by analysing its cardiac cycle. In addition, it stores the trend of 500 ventricular beats preceding the detection marker of the most recent AF episode, hereinafter called Flashback.

The results obtained when analysing the HRV features from the different clusters extracted from the Flashbacks showed that distinct triggers could be found. Although the inference of clinical information from unsupervised classification of patterns has relative reliability, the triggers that could potentially be identified in the clusters are premature atrial complexes (PACs), atrial tachycardia (AT), atrial flutter and spontaneous AF, i.e., no trigger. As mentioned before, this study is a first step towards aiding clinicians in determining the optimum ablation strategy before a first failed ablation attempt based on the AF trigger.

7.1.2. AF Characterization

This thesis approaches AF episode characterization focusing on two different aspects of the episodes. First, analysing individually each AF episode by studying the

variations of their f-wave frequency, i.e., atrial fibrillatory rate (AFR), and then, analysing the temporal aggregation of the AF episodes detected on a particular patient.

This study investigated the feasibility of modelling AFR based on RR series characteristics while accounting for possible effects of previous ablations, episode duration and onset date and time. In a previous study regarding AFR and HRV, the analysis was conducted only on patients with underlying congestive heart failure and didn't account for the presence of confounding factors[144]. This thesis assesses the use of a simple fixed-effect (FE) modelling approach using RR series features and compares it to a more complex mixed-effect (ME) modelling approach to study both the population and patient specific effects of RR series in AFR, and to another ME modelling approach that allowed correction for the effect of episode duration, previous ablations, and possible circadian variations. The ME modelling approach was shown to be superior to the FE modelling approach due to the heterogeneity of the patient population and the presence of confounding factors. The fixed effects extracted from the ME model showed that AFR is slightly higher in episodes of longer duration and with less organized RR series and is affected by catheter ablations. The use of ME models combined with long term monitoring of patients offers the chance of continuously estimating the AFR from RR series and episode-based characteristic and will lead to a more detailed characterization and a better understanding of the patients' condition which could potentially aid the clinicians in their decision-making process.

In recent years the problem of how to characterize episode patterns has received certain attention. However, it has been mainly focused on statistical analysis of either interepisode intervals, i.e. the interval between consecutive AF episodes [169–171] or inter-detection intervals, i.e. the intervals between onset of consecutive AF episodes [172]. The main drawback of this type of analysis is that it resides on the assumption that episodes are statistically independent, which may be questioned since AF episodes tend to cluster [170]. The alternating, bivariate Hawkes model evaluated in this thesis was developed to provide a model-based, statistical approach to characterizing the dynamics of episode patterns [174]. This thesis compared different parameters to determine the risk of AF recurrence in a cohort of continuously monitored AF patients outside of the restrictions 24-hour Holter devices entail. The proposed combination of Hawkes parameters, one accounting for the dominance of AF during the monitoring period and one describing the temporal aggregation of the episodes, was related to increased risk of AF recurrence within 1 year of the procedure for patients with more dominant AF and more episode clustering. The approach presented in this thesis represents a preliminary step to demonstrate the clinical significance of AF episode pattern characterization as well

as to popularize pre-ablation risk assessment which could be used in a more effective patient triage and reduce the economic and personal burden associated with the procedure.

7.1.3. AF Recurrence Prediction

Catheter ablation, specifically pulmonary vein isolation (PVI), has become over the decades a common treatment for AF patients, especially those highly symptomatic [7] or those where antiarrhythmic drug therapy has not been sufficient (or tolerated) for rhythm stabilization [83]. However, long-term outcomes of catheter ablation in AF reported single-procedure success rates as low as 66.6% in paroxysmal AF (PAF) patients and 51.9% in non-paroxysmal AF (NPAF) patients [8]. Several studies have investigated different methods of AF recurrence prediction by analysing the impact of different clinical scores. While thromboembolic risk predictors like $CHADS_2$ or CHA_2DS_2-VASc showed relatively modest prediction [10], other specific rhythm outcome predictors such as APPLE [11], SUCCESS [12], and MB-LATER [13] have been introduced yielding better results. However, these scoring systems have the disadvantage of relying on conventional Holter devices to detect AF recurrence in the patients and the need of image-based parameters such as LA diameter or EF while the method proposed in this thesis used easily obtainable clinical information and classical HRV features extracted from a ICM which continuously monitors the patient. This method is based on an optimally weighted combination of single classifiers which uses HRV and clinical features to predict AF recurrence. As mentioned before, this could be a first step into a more effective pre-ablation patient triage that could reduce economic and personal burden of the procedure by increasing the success rate of first catheter ablation to achieve long-term AF termination.

7.1.4. Clinical Significance

An appropriate characterization of patients diagnosed with AF is crucial for deciding the optimum course of treatment such as catheter ablation, which has relatively low success rates. ICMs with high AF detection accuracy offer the unique advantage of long-term monitoring periods and continuous monitoring of the patient. With the rapidly increasing use of these devices for AF patients, the need for methods to

characterize AF triggers and AF episodes which could be used in in tools that can help in clinical decisions, is increasingly important.

In particular and if confirmed in future studies, the use of these characterization methods to, for instance, aid clinicians in deciding the best catheter ablation strategy is potentially of significant clinical relevance for several reasons: first, catheter ablation of AF substrate is a procedure with high economic and personal burden; secondly, due to the epidemic character of AF prevalence, these interventions cannot be offered (even in countries with developed health-care systems) to all patients and third, the selection of patients with higher probability of long-term elimination of AF has high priority.

7.2. Future work

Some future research lines derived from this work are presented below.

The unsupervised classification of AF triggers offered insight in the different patterns that could be found in the beats preceding the AF onset. However, to be able to infer useful clinical information from the triggers, future studies including visual annotation of trigger patterns with the support of electrophysiologists and the development of a supervised trigger classifier are needed and is part of our ongoing project.

While the feasibility of modelling AFR from RR series and episode-based characteristics was shown, its clinical significance as AF recurrence risk predictor or as an indicator of the patients' condition was not evaluated. A study of the AFR trend before the catheter ablation procedure could offer insight on the progression of AF, could give indication on the best ablation strategy, and could help better understand the AF mechanics.

Similarly, the episode patterns studied in the thesis are a snapshot of the patients' condition before the catheter ablation procedure. Future studies evaluating the changes and trends of the Hawkes parameters are planned which could also help to better predict the catheter ablation outcome as well as potentially predict the patients' condition whether the patient undergoes the procedure or not.

The clinical annotation of the trigger, the evaluation of the AFR and temporal aggregation trends, and the use of other clinical information not accessible at the time of this study, could better characterize the patient and improve the AF recurrence predictive power of the Optimum Weighted with feature selection

algorithm presented in this thesis. With this in mind, a future study including these features as inputs for the algorithm is planned.

Lastly, the validation of the methods proposed with a higher number of patients. Throughout this thesis, the cohort of patients used in all the studies, albeit unique and with several advantages over studies restricted to 24-hour Holter recordings, offered limited clinical evidence. Therefore, increasing the number of patients with a prospective study would allow to fully evaluate the clinical significance of this thesis.

Chapter 8 Contributions

8.1. Journal Publications

Saiz-Vivo J, Corino VDA, Hatala R, de Melis M, Mainardi LT**. Heart Rate Variability and Clinical Features as Predictors of Atrial Fibrillation Recurrence After Catheter Ablation: A Pilot Study.** Front Physiol. 2021;12:672896. Published 2021 May 25. doi:10.3389/fphys.2021.672896

Saiz-Vivo J, Corino VDA, Martín-Yebra A, Mainardi LT, Hatala R, Sörnmo L. **Atrial fibrillation episode patterns as predictor of clinical outcome of catheter ablation**. Medical & Biological Engineering & Computing. 2022 Nov. DOI: 10.1007/s11517-022-02713-x. PMID: 36409405

8.2. Submitted publications

Saiz-Vivo J, Abdollahpur M, Mainardi LT, Corino VDA, De Melis M, Hatala R and Sandberg F. **Heart Rate Characteristic Based Modelling of Atrial Fibrillatory Rate using Implanted Cardiac Monitor Data**. Submitted to Physiological Measurements. Under review

8.3. Conference Proceedings

Saiz-Vivo J, Corino VDA, de Melis M, Mainardi LT. **Unsupervised Classification of Atrial Fibrillation Triggers Using Heart Rate Variability Features Extracted from Implantable Cardiac Monitor Data.** Annu Int Conf IEEE Eng Med Biol Soc. 2020 Jul;2020: 426-429. doi: 10.1109/EMBC44109.2020.9175369. PMID: 33018019.

Saiz-Vivo J, Abdollahpur M, Mainardi LT, Corino VDA, De Melis M and Sandberg F. **Atrial Fibrillatory Rate Characterization Extracted from Implanted Cardiac Monitor Data**, *2021 Computing in Cardiology (CinC)*, 2021, pp. 1-4, doi: 10.23919/CinC53138.2021.9662826.

8.4. Abstracts

Saiz-Vivo J, Corino VDA, de Melis M, Mainardi LT. **Clinical and heart rate variability feature analysis of pre-ablation AF patients leading to recurrence**. November 2021. Journal of Electrocardiology.

Saiz-Vivo J, Corino VDA, de Melis M, Mainardi LT**. Effect of Extra Lesions on AF burden of Continuously Monitored Patients Undergoing Single-Procedure Catheter Ablation.** October 2021. Atrial Signals

8.5. Indirectly related to the thesis

Saiz-Vivo J, Corino VDA, Rivolta MW, Sassi R and Mainardi LT. **Assessment of the Effect of Fibrillatory Waves in the Analysis of Spatial Heterogeneity of Ventricular Repolarization**, *2019 Computing in Cardiology (CinC)*, 2019, pp. 1-4, doi: 10.23919/CinC49843.2019.9005812. Finalists for the Rosanna Degani Young Investigator Award.

8.6. Patents

Saiz-Vivo J, de Melis M, Corino VDA, Mainardi LT. (Application filed, under review) **System Using Heart Rate Variability Features for Prediction of Medical Procedure Efficacy.** (United States of America, 89289406) Medtronic

Saiz-Vivo J, de Melis M, Corino VDA, Mainardi LT. (In preparation) **Medical Procedure Prediction Using Temporal Aggregation of Atrial Fibrillation Episodes.** Medtronic

References

1. Shukla A, Curtis AB. Avoiding permanent atrial fibrillation: Treatment approaches to prevent disease progression. Vasc Health Risk Manag. 2014;10:1–12.

2. Heeringa J, Van Der Kuip DAM, Hofman A, Kors JA, Van Herpen G, Stricker BHC, et al. Prevalence, incidence and lifetime risk of atrial fibrillation: The Rotterdam study. Eur Heart J. 2006;27(8):949–53.

3. Morillo CA, Banerjee A, Perel P, Wood D, Jouven X. Atrial fibrillation: The current epidemic. J Geriatr Cardiol. 2017;14(3):195–203.

4. Kuck KH, Hoffmann BA, Ernst S, Wegscheider K, Treszl A, Metzner A, et al. Impact of complete versus incomplete circumferential lines around the pulmonary veins during catheter ablation of paroxysmal atrial fibrillation: Results from the gap-atrial fibrillation-German atrial fibrillation competence network 1 trial. Circ Arrhythmia Electrophysiol. 2016;9(1):1–10.

5. Jones DG, Haldar SK, Hussain W, Sharma R, Francis DP, Rahman-Haley SL, et al. A randomized trial to assess catheter ablation versus rate control in the management of persistent atrial fibrillation in heart failure. J Am Coll Cardiol. 2013 May;61(18):1894–903.

6. Hindricks G, Potpara T, Dagres N, Bax JJ, Boriani G, Dan GA, et al. 2020 ESC Guidelines for the diagnosis and management of atrial fibrillation developed in collaboration with the European Association for Cardio-Thoracic Surgery (EACTS). Eur Heart J. 2021;42(5):373–498.

7. Arbelo E, Brugada J, Hindricks G, Maggioni AP, Tavazzi L, Vardas P, et al. The Atrial Fibrillation Ablation Pilot Study: An European Survey on Methodology and results of catheter ablation for atrial fibrillation conducted by the European Heart Rhythm Association. Eur Heart J. 2014;35(22):1466–78.

8. Ganesan AN, Shipp NJ, Brooks AG, Kuklik P, Lau DH, Lim HS, et al. Long-term outcomes of catheter ablation of atrial fibrillation: a systematic review and meta-analysis. J Am Heart Assoc. 2013;2(2):603.

9. Mansour M, Karst E, Heist EK, Dalal N, Wasfy JH, Packer DL, et al. The Impact of First Procedure Success Rate on the Economics of Atrial Fibrillation Ablation. JACC Clin Electrophysiol. 2017;3(2):129–38.

10. Letsas KP, Efremidis M, Giannopoulos G, Deftereos S, Lioni L, Korantzopoulos P, et al. CHADS2 and CHA2DS2-VASc scores as predictors of left atrial ablation outcomes for paroxysmal atrial fibrillation. Europace. 2014;16(2):202–7.

11. Kornej J, Hindricks G, Shoemaker MB, Husser D, Arya A, Sommer P, et al. The APPLE score: a novel and simple score for the prediction of rhythm outcomes after catheter ablation of atrial fibrillation. Clin Res Cardiol. 2015;104(10):871–6.

12. Jud FN, Obeid S, Duru F, Haegeli LM. A novel score in the prediction of rhythm outcome after ablation of atrial fibrillation: The SUCCESS score. Anatol J Cardiol. 2019;21(3):142–9.

13. Mujović N, Marinković M, Marković N, Shantsila A, Lip GYH, Potpara TS. Prediction of very late arrhythmia recurrence after radiofrequency catheter ablation of atrial fibrillation: The MB-LATER clinical score. Sci Rep. 2017;7(December 2016):1–12.

14. Ramkumar S, Nerlekar N, Souza DD, Pol DJ, Kalman JM, Marwick TH. Atrial fibrillation detection using single lead portable electrocardiographic monitoring : a systematic review and meta-analysis. 2018;1–16.

15. Hindricks G, Pokushalov E, Urban L, Taborsky M, Kuck KH, Lebedev D, et al. Performance of a new leadless implantable cardiac monitor in detecting and quantifying atrial fibrillation results of the XPECT trial. Circ Arrhythmia Electrophysiol. 2010;3(2):141–7.

16. Kapa S, Epstein AE, Callans DJ, Garcia FC, Lin D, Bala R, et al. Assessing arrhythmia burden after catheter ablation of atrial fibrillation using an implantable loop recorder: The abacus study. J Cardiovasc Electrophysiol. 2013;24(8):875–81.

17. Pokushalov E, Romanov A, Corbucci G, Artyomenko S, Turov A, Shirokova N, et al. Use of an implantable monitor to detect arrhythmia recurrences and select patients for early repeat catheter ablation for atrial fibrillation a pilot study. Circ Arrhythmia Electrophysiol. 2011;4(6):823–31.

18. Guyton AC, Hall JE. Textbook of medical physiology. Vol. 548. Saunders Philadelphia; 1986.

19. Antzelevitch C, Burashnikov A. Overview of Basic Mechanisms of Cardiac Arrhythmia. Card Electrophysiol Clin. 2011 Mar;3(1):23–45.

20. Sornmo L, Laguna P. Bioelectrical Signal Processing in Cardiac and Neurological Applications. Elsevier Science; 2005.

21. Aparicio HJ, Benjamin EJ, Callaway CW, Carson AP, Cheng S, Elkind MS V, et al. Heart Disease and Stroke Statistics-2021 Update A Report from the American Heart Association. Circulation. 2021. 254–743 p.

22. Murray C, Wang H, Naghavi M, Allen C, Barber R, Bhutta Z, et al. Global, regional, and national life expectancy, all-cause mortality, and cause-specific

mortality for 249 causes of death, 1980–2015: a systematic analysis for the Global Burden of Disease Study 2015. Lancet. 2016;388(10053):1459–544.

23. Mainardi L, Sörnmo L, Cerutti S. Understanding Atrial Fibrillation: The Signal Processing Contribution, Part II. Vol. 3, Synthesis Lectures on Biomedical Engineering. 2008.

24. Gibbs H, Freedman B, Rosenqvist M, Virdone S, Mahmeed W Al, Ambrosio G, et al. Clinical Outcomes in Asymptomatic and Symptomatic Atrial Fibrillation Presentations in GARFIELD-AF: Implications for AF Screening. Am J Med. 2021;134(7):893-901.e11.

25. Thrall G, Lane D, Carroll D, Lip GYH. Quality of Life in Patients with Atrial Fibrillation: A Systematic Review. Am J Med. 2006;119(5).

26. Serpytis R, Navickaite A, Serpytiene E, Barysiene J, Marinskis G, Jatuzis D, et al. Impact of Atrial Fibrillation on Cognitive Function, Psychological Distress, Quality of Life, and Impulsiveness. Am J Med [Internet]. 2018;131(6):703.e1-703.e5. Available from: https://doi.org/10.1016/j.amjmed.2017.12.044

27. Schnabel RB, Michal M, Wilde S, Wiltink J, Wild PS, Sinning CR, et al. Depression in atrial fibrillation in the general population. PLoS One. 2013;8(12).

28. Magnussen C, Niiranen TJ, Ojeda FM, Gianfagna F, Blankenberg S, Njølstad I, et al. Sex differences and similarities in atrial fibrillation epidemiology, risk factors, and mortality in community cohorts: Results from the biomarcare consortium (Biomarker for cardiovascular risk assessment in Europe). Circulation. 2017;136(17):1588–97.

29. Wolf PA, Abbott RD, Kannel WB. Atrial fibrillation as an independent risk factor for stroke: The framingham study. Stroke. 1991;22(8):983–8.

30. Platonov PG, Corino VDA, Seifert M, Holmqvist F, Sörnmo L. Atrial fibrillatory rate in the clinical context: Natural course and prediction of intervention outcome. Europace. 2014;16:iv110–9.

31. Raygor VP, Ng J, Goldberger JJ. Surface ECG f Wave Analysis of Dofetilide Drug Effect in the Atrium. J Cardiovasc Electrophysiol. 2015 Jun;26(6):644–8.

32. Aunes M, Egstrup K, Frison L, Berggren A, Stridh M, Sörnmo L, et al. Rapid slowing of the atrial fibrillatory rate after administration of AZD7009 predicts conversion of atrial fibrillation. J Electrocardiol [Internet]. 2014;47(3):316–23. Available from: http://dx.doi.org/10.1016/j.jelectrocard.2013.12.008

33. Black-Maier EW, Pokorney SD, Barnett AS, Liu P, Shrader P, Ng J, et al. Ranolazine reduces atrial fibrillatory wave frequency. Eur Eur pacing, arrhythmias, Card Electrophysiol J Work groups Card pacing, arrhythmias,

Card Cell Electrophysiol Eur Soc Cardiol. 2017 Jul;19(7):1096–100.

34. Nilsson F, Stridh M, Bollmann A, Sörnmo L. Predicting spontaneous termination of atrial fibrillation using the surface ECG. Med Eng Phys. 2006 Oct;28(8):802–8.

35. Petrutiu S, Sahakian A V, Swiryn S. Abrupt changes in fibrillatory wave characteristics at the termination of paroxysmal atrial fibrillation in humans. Europace. 2007;9:466–70.

36. Alcaraz R, Sandberg F, Sörnmo L, Rieta JJ. Classification of paroxysmal and persistent atrial fibrillation in ambulatory ECG recordings. IEEE Trans Biomed Eng. 2011 May;58(5):1441–9.

37. Wijffels MC, Kirchhof CJ, Dorland R, Allessie MA. Atrial fibrillation begets atrial fibrillation. A study in awake chronically instrumented goats. Circulation. 1995 Oct;92(7):1954–68.

38. Steinberg JS, O'Connell H, Li S, Ziegler PD. Thirty-Second Gold Standard Definition of Atrial Fibrillation and Its Relationship With Subsequent Arrhythmia Patterns: Analysis of a Large Prospective Device Database. Circ Arrhythm Electrophysiol. 2018 Jul;11(7):e006274.

39. Boriani G, Diemberger I, Ziacchi M, Valzania C, Gardini B, Cimaglia P, et al. AF burden is important - Fact or fiction? Int J Clin Pract. 2014;68(4):444–52.

40. https://www.urmc.rochester.edu/highland/departments-centers/cardiology/conditions/atrial-fibrillation.aspx.

41. Boriani G, Proietti M, Laroche C, Fauchier L, Marin F, Nabauer M, et al. Contemporary stroke prevention strategies in 11 096 European patients with atrial fibrillation: A report from the EURObservational Research Programme on Atrial Fibrillation (EORP-AF) Long-Term General Registry. Europace. 2018;20(5):747–57.

42. Pandey A, Kim S, Moore C, Thomas L, Gersh B, Allen LA, et al. Predictors and Prognostic Implications of Incident Heart Failure in Patients With Prevalent Atrial Fibrillation. JACC Heart Fail. 2017 Jan;5(1):44–52.

43. Ganesan AN, Chew DP, Hartshorne T, Selvanayagam JB, Aylward PE, Sanders P, et al. The impact of atrial fibrillation type on the risk of thromboembolism, mortality, and bleeding: A systematic review and meta-analysis. Eur Heart J. 2016;37(20):1591–602.

44. Nguyen BL, Fishbein MC, Chen LS, Chen P-S, Masroor S. Histopathological substrate for chronic atrial fibrillation in humans. Hear Rhythm. 2009 Apr;6(4):454–60.

45. Allessie MA, de Groot NMS, Houben RPM, Schotten U, Boersma E, Smeets JL, et al. Electropathological substrate of long-standing persistent atrial fibrillation in patients with structural heart disease: longitudinal dissociation. Circ Arrhythm Electrophysiol. 2010 Dec;3(6):606–15.

46. Spach MS, Josephson ME. Initiating reentry: the role of nonuniform anisotropy in small circuits. J Cardiovasc Electrophysiol. 1994 Feb;5(2):182–209.

47. Anné W, Willems R, Roskams T, Sergeant P, Herijgers P, Holemans P, et al. Matrix metalloproteinases and atrial remodeling in patients with mitral valve disease and atrial fibrillation. Cardiovasc Res. 2005 Sep;67(4):655–66.

48. Schotten U, Verheule S, Kirchhof P, Goette A. Pathophysiological mechanisms of atrial fibrillation: A translational appraisal. Physiol Rev. 2011;91(1):265–325.

49. Spach MS, Heidlage JF, Barr RC, Dolber PC. Cell size and communication: role in structural and electrical development and remodeling of the heart. Vol. 1, Heart rhythm. United States; 2004. p. 500–15.

50. Skalidis EI, Hamilos MI, Karalis IK, Chlouverakis G, Kochiadakis GE, Vardas PE. Isolated atrial microvascular dysfunction in patients with lone recurrent atrial fibrillation. J Am Coll Cardiol. 2008 May;51(21):2053–7.

51. Chen P-S, Chen LS, Fishbein MC, Lin S-F, Nattel S. Role of the autonomic nervous system in atrial fibrillation: pathophysiology and therapy. Circ Res. 2014 Apr;114(9):1500–15.

52. Haïssaguerre M, Jaïs P, Shah DC, Takahashi A, Hocini M, Quiniou G, et al. Spontaneous Initiation of Atrial Fibrillation by Ectopic Beats Originating in the Pulmonary Veins. N Engl J Med [Internet]. 1998;339(10):659–66. Available from: http://www.nejm.org/doi/abs/10.1056/NEJM199809033391003

53. Moe GK, Abildskov JA. Atrial fibrillation as a self-sustaining arrhythmia independent of focal discharge. Am Heart J [Internet]. 1959;58(1):59–70. Available from: https://www.sciencedirect.com/science/article/pii/0002870359902741

54. Haissaguerre M, Hocini M, Denis A, Shah AJ, Komatsu Y, Yamashita S, et al. Driver domains in persistent atrial fibrillation. Circulation. 2014;130(7):530–8.

55. Palatini P. Parental atrial fibrillation as a risk factor for atrial fibrillation in offspring. Vol. 292, JAMA. United States; 2004. p. 1174–5.

56. Olesen MS, Nielsen MW, Haunsø S, Svendsen JH. Atrial fibrillation: the role of common and rare genetic variants. Eur J Hum Genet [Internet].

2014;22(3):297–306. Available from: https://doi.org/10.1038/ejhg.2013.139

57. Charitos EI, Pürerfellner H, Glotzer T V, Ziegler PD. Clinical classifications of atrial fibrillation poorly reflect its temporal persistence: insights from 1,195 patients continuously monitored with implantable devices. J Am Coll Cardiol. 2014 Jul;63(25 Pt A):2840–8.

58. Lip GYH. The ABC pathway: An integrated approach to improve AF management. Nat Rev Cardiol [Internet]. 2017;14(11):627–8. Available from: http://dx.doi.org/10.1038/nrcardio.2017.153

59. Lip G, Freedman B, De Caterina R, Potpara TS. Stroke prevention in atrial fibrillation: Past, present and future. Comparing the guidelines and practical decision-making. Thromb Haemost. 2017 Jun;117(7):1230–9.

60. Al-Khatib SM, Allen LaPointe NM, Chatterjee R, Crowley MJ, Dupre ME, Kong DF, et al. Rate- and rhythm-control therapies in patients with atrial fibrillation: a systematic review. Ann Intern Med. 2014 Jun;160(11):760–73.

61. Dankner R, Shahar A, Novikov I, Agmon U, Ziv A, Hod H. Treatment of stable atrial fibrillation in the emergency department: a population-based comparison of electrical direct-current versus pharmacological cardioversion or conservative management. Cardiology. 2009;112(4):270–8.

62. Khan IA. Pharmacological cardioversion of recent onset atrial fibrillation. Eur Heart J. 2004;25(15):1274–6.

63. Khan IA. Oral loading single dose flecainide for pharmacological cardioversion of recent-onset atrial fibrillation. Int J Cardiol. 2003 Feb;87(2–3):121–8.

64. Khan IA. Single oral loading dose of propafenone for pharmacological cardioversion of recent-onset atrial fibrillation. J Am Coll Cardiol [Internet]. 2001;37(2):542–7. Available from: http://dx.doi.org/10.1016/S0735-1097(00)01116-5

65. Roy D, Pratt CM, Torp-Pedersen C, Wyse DG, Toft E, Juul-Moller S, et al. Vernakalant hydrochloride for rapid conversion of atrial fibrillation: A phase 3, randomized, placebo-controlled trial. Circulation. 2008;117(12):1518–25.

66. Letelier LM, Udol K, Ena J, Weaver B, Guyatt GH. Effectiveness of amiodarone for conversion of atrial fibrillation to sinus rhythm: A meta-analysis. Arch Intern Med. 2003;163(7):777–85.

67. Alboni P, Botto GL, Baldi N, Luzi M, Russo V, Gianfranchi L, et al. Outpatient Treatment of Recent-Onset Atrial Fibrillation with the “Pill-in-the-Pocket” Approach. N Engl J Med. 2004;351(23):2384–91.

68. Inácio JFS, da Rosa M dos SG, Shah J, Rosário J, Vissoci JRN, Manica ALL, et al.

Monophasic and biphasic shock for transthoracic conversion of atrial fibrillation: Systematic review and network meta-analysis. Resuscitation. 2016 Mar;100:66–75.

69. Kirchhof P, Eckardt L, Loh P, Weber K, Fischer R-J, Seidl K-H, et al. Anterior-posterior versus anterior-lateral electrode positions for external cardioversion of atrial fibrillation: a randomised trial. Lancet (London, England). 2002 Oct;360(9342):1275–9.

70. Valembois L, Audureau E, Takeda A, Jarzebowski W, Belmin J, Lafuente-Lafuente C. Antiarrhythmics for maintaining sinus rhythm after cardioversion of atrial fibrillation. Cochrane database Syst Rev. 2019 Sep;9(9):CD005049.

71. Nielsen JC, Johannessen A, Raatikainen P, Hindricks G, Walfridsson H, Pehrson SM, et al. Long-term efficacy of catheter ablation as first-line therapy for paroxysmal atrial fibrillation: 5-year outcome in a randomised clinical trial. Heart. 2017 Mar;103(5):368–76.

72. Di Biase L, Mohanty P, Mohanty S, Santangeli P, Trivedi C, Lakkireddy D, et al. Ablation Versus Amiodarone for Treatment of Persistent Atrial Fibrillation in Patients With Congestive Heart Failure and an Implanted Device: Results From the AATAC Multicenter Randomized Trial. Circulation. 2016;133(17):1637–44.

73. De Vecchis R. Is an elevated burden of antiarrhythmic drug (AAD) side-effects the unavoidable price to be traded for a durable suppression of AF relapses in ablated patients? The weaknesses and risks of the AAD suppression algorithm used by current models of AF seconda. Eur J Clin Pharmacol. 2019;873–4.

74. MacNeil DJ. The side effect profile of class III antiarrhythmic drugs: Focus on d,l- sotalol. Am J Cardiol. 1997;80(8 A).

75. Kirchhof P, Andresen D, Bosch R, Borggrefe M, Meinertz T, Parade U, et al. Short-term versus long-term antiarrhythmic drug treatment after cardioversion of atrial fibrillation (Flec-SL): a prospective, randomised, open-label, blinded endpoint assessment trial. Lancet (London, England). 2012 Jul;380(9838):238–46.

76. Fürnkranz A, Brugada J, Albenque J-P, Tondo C, Bestehorn K, Wegscheider K, et al. Rationale and Design of FIRE AND ICE: A multicenter randomized trial comparing efficacy and safety of pulmonary vein isolation using a cryoballoon versus radiofrequency ablation with 3D-reconstruction. J Cardiovasc Electrophysiol. 2014 Dec;25(12):1314–20.

77. Kuck K-H, Fürnkranz A, Chun KRJ, Metzner A, Ouyang F, Schlüter M, et al. Cryoballoon or radiofrequency ablation for symptomatic paroxysmal atrial

fibrillation: reintervention, rehospitalization, and quality-of-life outcomes in the FIRE AND ICE trial. Eur Heart J. 2016 Oct;37(38):2858–65.

78. Luik A, Radzewitz A, Kieser M, Walter M, Bramlage P, Hörmann P, et al. Cryoballoon versus open irrigated radiofrequency ablation in patients with paroxysmal atrial fibrillation. Circulation. 2015;132(14):1311–9.

79. Schmidt M, Dorwarth U, Andresen D, Brachmann J, Kuck K-H, Kuniss M, et al. Cryoballoon versus RF ablation in paroxysmal atrial fibrillation: results from the German Ablation Registry. J Cardiovasc Electrophysiol. 2014 Jan;25(1):1–7.

80. Kuck KH, Brugada J, Fürnkranz A, Metzner A, Ouyang F, Chun J, et al. Cryoballoon or radiofrequency ablation for paroxysmal atrial fibrillation. J Cardiopulm Rehabil Prev. 2016;36(5):393–4.

81. Haïssaguerre M, Hocini M, Sanders P, Sacher F, Rotter M, Takahashi Y, et al. Catheter ablation of long-lasting persistent atrial fibrillation: clinical outcome and mechanisms of subsequent arrhythmias. J Cardiovasc Electrophysiol. 2005 Nov;16(11):1138–47.

82. Kornej J, Hindricks G, Arya A, Sommer P, Husser D, Bollmann A. The APPLE score - A novel score for the prediction of rhythm outcomes after repeat catheter ablation of atrial fibrillation. PLoS One. 2017;12(1):1–9.

83. Kirchhof P, Benussi S, Kotecha D, Ahlsson A, Atar D, Casadei B, et al. 2016 ESC Guidelines for the management of atrial fibrillation developed in collaboration with EACTS The Task Force for1. Task A, Members F, Kirchhof P, Uk C, Uk DK, Uk BC, et al. 2016 ESC Guidelines for the management of atrial fibrillation developed in c. 2017;(November):2893–962.

84. Nikolaidou T, Channer KS. Chronic atrial fibrillation: a systematic review of medical heart rate control management. Postgrad Med J. 2009 Jun;85(1004):303–12.

85. Heist EK, Mansour M, Ruskin JN. Rate control in atrial fibrillation: Targets, methods, resynchronization considerations. Circulation. 2011;124(24):2746–55.

86. Goldberger ZD, Alexander GC. Digitalis use in contemporary clinical practice: refitting the foxglove. JAMA Intern Med. 2014 Jan;174(1):151–4.

87. Ziff OJ, Lane DA, Samra M, Griffith M, Kirchhof P, Lip GYH, et al. Safety and efficacy of digoxin: systematic review and meta-analysis of observational and controlled trial data. BMJ. 2015 Aug;351:h4451.

88. Lim K-T, Davis MJE, Powell A, Arnolda L, Moulden K, Bulsara M, et al. Ablate and pace strategy for atrial fibrillation: long-term outcome of AIRCRAFT trial.

Eur Eur pacing, arrhythmias, Card Electrophysiol J Work groups Card pacing, arrhythmias, Card Cell Electrophysiol Eur Soc Cardiol. 2007 Jul;9(7):498–505.

89. Wood MA, Brown-Mahoney C, Kay GN, Ellenbogen KA. Clinical outcomes after ablation and pacing therapy for atrial fibrillation : a meta-analysis. Circulation. 2000 Mar;101(10):1138–44.

90. Dzeshka MS, Shantsila A, Shantsila E, Lip GYH. Atrial Fibrillation and Hypertension. Hypertension. 2017;70(5):854–61.

91. Anter E, Jessup M, Callans DJ. Atrial fibrillation and heart failure: Treatment considerations for a dual epidemic. Circulation. 2009;119(18):2516–25.

92. Michniewicz E, Mlodawska E, Lopatowska P, Tomaszuk-Kazberuk A, Malyszko J. Patients with atrial fibrillation and coronary artery disease - Double trouble. Adv Med Sci. 2018 Mar;63(1):30–5.

93. Pallisgaard JL, Schjerning A-M, Lindhardt TB, Procida K, Hansen ML, Torp-Pedersen C, et al. Risk of atrial fibrillation in diabetes mellitus: A nationwide cohort study. Eur J Prev Cardiol. 2016 Apr;23(6):621–7.

94. Movahed M-R, Hashemzadeh M, Jamal MM. Diabetes mellitus is a strong, independent risk for atrial fibrillation and flutter in addition to other cardiovascular disease. Int J Cardiol. 2005 Dec;105(3):315–8.

95. Linz D, Baumert M, Catcheside P, Floras J, Sanders P, Lévy P, et al. Assessment and interpretation of sleep disordered breathing severity in cardiology: Clinical implications and perspectives. Int J Cardiol. 2018 Nov;271:281–8.

96. Gami AS, Pressman G, Caples SM, Kanagala R, Gard JJ, Davison DE, et al. Association of atrial fibrillation and obstructive sleep apnea. Circulation. 2004 Jul;110(4):364–7.

97. Huxley RR, Misialek JR, Agarwal SK, Loehr LR, Soliman EZ, Chen LY, et al. Physical activity, obesity, weight change, and risk of atrial fibrillation: the Atherosclerosis Risk in Communities study. Circ Arrhythm Electrophysiol. 2014 Aug;7(4):620–5.

98. Baek Y-S, Yang P-S, Kim T-H, Uhm J-S, Park J, Pak H-N, et al. Associations of Abdominal Obesity and New-Onset Atrial Fibrillation in the General Population. J Am Heart Assoc. 2017 Jun;6(6).

99. Mukamal KJ, Tolstrup JS, Friberg J, Jensen G, Grønbaek M. Alcohol consumption and risk of atrial fibrillation in men and women: the Copenhagen City Heart Study. Circulation. 2005 Sep;112(12):1736–42.

100. Liang Y, Mente A, Yusuf S, Gao P, Sleight P, Zhu J, et al. Alcohol consumption and the risk of incident atrial fibrillation among people with cardiovascular

disease. C Can Med Assoc J = J l'Association medicale Can. 2012 Nov;184(16):E857-66.

101. Nielsen JR, Wachtell K, Abdulla J. The Relationship Between Physical Activity and Risk of Atrial Fibrillation-A Systematic Review and Meta-Analysis. J Atr Fibrillation. 2013;5(5):789.

102. Abed HS, Wittert GA, Leong DP, Shirazi MG, Bahrami B, Middeldorp ME, et al. Effect of weight reduction and cardiometabolic risk factor management on symptom burden and severity in patients with atrial fibrillation: a randomized clinical trial. JAMA. 2013 Nov;310(19):2050–60.

103. Voskoboinik A, Kalman JM, De Silva A, Nicholls T, Costello B, Nanayakkara S, et al. Alcohol Abstinence in Drinkers with Atrial Fibrillation. N Engl J Med. 2020 Jan;382(1):20–8.

104. Davis RC, Hobbs FDR, Kenkre JE, Roalfe AK, Iles R, Lip GYH, et al. Prevalence of atrial fibrillation in the general population and in high-risk groups: the ECHOES study. Eur Eur pacing, arrhythmias, Card Electrophysiol J Work groups Card pacing, arrhythmias, Card Cell Electrophysiol Eur Soc Cardiol. 2012 Nov;14(11):1553–9.

105. Freeman J V, Simon DN, Go AS, Spertus J, Fonarow GC, Gersh BJ, et al. Association Between Atrial Fibrillation Symptoms, Quality of Life, and Patient Outcomes: Results From the Outcomes Registry for Better Informed Treatment of Atrial Fibrillation (ORBIT-AF). Circ Cardiovasc Qual Outcomes. 2015 Jul;8(4):393–402.

106. Philippsen TJ, Christensen LS, Hansen MG, Dahl JS, Brandes A. Detection of Subclinical Atrial Fibrillation in High-Risk Patients Using an Insertable Cardiac Monitor. 2017;3(13).

107. Turchioe MR, Jimenez V, Isaac S, Alshalabi M, Slotwiner D, Creber RM. Review of mobile applications for the detection and management of atrial fi brillation. Hear Rhythm O2 [Internet]. 2020;1(1):35–43. Available from: https://doi.org/10.1016/j.hroo.2020.02.005

108. Paudel B, Paudel K. The diagnostic significance of the holter monitoring in the evaluation of palpitation. J Clin Diagn Res. 2013 Mar;7(3):480–3.

109. Onder H, Yilmaz S. The Rationale of Holter Monitoring After Stroke. Angiology [Internet]. 2017 Apr 7;68(10):926–7. Available from: https://doi.org/10.1177/0003319717703003

110. Hingorani P, Karnad DR, Rohekar P, Kerkar V, Lokhandwala YY, Kothari S. Arrhythmias Seen in Baseline 24-Hour Holter ECG Recordings in Healthy Normal Volunteers During Phase 1 Clinical Trials. J Clin Pharmacol. 2016

Jul;56(7):885–93.

111. Chudzik M, Klimczak A, Wranicz JK. Ambulatory Holter monitoring in asymptomatic patients with DDD pacemakers - do we need ACC/AHA Guidelines revision? Arch Med Sci [Internet]. 2013/11/05. 2013 Oct 31;9(5):815–20. Available from: https://pubmed.ncbi.nlm.nih.gov/24273562

112. Kwon S, Lee SR, Choi EK, Ahn HJ, Song HS, Lee YS, et al. Comparison Between the 24-hour Holter Test and 72-hour Single-Lead Electrocardiogram Monitoring With an Adhesive Patch-Type Device for Atrial Fibrillation Detection: Prospective Cohort Study. J Med Internet Res. 2022;24(5):e37970.

113. Hanke T, Charitos EI, Stierle U, Karluss A, Kraatz E, Graf B, et al. Twenty-four - hour holter monitor follow-up does not provide accurate heart rhythm status after surgical atrial fibrillation ablation therapy up to 12 months experience with a novel permanently implantable heart rhythm monitor device. Circulation. 2009;120(SUPPL. 1):177–84.

114. Verma A, Champagne J, Sapp J, Essebag V, Novak P, Skanes A, et al. Discerning the incidence of symptomatic and asymptomatic episodes of atrial fibrillation before and after catheter ablation (DISCERN AF): a prospective, multicenter study. JAMA Intern Med. 2013 Jan;173(2):149–56.

115. Mittal S, Pokushalov E, Romanov A, Ferrara M, Arshad A, Musat D, et al. Long-term ECG monitoring using an implantable loop recorder for the detection of atrial fibrillation after cavotricuspid isthmus ablation in patients with atrial flutter. Hear Rhythm [Internet]. 2013;10(11):1598–604. Available from: https://www.sciencedirect.com/science/article/pii/S1547527113007911

116. Etgen T, Hochreiter M, Mundel M, Freudenberger T. Insertable cardiac event recorder in detection of Atrial fibrillation after cryptogenic stroke: An audit report. Stroke. 2013;44(7):2007–9.

117. Sarkar S, Ritscher D, Mehra R. A detector for a chronic implantable atrial tachyarrhythmia monitor. IEEE Trans Biomed Eng. 2008;55(3):1219–24.

118. Pürerfellner H, Pokushalov E, Sarkar S, Koehler J, Zhou R, Urban L, et al. P-wave evidence as a method for improving algorithm to detect atrial fibrillation in insertable cardiac monitors. Hear Rhythm [Internet]. 2014;11(9):1575–83. Available from: http://dx.doi.org/10.1016/j.hrthm.2014.06.006

119. Sanders P, Pürerfellner H, Pokushalov E, Sarkar S, Di Bacco M, Maus B, et al. Performance of a new atrial fibrillation detection algorithm in a miniaturized insertable cardiac monitor: Results from the Reveal LINQ Usability Study. Hear Rhythm. 2016;13(7):1425–30.

120. Bou Ezzeddine H, Vachulova A, Svetlosak M, Urban L, Hlivak P, Margitfalvi P, et al. Occurrence of symptoms after catheter ablation of atrial fibrillation. Bratislava Med J. 2015;116(8):461–4.

121. Naghdy GA, Todd C, Olaode A, Naghdy G. Unsupervised Classification of Images: A Review. Int J Image Process [Internet]. 2014;(8):325. Available from: https://www.researchgate.net/publication/265729668

122. Mietus JE, Peng CK, Henry I, Goldsmith RL, Goldberger AL. The pNNx files: Re-examining a widely used heart rate variability measure. Heart. 2002;88(4):378–80.

123. Pincus SM. Approximate entropy: A complexity measure for biological time series data. Bioengineering, Proceedings of the Northeast Conference. 1991. p. 35–6.

124. Delgado-Bonal A, Marshak A. Approximate entropy and sample entropy: A comprehensive tutorial. Vol. 21, Entropy. 2019.

125. Tayel M, AlSaba E. Poincaré Plot for Heart Rate Variability. Int J Medical, Heal Biomed Bioeng Pharm Eng [Internet]. 2015;9(9):708–11. Available from: https://pdfs.semanticscholar.org/dddb/0af509fc75b5dbdc6e04dd4321d85401911b.pdf

126. Obaid HS, Dheyab SA, Sabry SS. The Impact of Data Pre-Processing Techniques and Dimensionality Reduction on the Accuracy of Machine Learning. IEEE. 2019;Annual Inf.

127. Samuels P. Advice on Exploratory Factor Analysis. 2016;(June).

128. Lamrous S, Taïleb M. Divisive hierarchical K-means. CIMCA 2006 Int Conf Comput Intell Model Control Autom Jointly with IAWTIC 2006 Int Conf Intell Agents Web Technol . 2006;(2):0–5.

129. Holm S. A Simple Sequentially Rejective Multiple Test Procedure. Scand J Stat [Internet]. 1979 Jan 30;6(2):65–70. Available from: http://www.jstor.org/stable/4615733

130. Shaffer F, Ginsberg JP. An Overview of Heart Rate Variability Metrics and Norms. Front Public Heal. 2017;5(September):1–17.

131. Ciccone AB, Siedlik JA, Wecht JM, Deckert JA, Nguyen ND, Weir JP. Reminder: RMSSD and SD1 are identical heart rate variability metrics. Muscle and Nerve. 2017;56(4):674–8.

132. Hoshi RA, Pastre CM, Vanderlei LCM, Godoy MF. Poincaré plot indexes of heart rate variability: Relationships with other nonlinear variables. Auton Neurosci Basic Clin [Internet]. 2013;177(2):271–4. Available from:

http://dx.doi.org/10.1016/j.autneu.2013.05.004

133. Camm AJ, Malik M, Bigger JT, Breithardt G, Cerutti S, Cohen RJ, et al. Heart rate variability Standards of measurement, physiological interpretation, and clinical use. Eur Heart J [Internet]. 1996;17:354–81. Available from: http://www.mendeley.com/research/guidelines-heart-rate-variability-2/

134. Salahuddin L, Cho J, Jeong MG, Kim D. Ultra short term analysis of heart rate variability for monitoring mental stress in mobile settings. Annu Int Conf IEEE Eng Med Biol - Proc. 2007;4656–9.

135. Baek HJ, Cho CH, Cho J, Woo JM. Reliability of ultra-short-term analysis as a surrogate of standard 5-min analysis of heart rate variability. Telemed e-Health. 2015;21(5):404–14.

136. Rottner L, Bellmann B, Lin T, Reissmann B, Tönnis T, Schleberger R, et al. Catheter Ablation of Atrial Fibrillation: State of the Art and Future Perspectives. Cardiol Ther. 2020 Jun;9(1):45–58.

137. Saglietto A, Ballatore A, Gaita F, Scaglione M, De Ponti R, De Ferrari GM, et al. Comparative efficacy and safety of different catheter ablation strategies for persistent atrial fibrillation: a network meta-analysis of randomized clinical trials. Eur Hear journal Qual care Clin outcomes. 2021 Sep;

138. Stridh M, Sörnmo L. Spatiotemporal QRST Cancellation Techniques for Analysis of Atrial Fibrillation. 2001;48(1):105–11.

139. Corino VDA, Mainardi LT, Bollmann A, Husser D, Stridh M, Sörmno L. A Gaussian mixture model for time-frequency analysis of atrial fibrillation electrocardiograms. Annu Int Conf IEEE Eng Med Biol - Proc. 2007;271–4.

140. Alcaraz R, Rieta JJ. Wavelet bidomain regularity analysis to predict spontaneous termination of atrial fibrillation. Annu Int Conf IEEE Eng Med Biol - Proc. 2007;1838–41.

141. Platonov PG, Corino VDA, Seifert M, Holmqvist F, Sörnmo L. Atrial fibrillatory rate in the clinical context: Natural course and prediction of intervention outcome. Europace. 2014;16:iv110–9.

142. Bollmann A, Husser D, Steinert R, Stridh M, Soernmo L, Olsson SB, et al. Echocardiographic and Electrocardiographic Predictors for Atrial Fibrillation Recurrence Following Cardioversion. J Cardiovasc Electrophysiol. 2003;14(10 SUPPL.).

143. Bollmann A, Tveit A, Husser D, Stridh M, Sörnmo L, Smith P, et al. Fibrillatory rate response to candesartan in persistent atrial fibrillation. Europace. 2008;10(10):1138–44.

144. Corino VDA, Cygankiewicz I, Mainardi LT, Stridh M, Vasquez R, Bayes De Luna A, et al. Association between atrial fibrillatory rate and heart rate variability in patients with atrial fibrillation and congestive heart failure. Ann Noninvasive Electrocardiol. 2013;18(1):41–50.

145. Bollmann A, Sonne K, Esperer HD, Toepffer I, Klein HU. Circadian variations in atrial fibrillatory frequency in persistent human atrial fibrillation. PACE - Pacing Clin Electrophysiol. 2000;23(11 II):1867–71.

146. Meurling CJ, Waktare JEP, Holmqvist F, Hedman A, Camm AJ, Olsson SB, et al. Diurnal variations of the dominant cycle length of chronic atrial fibrillation. Am J Physiol - Hear Circ Physiol. 2001;280(1 49-1):401–6.

147. Cosson S, Maison-Blanche P, Bertil Olsson S, Leenhardt A, Badilini F, Coumel P. Circadian modulation of atrial cycle length in human chronic permanent atrial fibrillation: A noninvasive assessment using long-term surface ECG. Ann Noninvasive Electrocardiol. 2000;5(3):270–8.

148. Sandberg F, Bollmann A, Husser D, Stridh M, Sörnmo L. Circadian variation in dominant atrial fibrillation frequency in persistent atrial fibrillation. Physiol Meas. 2010;31(4):531–42.

149. Bollmann A, Sonne K, Esperer HD, Toepffer I, Langberg JJ, Klein HU. Non-invasive assessment of fibrillatory activity in patients with paroxysmal and persistent atrial fibrillation using the Holter ECG. Cardiovasc Res. 1999;44(1):60–6.

150. Platonov PG, Stridh M, de Melis M, Urban L, Carlson J, Corbucci G, et al. Analysis of atrial fibrillatory rate during spontaneous episodes of atrial fibrillation in humans using implantable loop recorder electrocardiogram. J Electrocardiol. 2012;45(6):723–6.

151. Henriksson M, Petrenas A, Marozas V, Sandberg F, Sornmo L. Model-based assessment of f-wave signal quality in patients with atrial fibrillation. IEEE Trans Biomed Eng. 2018;65(11):2600–11.

152. Stroup WW. Generalized Linear Mixed Models: Modern Concepts, Methods and Applications by Walter W. Stroup. Vol. 81, Texts in Statistical Science Series. 2013. 482–483 p.

153. Akaike H. A New Look at the Statistical Model Identification. IEEE Trans Automat Contr. 1974;19(6):716–23.

154. Zeng T, Li Y, Yu J. Deviance information criterion for comparing var models. Adv Econom. 2014;33:615–37.

155. Wright S. Correlation and causation. J Agric Res. 1921;20:557–85.

156. Saiz-Vivo J, Abdollahpur M, Mainardi LT, Corino VDA, De Melis M, Sandberg F. Atrial Fibrillatory Rate Characterization Extracted from Implanted Cardiac Monitor Data. In: 2021 Computing in Cardiology (CinC). 2021. p. 1–4.

157. Lee R, Mittal S. Utility and limitations of long-term monitoring of atrial fibrillation using an implantable loop recorder. Hear Rhythm. 2018 Feb;15(2):287–95.

158. Corino VDA, Ulimoen SR, Enger S, Mainardi LT, Tveit A, Platonov PG. Rate-control drugs affect variability and irregularity measures of RR intervals in patients with permanent atrial fibrillation. J Cardiovasc Electrophysiol. 2015 Feb;26(2):137–41.

159. Cygankiewicz I, Corino V, Vazquez R, Bayes-Genis A, Mainardi L, Zareba W, et al. Reduced Irregularity of Ventricular Response During Atrial Fibrillation and Long-term Outcome in Patients With Heart Failure. Am J Cardiol. 2015 Oct;116(7):1071–5.

160. Platonov PG, Cygankiewicz I, Stridh M, Holmqvist F, Vazquez R, Bayes-Genis A, et al. Low atrial fibrillatory rate is associated with poor outcome in patients with mild to moderate heart failure. Circ Arrhythm Electrophysiol. 2012 Feb;5(1):77–83.

161. Patel HC, Hayward C, Wardle AJ, Middleton L, Lyon AR, Di Mario C, et al. The effect of head-up tilt upon markers of heart rate variability in patients with atrial fibrillation. Ann Noninvasive Electrocardiol. 2018;23(3):1–11.

162. Plappert F, Wallman M, Platonov P, Sandberg F. Changes in RR Series Characteristics During Atrial Fibrillation: An AV Node Simulation Study. In: 2021 Computing in Cardiology (CinC). 2021. p. 1–4.

163. Swartz MF, Fink GW, Lutz CJ, Taffet SM, Berenfeld O, Vikstrom KL, et al. Left versus right atrial difference in dominant frequency, K+ channel transcripts, and fibrosis in patients developing atrial fibrillation after cardiac surgery. Hear Rhythm. 2009;6(10):1415–22.

164. Carnagarin R, Kiuchi MG, Ho JK, Matthews VB, Schlaich MP. Sympathetic nervous system activation and its modulation: Role in atrial fibrillation. Front Neurosci. 2019;13(JAN):1–16.

165. Heijman J, Guichard J-B, Dobrev D, Nattel S. Translational Challenges in Atrial Fibrillation. Circ Res. 2018 Mar;122(5):752–73.

166. Karamichalakis N, Letsas KP, Vlachos K, Georgopoulos S, Bakalakos A, Efremidis M, et al. Managing atrial fibrillation in the very elderly patient: challenges and solutions. Vasc Health Risk Manag. 2015;11:555–62.

167. Chen LY, Chung MK, Allen LA, Ezekowitz M, Furie KL, McCabe P, et al. Atrial

Fibrillation Burden: Moving Beyond Atrial Fibrillation as a Binary Entity: A Scientific Statement From the American Heart Association. Circulation. 2018 May;137(20):e623–44.

168. Go AS, Reynolds K, Yang J, Gupta N, Lenane J, Sung SH, et al. Association of Burden of Atrial Fibrillation With Risk of Ischemic Stroke in Adults With Paroxysmal Atrial Fibrillation: The KP-RHYTHM Study. JAMA Cardiol. 2018 Jul;3(7):601–8.

169. Greer GS, Wilkinson WE, McCarthy EA, Pritchett ELC. Random and nonrandom behavior of symptomatic paroxysmal atrial fibrillation. Am J Cardiol. 1989;64(5):339–42.

170. Gillis AM, Rose MS. Temporal patterns of paroxysmal atrial fibrillation following DDDR pacemaker implantation. Am J Cardiol. 2000;85(12):1445–50.

171. Kaemmerer WF, Rose MS, Mehra R. Distribution of patients' paroxysmal atrial tachyarrhythmia episodes: Implications for detection of treatment efficacy. J Cardiovasc Electrophysiol. 2001;12(2):121–30.

172. Shehadeh LA, Liebovitch LS, Wood MA. Temporal patterns of atrial arrhythmia recurrences in patients with implantable defibrillators: Implications for assessing antiarrhythmic therapies. J Cardiovasc Electrophysiol. 2002;13(4):303–9.

173. Gillis AM. Modeling temporal patterns of atrial tachyarrhythmias: A new surrogate outcome measure for clinical studies? J Cardiovasc Electrophysiol. 2002;13(4):310–1.

174. Henriksson M, Martin-Yebra A, Butkuviene M, Rasmussen JG, Marozas V, Petrenas A, et al. Modeling and Estimation of Temporal Episode Patterns in Paroxysmal Atrial Fibrillation. IEEE Trans Biomed Eng. 2021;68(1):319–29.

175. Charitos EI, Ziegler PD, Stierle U, Sievers HH, Paarmann H, Hanke T. Atrial fibrillation density: A novel measure of atrial fibrillation temporal aggregation for the characterization of atrial fibrillation recurrence pattern. Appl Cardiopulm Pathophysiol. 2013;17(1):3–10.

176. Chen Z, Brown EN, Barbieri R. Characterizing nonlinear heartbeat dynamics within a point process framework. IEEE Trans Biomed Eng. 2010 Jun;57(6):1335–47.

177. Daley DJ, Vere-Jones D. An Introduction to the Theory of Point Processes: Volume I: Elementary Theory and Methods. 2nd ed. New York: Springer; 2003.

178. Andrade JG, Yao RRJ, Deyell MW, Hawkins NM, Rizkallah J, Jolly U, et al.

Clinical assessment of AF pattern is poorly correlated with AF burden and post ablation outcomes: A CIRCA-DOSE sub-study. J Electrocardiol [Internet]. 2020;60:159–64. Available from: https://doi.org/10.1016/j.jelectrocard.2020.03.008

179. Lombardi F, Colombo A, Basilico B, Ravaglia R, Garbin M, Vergani D, et al. Heart rate variability and early recurrence of atrial fibrillation after electrical cardioversion. J Am Coll Cardiol [Internet]. 2001;37(1):157–62. Available from: http://dx.doi.org/10.1016/S0735-1097(00)01039-1

180. Akyürek Ö, Diker E, Güldal M, Oral D. Predictive value of heart rate variability for the recurrence of chronic atrial fibrillation after electrical cardioversion. Clin Cardiol. 2003;26(4):196–200.

181. Seaborn GEJ, Todd K, Michael KA, Baranchuk A, Abdollah H, Simpson CS, et al. Heart rate variability and procedural outcome in catheter ablation for atrial fibrillation. Ann Noninvasive Electrocardiol. 2014;19(1):23–33.

182. Hsieh MH, Chiou CW, Wen ZC, Wu CH, Tai CT, Tsai CF, et al. Alterations of heart rate variability after radiofrequency catheter ablation of focal atrial fibrillation originating from pulmonary veins. Circulation. 1999;100(22):2237–43.

183. Kang KW, Kim TH, Park J, Uhm JS, Joung B, Hwang C, et al. Long-term changes in heart rate variability after radiofrequency catheter ablation for atrial fibrillation: 1-year follow-up study with irrigation tip catheter. J Cardiovasc Electrophysiol. 2014;25(7):693–700.

184. Kocovic DZ, Harada T, Shea JB, Soroff D, Friedman PL. Alterations of heart rate and of heart rate variability after radiofrequency catheter ablation of supraventricular tachycardia: Delineation of parasympathetic pathways in the human heart. Circulation. 1993;88(4 I):1671–81.

185. Christianini N, Shawe-Taylor J. An Introduction to Support Vector Machines and Other Kernel-Based Learning Methods. Cambridge University Press; 2013.

186. Djerioui M, Brik Y, Ladjal M, Attallah B. Neighborhood component analysis and support vector machines for heart disease prediction. Ing des Syst d'Information. 2019;24(6):591–5.

187. Hosseini M-P, Hosseini A, Ahi K. A Review on Machine Learning for EEG Signal Processing in Bioengineering. IEEE Rev Biomed Eng. 2020;3333(c):1–1.

188. Calkins H, Kuck KH, Cappato R, Brugada J, Camm AJ, Chen SA, et al. 2012 HRS/EHRA/ECAS Expert Consensus Statement on Catheter and Surgical Ablation of Atrial Fibrillation: Recommendations for Patient Selection,

Procedural Techniques, Patient Management and Follow-up, Definitions, Endpoints, and Research Trial Design. Hear Rhythm [Internet]. 2012;9(4):632-696.e21. Available from: http://dx.doi.org/10.1016/j.hrthm.2011.12.016

189. Camm AJ, Malik M, Bigger JT, Breithardt G, Cerutti S, Cohen RJ, et al. Heart rate variability: Standards of Measurement, Physiological. Eur Heart J [Internet]. 1996;17:354–81. Available from: http://www.mendeley.com/research/guidelines-heart-rate-variability-2/

190. Peng CK, Havlin S, Stanley HE, Goldberger AL. Quantification of scaling exponents and crossover phenomena in nonstationary heartbeat time series. Chaos. 1995;5(1):82–7.

191. Somol P, Novovičová J, Pudil P. Flexible-hybrid sequential floating search in statistical feature selection. Lect Notes Comput Sci (including Subser Lect Notes Artif Intell Lect Notes Bioinformatics). 2006;4109 LNCS:632–9.

192. Corino VDA, Montin E, Messina A, Casali PG, Gronchi A, Marchianò A, et al. Radiomic analysis of soft tissues sarcomas can distinguish intermediate from high-grade lesions. J Magn Reson Imaging. 2018;47(3):829–40.

193. Kononenko I. Machine learning for medical diagnosis: History, state of the art and perspective. Artif Intell Med. 2001;23(1):89–109.

194. Potpara TS, Mujovic N, Sivasambu B, Shantsila A, Marinkovic M, Calkins H, et al. Validation of the MB-LATER score for prediction of late recurrence after catheter-ablation of atrial fibrillation. Int J Cardiol [Internet]. 2019;276:130–5. Available from: https://doi.org/10.1016/j.ijcard.2018.08.018

195. Balk EM, Garlitski AC, Alsheikh-Ali AA, Terasawa T, Chung M, Ip S. Predictors of atrial fibrillation recurrence after radiofrequency catheter ablation: A systematic review. J Cardiovasc Electrophysiol. 2010;21(11):1208–16.

Appendix A

Table A1 Parameters computed for each HRV derived feature, group and class (NR: No Recurrence, R: Recurrence). The groups shown are FB: Flashback, and L100: Last 100 beats. Pair of values with significant differences between classes shown in bold for clarity reasons.

Feature	FB NR	FB R	L100 NR	L100 R
Mean (ms)	824 ± 173	826 ± 172	816 ± 176	820 ± 185
pNN50 (%)	13.6 (35.8)	39.7 (66.6)	19.1 (43.9)	38.7 (61.6)
pNN20 (%)	**51.3 (45.6)***	**65.0 (48.5)***	57.0 (48.4)	64.8 (47.4)
RMSSD (ms)	96 (75)	129 (146)	93 (93)	122 (126)
SDNN (ms)	103 (81)	128 (82)	89 (77)	112 (63)
TINN (ms)	0.14 (0.10)	0.17 (0.14)	0.07 (0.07)	0.09 (0.07)
TRI	12.5 (7.5)	14.1 (8.5)	8.7 (5.1)	10.3 (8.0)
ApEn	0.81 (0.42)	0.96 (0.65)	0.61 ± 0.15	0.61 ± 0.15
SamEn	0.75 (0.59)	1.11 (1.25)	1.01 (0.84)	1.36 (1.12)
SD1	68.0 (53.3)	91.8 (103.4)	65.8 (65.7)	86.8 (89.1)
SD2	120 (111)	153 (71)	105 (104)	127 (75)
SD1SD2ratio	0.54 ± 0.22	0.60 ± 0.28	0.65 ± 0.32	0.70 ± 0.34
DFA alpha 1	0.75 (0.22)	0.81 (0.36)	0.79 (0.43)	0.87 (0.54)
DFA alpha 2	0.96 ± 0.25	0.91 ± 0.32	0.83 (0.47)	0.89 (0.68)

Normally distributed values are given as Mean ± Standard Deviation
Non-normally distributed values are given as Median (Interquartile Range)
Pair of parameters with a p-value<0.05 (*)

Table A2 Parameters computed for each HRV derived feature, group and class (NR: No Recurrence, R: Recurrence) Continued. The groups shown are Delta and AF: first 2 minutes of AF episode. Pair of values with significant differences between classes shown in bold for clarity reasons.

Feature	**Delta NR**	**Delta R**	**AF NR**	**AF R**
Mean (ms)	0.79 (16.52)	0.48 (11.12)	679 (264)	741 (290)
pNN50 (%)	-	-	43.7 (27.5)	55.1 (31.0)
pNN20 (%)	-	-	70.2 ± 13.2	75.6 ± 13.3
RMSSD (ms)	-15 (102)	-19 (49)	172 (69)	205 (124)
SDNN (ms)	-9 (87)	-4 (35)	138 (107)	167 (96)
TINN (ms)	43.65 (75.49)	-12.81 (73.38)	0.12 (0.14)	0.16 (0.16)
TRI	**8.3 (48.1)***	**16.9 (48.1)***	11.9 (14.6)	15.6 (10.9)
ApEn	27.26 (29.69)	20.92 (36.06)	0.89 (0.43)	0.16 (0.16)
SamEn	2.71 (58.99)	-43.52 (110.11)	**0.59 (0.64)***	**0.97 (0.48)***
SD1	-14.9 (102.0)	-19.7 (49.1)	122.2 (49.2)	0.9 (1.0)
SD2	-10.72 (67.00)	-2.39 (53.58)	156.26 (130.45)	145.35 (88.18)
SD1SD2ratio	-2.25 (62.79)	-25.10 (50.02)	0.75 (0.42)	185.67 (93.90)
DFA alpha 1	-5.95 (72.51)	-20.17 (57.27)	$-1.07 \times 10^{-15} \pm 4.36 \times 10^{-16}$	$-1.09 \times 10^{-15} \pm 5.04 \times 10^{-16}$
DFA alpha 2	13.96 (81.63)	-23.13 (67.83)	$-2.43 \times 10^{-16} \pm 7.92 \times 10^{-16}$	$-2.03 \times 10^{-16} \pm 7.35 \times 10^{-16}$

Normally distributed values are given as Mean ± Standard Deviation
Non-normally distributed values are given as Median (Interquartile Range)
Pair of parameters with a p-value<0.05 (*)